



Universitetet
i Stavanger

FACULTY OF SCIENCE AND TECHNOLOGY

MASTER'S THESIS

Study programme/specialization: Petroleum Engineering- Drilling Technology	Spring semester, 2019 Open/ Confidential
Author: Kamilla Helland	Digital submission (signature of author)
Faculty supervisor: Professor Kjell Kåre Fjelde External supervisor(s): Lasse Staff Jensen (Oliasoft), Lene Lykke Erichsen (Oliasoft), Dalia Gomes (UIS)	
Title of master's thesis: Blowout Flow Rate Modelling	
Credits (ECTS): 30	
Keywords: - Well Control - Blowout - Steady State Model - Black Oil Model - BlowFlow - Matlab - Inflow Model	Number of pages: 138 + supplemental material/other: 18 Stavanger, 12 th of June, 2019 date/year

Abstract

A blowout represent one of the major concerns associated with drilling, completion, maintenance and production of an oil field. Calculation of blowout rate is commonly one of the first steps in an Environmental Risk Analysis, as well as being a measure of the environmental and economic damage caused by a blowout. An increasing focus on preserving and protecting the environment, enlarges the requirement for improved numerical simulators within well control assessment. BlowFlow is an example of a software tool applied for oil-spill calculations. The engine combines flow modelling with uncertainty modelling to produce statistical distributions of blowout rates, volumes and duration. A simulation example performed in Oliasoft Blowout Simulator is presented in this thesis to illustrate a possible approach of performing oil-spill calculations.

A numerical simulator based on the black oil model, multiphase flow model, simple friction model and inflow model, has been developed with the purpose of estimating blowout rates. The starting point was a steady two-phase flow model developed by Gomes (2016). This code has been tested and documented, resulting in a number of modifications. The major improvement made to this point, is that the program is extended to include an inflow model for both single-phase and multiphase inflow conditions. Because the modified model is based on an initial guess of the BHP, while utilizing a shooting technique from the bottom of the well and up, made it possible to determine the actual oil inflow rate of a blowing well directly from the simulation.

This study provides an overview of two modelling approaches available for simulating blowout rates. Both methods presents reasonable result depending on the conditions in the reservoir. The case studies shows that the approach varying

the liquid rates at surface conditions, and finding a solution at the intersection point between the IPR and TPR curves, is less efficient than implementing an inflow directly in the simulator. This is the case as long as the model is based on a technique of numerical calculation from bottom to top.

Acknowledgement

This master thesis marks the end of my master degree in Petroleum Engineering with specialization in Drilling Technology at the University of Stavanger.

First of all, I would like to thank my supervisor Professor Kjell Kåre Fjelde for providing me with this challenging and interesting thesis, and for all his guidance and involvement during the process. I would also like to thank Oliasoft for giving me the opportunity to test their BlowFlow software. A special gratitude expressed to Lene Lykke Erichsen for guidance in the use of their program.

Finally, I would like to acknowledge my friends and family for their endless support through my years of study.

Table of content

1	Introduction	1
1.1	Study Objective	2
1.2	Structure of the Thesis	3
2	Well Containment	4
2.1	Well Barriers	4
2.2	Blowout	6
2.2.1	Kick and Well Kill Methods	8
2.2.2	Reasons for Blowout	9
2.2.3	Techniques for Killing a Blowout	12
2.2.4	Oil Spill Preparedness Systems	15
2.2.5	Blowout Control	18
2.2.6	Blowout Spill Consequences	22
2.2.7	Blowout Statistics	24
2.3	Blowout Modelling	25
2.3.1	Models for Analysing Blowouts	28
3	BlowFlow	33
3.1	Design Philosophy	34
3.2	Model Structure	36
3.2.1	PVT Model	37
3.2.2	Inflow Model	38
3.2.3	Outflow Model	39
3.3	The BlowFlow Analysis Process	40
3.3.1	Assessment of Input Data	40
3.3.2	BlowFlow Analysis	43
3.3.3	Evaluation of Results	43
4	Simulation in Oliasoft Blowout Simulator	45
4.1	Well Input	45

4.1.1	Topside	45
4.1.2	Formation	46
4.1.3	Drill String Data	48
4.1.4	Reservoir Characteristics	48
4.2	Casing Design	51
4.3	Trajectory	53
4.4	Blowout Simulation	54
4.4.1	Simulation Settings	54
4.4.2	Simulation Scenarios	54
4.5	Blowout Summary	59
4.5.1	Flow Rate	60
4.5.2	Volume	64
4.5.3	Duration	66
5	Mathematical Model for Steady State Flow	68
5.1	Conservation Laws	68
5.1.1	Steady State Model	69
5.2	Black Oil Model	71
5.2.1	Required Initial Parameters	73
5.2.2	Preliminary Calculations	74
5.2.3	Empirical Correlations	75
5.2.4	Phase Properties Calculations	81
5.3	Multiphase Flow Model	83
5.3.1	Calculation of Liquid Holdup	83
5.3.2	Pressure Drop	87
6	Calculation Approach for Steady State Flow Model	90
6.1	Model Description	90
6.2	Computational Method	91
6.2.1	Discretization Process	91
6.2.2	Shooting Method	92
6.2.3	The Bisection Method	93
6.2.4	Calculation Procedure	95
6.3	Code Structure	97
6.3.1	Main.m	97
6.3.2	Itsolver.m	98
6.3.3	Wellpressure.m	99

7	Blowout Flow Rate Model	103
7.1	Inflow Model	104
7.1.1	Simple Inflow Model	104
7.1.2	Empirical Inflow Models	105
7.2	Modelling Procedures	106
7.2.1	Case Study #1	108
7.2.2	Case Study #2	110
7.2.3	Case Study #3	120
7.3	Sensitivity Analysis	125
7.3.1	Friction Model	125
7.3.2	GOR	126
7.3.3	Productivity Index	126
7.3.4	Outlet Pressure - The real pressure at surface	127
7.4	Discussion of Results	128
7.5	Additional Improvements	132
7.6	Further Work	133
8	Conclusion	136
A	Appendix	145
A.1	Simple Inflow Model Calculations	145
A.2	Modified Code with Implemented Inflow Model	146
A.2.1	Main.m	146
A.2.2	Itsolver.m	146
A.2.3	Wellpressure.m	148
A.2.4	Function for solubility ratio	152
A.2.5	Function for bubble point pressure	152
A.2.6	Function for frictional pressure loss	152
A.2.7	Function for oil formation volume factor	153
A.2.8	Function for gas formation volume factor	154
A.2.9	Function for liquid holdup	154
A.2.10	Function for liquid velocity number	155
A.2.11	Function for gas velocity number	155
A.2.12	Function for viscosity liquid number	155
A.2.13	Function for diameter number	155
A.2.14	Function for tension	155
A.2.15	Function for compressibility factor of gas	156

List of Figures

2.1	Well barrier schematics during drilling operation (NORSOK D010, 2013).	5
2.2	Surface Blowout at the Macondo Deepwater Horizon Rig in the Gulf of Mexico, April 2010 (Herbst, 2017).	7
2.3	Example of planned well paths for two relief wells to the target well (Statoil, 2010).	14
2.4	Boom deployed in an U configuration between two vessels to capture oil (ITOPF, 2018).	17
2.5	Well control equipment (Fjelde, 2016).	21
2.6	A schematic of a BOP (Belayneh, 2018b).	22
2.7	Blowout risk analysis (Arild et al., 2008).	24
2.8	Amount of blowouts experienced during different petroleum activities (SINTEF, 2017).	25
2.9	Models for analysing blowout, categorized by their purpose.	28
2.10	BlowFlow model framework (Karlsen and Ford, 2014a).	31
3.1	BlowFlows role in an ERA (Karlsen and Ford, 2014a).	33
3.2	The Monte Carlo Simulation process in BlowFlow.	35
3.3	The BlowFlow model structure (Ford, 2012).	36
3.4	A VLP and IPR curve showing the outflow/inflow from annulus to surface and the intersection point.	39
3.5	The BlowFlow work process (Arild et al., 2008).	40
3.6	Example of two types of distribution models available in BlowFlow. The first being a triangle distribution model, while the second is a continuous uniform distribution model.	43
3.7	Example of result from the simulator, expressed through probability distributions of rates, volumes and durations.	44
4.1	Schematic representation of the platform and water depth.	46

4.2	Estimated formation temperature throughout the well.	46
4.3	The formation pressure profile, with corresponding casing setting depths.	47
4.4	Triangle distribution of the reservoir pressure.	50
4.5	Reservoir zone properties with the use of OilBasic model.	51
4.6	Wellbore schematic showing the casing program and open hole section.	52
4.7	Illustration of the vertical well trajectory.	53
4.8	Probabilistic scenarios of blowout exit points and flow path.	55
4.9	BOP settings used in the case study.	56
4.10	Reservoir penetration depth distributions.	57
4.11	The different phases of a relief well process, with corresponding estimated duration.	58
4.12	Probabilistic oil flow rate distribution at day 0.	60
4.13	Probabilistic flow rate distribution at day 32.	63
4.14	Probabilistic flow rate distribution at day 45 and 65, respectively.	64
4.15	Probabilistic indication of total blowout volume released until the well is killed.	64
4.16	Blowout duration probability distribution.	67
5.1	Illustration of the conservation of mass in a discretized pipe.	69
5.2	Petroleum fluids and their characteristics (Petrowiki, 2015c).	71
5.3	Essential variables defined in the black oil model (Gomes, 2016).	72
5.4	The relationship between R_s and GOR (Pettersen, 1990).	73
5.5	Typical response of the important parameters in the black oil model (Pettersen, 1990).	76
5.6	The curve used to determine C_{NL} (Economides et al., 1994).	85
5.7	The plot used to determine $\frac{H_L}{\psi}$ (Economides et al., 1994).	85
5.8	The graph used to determine ψ (Economides et al., 1994).	86
6.1	The discretization process in a vertical well.	92
6.2	Calculation procedure of the bisection method (Fjelde, 2017b).	94
6.3	Calculation procedure from bottom to top in the steady state flow model.	95
6.4	Calculation procedure from node (i) to (i+1).	96
6.5	Base code structure.	97
7.1	Plot used to determine the actual flow rate and corresponding BHP.	108
7.2	IPR and TPR curves plotted in Excel.	110

7.3	New code structure of the improved model.	112
7.4	Pressure drop profile in the well.	115
7.5	Oil formation volume factor profile.	116
7.6	Gas formation volume factor profile.	117
7.7	Oil density profile.	117
7.8	Gas density profile.	118
7.9	Liquid holdup profile.	119
7.10	Liquid holdup profile for example 3.	124
7.11	Sensitivity analysis of the impact of GOR.	126
7.12	Sensitivity analysis of the impact of productivity index.	127
7.13	Sensitivity analysis of the effect of applying a backpressure at surface.	128

List of Tables

2.1	Barriers failures causing blowouts from 2000 to 2015 (Holand, 2017).	11
3.1	Input parameters required in BlowFlow (Arild et al., 2008).	41
4.1	Drill string components and their dimensions.	48
4.2	Casing program used as input in the Oliasoft Blowout Simulator.	52
4.3	Reservoir input data for the simulation.	59
4.4	Mean potential surface blowout rate.	61
4.5	Mean potential subsea blowout rate.	62
4.6	Potential mean blowout volumes in case of a surface blowout.	65
4.7	Potential mean blowout volumes in case of a seabed blowout.	66
5.1	Definition of variables used in the conservation laws.	70
5.2	Initial parameter needed to be defined in the black oil model (Gomes, 2016).	73
6.1	Input parameters for the main program.	98
6.2	Adjustments made to the units of the input variables.	100
6.3	Input parameters for the wellpressure function.	101
7.1	Input parameters for the case studies.	107
7.2	New parameters declared in wellpressure.m for case study #2.	113
7.3	Parameters declared in wellpressure.m for case study #3.	121
7.4	Parameters in example 1.	122
7.5	Parameters in example 2.	123
7.6	Parameters in example 3.	124
7.7	Result from the case studies.	129
7.8	Result from the examples in case study #3.	130

List of Symbols

α_g	Gas volume fraction
α_l	Liquid volume fraction
Δp	Total pressure drop
Δp_{fric}	Frictional pressure drop
Δp_{hyd}	Hydrostatic pressure drop
Δz	Vertical displacement
γ_g	Gas gravity
γ_o	Oil gravity
γ_{API}	API grade
μ_g	Gas viscosity
μ_l	Liquid viscosity
μ_w	Water viscosity
μ_{mix}	Mixture viscosity
ρ_f	Formation density
ρ_g	Gas density
ρ_l	Liquid density
ρ_w	Water density
ρ_{air}	Air density
ρ_{do}	Dead oil density

ρ_{gst}	Gas density at standard conditions
ρ_{mix}	Mixture density
ρ_{pr}	Pseudoreduced gas density
σ	Interfacial tension
σ_{gc}	Gas-condensate interfacial tension
A	Flow area
ABC	Advanced Blowout Control
B_g	Gas formation volume factor
B_o	Oil formation volume factor
B_{ob}	Formation volume factor for oil at bubble point pressure
BHA	Bottomhole Assembly
BHP	Bottomhole pressure
BOP	Blowout Preventer
C	Correction factor
c_g	Gas isothermal compressibility
c_o	Oil compressibility
C_{NL}	Viscosity number coefficient
d_{in}	Inner diameter
d_{out}	Outer diameter
e	Inner roughness
ERA	Environmental Risk Analysis
F	Internal variable
f	Friction factor
f_w	Water fraction

g	Gravity constant
GOR	Gas Oil Ratio
h	Well depth
H_G	Gas holdup
H_L	Liquid holdup
$HPHT$	High Pressure High Temperature
ID	Inner diameter
IPR	Inflow Performance Relationship
J	Productivity index
K	Relative roughness
M_{air}	Air molar mass
n	Number of moles of gas
N_d	Diameter number
N_l	Viscosity liquid number
N_{vg}	Gas velocity number
N_{vl}	Liquid velocity number
NCS	Norwegian Continental Shelf
OD	Outer diameter
OLF	Norwegian Oil and Gas Association
$OSRA$	Oil Spill Response Analysis
p	Pressure
P_b	Bubble point pressure
P_N	Outlet pressure
P_{atm}	Atmospheric pressure

P_{guess}	Initial guess of the bottomhole pressure
P_{pc}	Pseudocritical pressure
P_{pr}	Pseudoreduced pressure
P_{res}	Average reservoir pressure
P_{st}	Pressure at standard conditions
P_{surf}	Pressure at surface
P_{wf}	Bottomhole pressure
PI	Productivity index
PSA	Petroleum Safety Authority Norway
PVT	Pressure, Volume and Temperature
Q_l	Liquid flow rate at standard conditions
Q_{gst}	Gas flow rate at standard conditions
q_g	Gas flow rate at downhole conditions
q_{IPR}	Inflow performance relation flow
$q_{o,max}$	Maximum oil rate
Q_{ost}	Oil flow rate at standard conditions
q_o	Oil flow rate at downhole conditions
q_{TPR}	Tubing performance relation flow
R	Universal gas constant
R_s	Solution ratio
R_{sb}	Solubility ratio at bubble point
Re	The Reynolds number
$RWIS$	Relief Well Injection Spool
SC	Standard conditions

STC	Stock tank conditions
T	Temperature
T_{pc}	Pseudocritical temperature
T_{pr}	Pseudoreduced temperature
T_{st}	Temperature at standard conditions
TPR	Tubular Performance Relationship
TRA	Total Risk Analysis
TVD	True Vertical Depth
V_g	Volume of free gas at reservoir conditions
v_g	Gas velocity
v_l	Liquid velocity
V_o	Oil volume at reservoir conditions
V_{gsc}	Volume of gas at standard conditions
v_{mix}	Mixture velocity
V_{ost}	Oil volume at standard conditions
v_{SG}	Superficial gas velocity
v_{SL}	Superficial liquid velocity
VLP	Vertical Lift Performance
WCD	Worst Case Discharge
y_g	Internal variable
Z	Gas compressibility factor

1. Introduction

Management of well control is considered to be of high importance during all stages of a well. A blowout is a severe event that may occur if the well containment is not sufficient, and is typically a result of series of events that can be traced back to equipment failure or human error (Schubert, 1995; Schubert et al., 2004). Uncontrolled release of hydrocarbons to surface or seabed, can lead to large oil spills, causing negative impact on the environment. Although statistics show that blowouts are a rare phenomena, the possible consequences of such an event is of too high magnitude to simply ignore (SINTEF, 2017). By studying the Macondo accident in the Gulf of Mexico April 2010, one clearly see the importance of preventing and estimating blowouts. Loss in well control resulted in over 4.9 million barrels of oil spilled through a surface blowout, causing 11 casualties and enormous damages on the environment. It took the operator several months to stop the leak and regain control of the situation (National Commision, 2011).

With an increasing focus on both safety and preserving the environment, in combination with the petroleum industry facing more and bigger challenges as the industry moves into more harsh environment, contributes to making blowout prevention and estimation of possible spills a top priority in the petroleum industry. Hence, numerical simulators have become important tools in the industry.

Environmental Risk Analysis (ERA) is an example of risk analysis operators on the Norwegian continental shelf (NCS) have to conduct, by law, in order to quantify and predict the risk of petroleum activities (Karlsen and Ford, 2014b). Environmental Risk Assessment of Exploration Drilling in Nordland VI (DNV, 2010), is an example of such a risk analysis. Blowouts represents one of the major threats associated with the oil and gas industry. Hence, calculation of potential

blowout rates, volumes and durations are needed as input in ERAs, to dimension the appropriate oil spill emergency preparedness (Nilsen, 2014).

There are generally two types of numerical simulation softwares available related to blowout modelling. One focuses on killing a blowout and how this should be done hydraulically, while the other type of simulator focuses on estimating the rate, volume and duration of a blowout, hence studying the oil spill (Arild et al., 2008; Karlsen and Ford, 2014b). Various softwares have been developed over the last couple of years, due to the increasing demand for improved tools within well control assessment. BlowFlow, developed by NORCE, is an example of such a software tool. The software, currently being commercialized by Oliasoft, combines flow modelling with uncertainty modelling to produce statistical distributions for the flow rates, duration and discharged volumes. Unlike other simulators on the market, this model apply a stochastic modelling approach, where probability distributions for a certain number of inputs are used instead of fixed numbers. This approach is applied to model the uncertainty related to the consequences of a blowout (Ford, 2012).

Multiphase flow models, like the steady state flow model, are widely used in the petroleum industry, and one of the various application of such a model is to simulate blowout flow rate.

1.1 Study Objective

One of the purposes of this thesis is to describe the BlowFlow model in more detail, and in collaboration with Oliasoft, present a simulation example using Oliasoft Blowout Simulator. The objective of this simulation example is to show one alternative approach of performing blowout modelling.

Furthermore, this thesis aims to check and document the developed model by Gomes (2016), as well as extending the original code to being valid both for annular geometry and tubular configuration.

The main objective of this thesis is to develop a blowout flow model based on Gomes (2016), with an integrated inflow model valid for both multiphase and single-phase inflow. A shooting technique will be employed, guessing for the bottomhole pressure (BHP) and iterating until the outlet boundary condition has been met at surface. The fact that the shooting is performed from bottom to top, makes it possible to include an inflow model directly in the flow model. If an inflow model is successfully implemented in the steady state flow model, it would be possible to determine the solution point flow rate of a blowing well directly from the simulation rather than needing to find the solution from the intersection point between the Inflow Performance Relationship (IPR) and Tubular Performance Relationship (TPR) curves. This approach differs from the approach used by Gomes (2016), where various inlet rates are used to calculate the corresponding BHP. These two modelling approaches available for modelling the blowout rates will be tested, where the main focus will be on studying the benefits of including an inflow model directly in the program, when the shooting technique is applied from the bottom of the well and up.

1.2 Structure of the Thesis

The thesis is divided into eight chapters. Chapter 2 gives a theoretical review of blowout, and blowout calculations use in oil spill preparedness planning. Chapter 3 describes the BlowFlow engine, while a simulation example using Oliasoft Blowout Simulator is presented in chapter 4. Chapter 5 presents the mathematical model forming the base for the simulation. The calculation approach and the structure of the steady state flow model developed on basis of Gomes (2016) are covered in chapter 6. Chapter 7 gives a review of inflow models, and how they may be included in the flow model. This chapter also presents three case studies of blowout modelling, discussion of results, and future recommendations. Finally, chapter 8 presents a conclusion of the work conducted.

2. Well Containment

During the lifetime of a well, the management of well control is considered to be of high importance. It is crucial to maintain and control the well pressures, and ensure no unwanted influx of formation fluids into the wellbore at all time (Schubert, 1995). The oil and gas industry is today facing more and bigger challenges as the industry is moving into more harsh environments, in combination with an increasing focus on both safety and preserving the environment. These issues contributes to making well control a top priority in the petroleum industry (Liu et al., 2015; Arild et al., 2008).

2.1 Well Barriers

The importance of well control cannot be underestimated. To ensure well control, at least two independent well barriers have to be present in each well at all time. A well barrier consist of one or several well barrier elements, which prevents fluids from flowing uncontrolled from the formation. One single barrier element is not sufficient to act as a barrier alone, which is why several barrier elements are needed to close the envelope, and restore well control. The main objectives of these envelopes of barriers are to avoid a catastrophic event, and have the ability to regain well control (NORSOK D010, 2013). Figure 2.1 shows a typical well barrier envelope for a drilling operation.

Norway has regulations relating to design and outfitting in the petroleum industry, called *The Facilities Regulations*. According to this regulation, section 48: *"The well barriers shall be designed such that well integrity is ensured, and the barrier functions are safeguarded during the well's lifetime"* (PSA, 2019c). In addition, the NORSOK Standard D-010 is heavily used as guideline for well

integrity during different petroleum activities on the NCS.

In terms of well barriers, it is common to distinguish between primary and secondary barriers. The primary barrier is the first protection against unwanted influx of reservoir fluid to the wellbore. It is in most cases the operation of maintaining the hydrostatic pressure in the well. The well pressure has to be greater than the pore pressure, but lower than the fracture pressure. This is controlled by monitoring the mud column, outlined in blue in figure 2.1 (Petrowiki, 2015b).

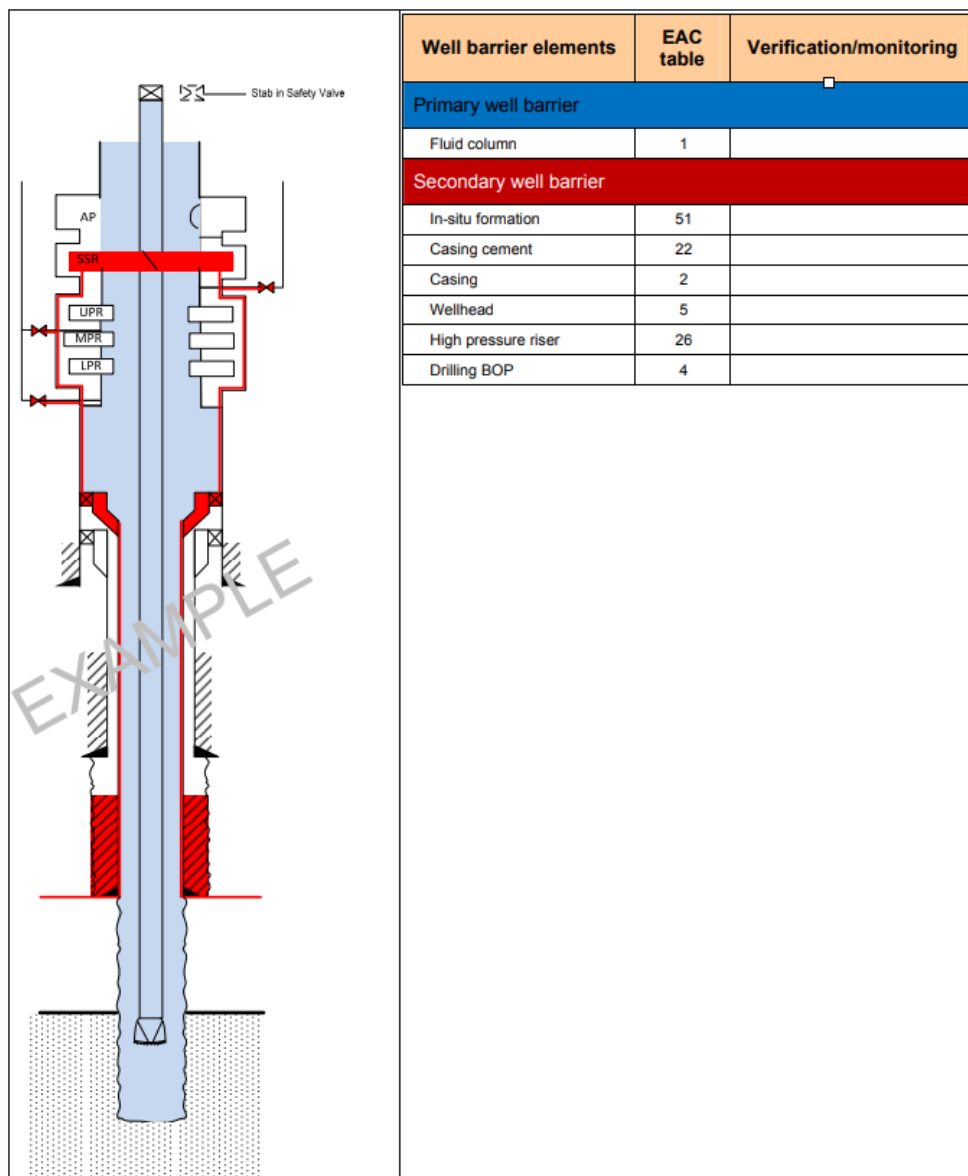


Figure 2.1: Well barrier schematics during drilling operation (NORSOK D010, 2013).

Failure in the primary well barrier may result in a kick, defined as flow of formation fluids into the wellbore during drilling operations. When a kick occur, the drilling mud is displaced from the well by less dense reservoir fluid (Willson, 2012). This will affect the pressure by reducing the bottomhole pressure to lower than the formation pressure, which is the condition for a kick to develop. Due to a failure in the primary well barriers, the further operation is relayed on the secondary barriers to work and restore control of the well (NORSOK D010, 2013).

The main intention of secondary well barrier is to stop the inflow of formation fluids from reaching the surface, hence loosing the control of the kick (NORSOK D010, 2013). In most cases, the well is installed with a blowout preventer (BOP) on top of the wellhead, acting as a secondary barrier. A BOP consist of a set of valves and shear rams, which can seal off the annulus or cut the drillstring, and shut in the well in case of a kick (NORSOK D010, 2013). Other secondary barriers include wellhead, cement and surface casing (Vandenbussche et al., 2012). The BOP located on top of the wellhead, as well as other possible secondary barriers, are outlined in red in the figure 2.1.

2.2 Blowout

A blowout occur when a kick cannot be controlled, the drilling fluid is fully displaced from the well, and there is an emission of formation fluids from the well either at the sea-floor or at surface. The discharge point may be used to classify the different types of blowout (Willson, 2012);

- Seabed blowout
- Surface blowout
- Underground blowout

An example of a surface blowout, the Macondo Deepwater Horizon Rig in the Gulf of Mexico, April 2010, is shown in figure 2.2.



Figure 2.2: *Surface Blowout at the Macondo Deepwater Horizon Rig in the Gulf of Mexico, April 2010 (Herbst, 2017).*

The release point will depend upon the integrity of the well and possible riser installation. If a riser is part of the well design, or has not yet been disconnected, the blowout will occur at surface. For seabed blowouts, the flow typically exits the well at sea-floor, directly into the sea. The well pressure during a kick is affected by the hydrostatic pressure, choke pressure and friction pressure. If this well pressure is greater than the fracture pressure in the borehole, it is possible to get an underground blowout (Willson, 2012). During an underground blowout, the formation fluids will flow from one formation zone to another (Schubert et al., 2004).

The discharge point has a great impact on the flow rate and the possible oil-spill. According to Liu et al. (2015), a surface blowout is normally of highest detrimental. This statement is based on the fact that such a blowout usually result in a much higher gas fraction, much higher mixture velocity and much lower pressure at the bottom of the well compared to the reservoir, all in which causes a more severe discharge rate.

2.2.1 Kick and Well Kill Methods

As described earlier, failure in the primary well barriers may result in a kick. The development of a kick can be caused by various of reasons, including (Petrowiki, 2015b; Belayneh, 2018a);

- Insufficient mud weight
- Improper hole fill-up on trips
- Swabbing
- Gas cut mud
- Lost circulation

All these accidents mentioned above causes an imbalance of pressure in the well, which may lead to an influx of formation fluids to the wellbore. However, this influx does not necessarily cause a blowout. There are a variety of actions taken to shut in the well and kill the kick, before the situation gets the opportunity to developed into a full blowout. The first response is to stop the operation, and isolate the borehole from the surface by activating the secondary barriers. The well kill procedure may start after the well is shut in (Fjelde, 2017a).

Killing a well, means to circulate the gas out of the well through a choke, and replace the original mud with a heavier mud to avoid further influx. Heavy mud, referred to as kill mud, is circulated down the well to balance the BHP (Petrowiki, 2015b). There are mainly three well kill methods available (Belayneh, 2018a);

- **Driller's method (Two circulation method):** The basic principle is to keep the BHP constant while killing the well. First, the kick is circulated out of the well using old mud. The next step is to weight the kill mud up to required density, and replace the old mud.
- **Wait and weight method (One circulation method):** The kill mud is weighted up to the desired density from the start, and circulated down the drillstring. In the same circulation, kill mud moves up through the annulus, while the stand pipe pressure is kept constant by proper choke adjustments.
- **Bullheading:** The well is killed by forcing formation fluids back into the formation by pumping kill weight fluid down the annulus.

2.2.2 Reasons for Blowout

The first sign of a possible blowout is usually a kick. If the kick is not properly controlled, it may lead to a blowout. However, blowouts are typically a result of series of events traced back to either equipment failure or human error (Schubert et al., 2004). A blowout only occur if both well barriers fail. This means that both the primary barrier, represented by the mud-column, and the secondary barriers represented by the BOP, wellhead, cement or surface casing, have to fail (Vandenbussche et al., 2012). In the following, some of the situations which may lead to a blowout will be described.

Undetected kick is a phenomena that may occur when drilling with oil based mud. If the kick volume is small enough it may go undetected, and dissolve in the oil based drilling mud. The barriers will then fail to kill the kick, and it will be transported with the mud to surface. As the kick migrates upwards in the well, in combination with suitable temperature and pressure, the gas will boil out at surface (Belayneh, 2018a). Although the initial amount of gas was minimal, the volume of gas in the mud increases at the top section of the well, which may cause severe consequences.

During the well kill procedure, while waiting for the pressure build-up to stabilize, a *formation fracture* may develop at the weakest point in the well. The weakest point is normally just below the last casing shoe. As a result, a combination of drilling and formation fluid enters the formation before the pressure at the bottom of the well is sufficient to stop the uncontrolled flow (Watson et al., 2003). To deal with such situations, it is necessary to increase the BHP while decreasing the pressure at fracture point. This may eventually cause the well pressure to exceed the formation pressure, and thus fracture the well all the way to surface. If this fracturing process is not controlled, it may cause a blowout to occur (Halle, 2010).

In order to run a large diameter hole opener, one need to disconnect the riser from the BOP. During the *disconnection of riser* a blowout may develop. When

performing this operation it is of high importance to keep the well stable. By displacing the fluids in the well up to the BOP with a heavy kill mud, an adequate overbalanced well pressure is kept, which reduces the probability of a blowout (Holand, 1996).

Failure in BOP or in any of the other secondary barrier elements installed in the well, may cause a blowout to occur. This can either be failure in the mechanics or restrictions in the pipe, making it impossible for the barriers to completely seal the well or fully engage. It should be noted that there may also be failure in the other valves control systems in the well, causing uncontrolled flow of hydrocarbons (Nilsen, 2014).

The operations of drilling and setting the first casing are conducted in shallow zones. In some cases, these areas may contain gas. Because these *shallow gas zones* are penetrated before the installation of surface casing and BOP, there are no barriers available to prevent uncontrolled flow of formation fluid to surface. The uppermost layers in a formation are too thin and weak to handle a shut-in pressure, making the BOP useless. This is why the BOP is not in general installed before after the surface casing has been set and cemented. Due to the lack of well control equipment installed when drilling in shallow gas zones, a blowout may occur (Holand, 1996).

Poor cementing job or a failure in the casing, may cause a blowout to develop outside the casing. In such cases, the uncontrolled flow of formation fluid will flow outside the casing wall towards surface. Because other constituents of the secondary barrier have failed, the BOP will fail to kill the blowout (Holand, 1996).

Moreover, it is necessary to mention that sometimes a blowout may be caused by *external causes*, including storms, military activities, ship collisions, fire and earthquake (Holand, 2017; SINTEF, 2017).

Table 2.1 presents the primary and secondary barrier failure causes for deep-water blowouts in the US GoM and regulated areas, among others Norway, UK, Australia, Canada, Brazil and US Pacific, from 2000 to 2015 (Holand, 2017).

Table 2.1: *Barriers failures causing blowouts from 2000 to 2015 (Holand, 2017).*

Primary barrier failure	Secondary barrier failure	Total blowouts
Too low mud weight	Casing head failed	1
Gas cut mud	Poor cement	1
Improper fill up, annular losses, packer leakage	Wellhead failed	1
Disconnected riser	Failed to close BOP	1
Unexpected high well pressure	Formation breakdown, poor cement, casing leakage	5
Reservoir depth uncertainty	String safety valves failed, inner casing failed	2
While cement setting	BOP failed after closure, BOP not in place, wellhead failed	4
Casing plug failure	Failed to close BOP, only one barrier present	2

As seen from the figure above, most of the blowouts occurred due to unexpected high well pressure or while cement setting. The two incidents with casing plug failure as source for loss of the primary barrier, are the Deepwater Horizon blowout in 2010 and the Montara blowout in 2009. Although the severity of those two blowouts differs, they are both considered extreme blowouts. The Montara well in Australia spilled a total of 29 600 bbl, which is 140 times less than the Macondo incident in the Gulf of Mexico. The Montara blowout occurred because the well only had one barrier present, while the Macondo accident originated from several human and equipment errors, causing failure in closing the BOP (Holand, 2017; National Commission, 2011).

2.2.3 Techniques for Killing a Blowout

The blowout duration depends on how long it takes to kill the blowing well. There are various intervention methods available to kill a blowout and regain control of the well. These methods are often referred to as kill mechanisms, and can be categorized depending on the intervention location, like surface intervention and relief well intervention (Oskarsen et al., 2016). According to *The Activities Regulation* section 86, published by The Petroleum Safety Authority Norway (PSA), it should always be possible to regain well control by intervening directly or by drilling one relief well (PSA, 2019b).

Surface intervention is always the first action taken to kill a blowout. The objective of this type of intervention is to control the blowout by direct access to the discharge point or the wellhead of the blowing well (Lage et al., 2006). On occasion, surface intervention is impractical or cannot be used to establish control over the well (Schubert et al., 2004). This is typical for deep water scenarios, such as the Macondo incident. Such situations often require an alternative approach in order to kill the blowing well. This can be accomplished by drilling a relief well, and thus utilize this additional well to regain control of the target well (Oskarsen et al., 2016).

Furthermore, blowout intervention can be classified depending on the intervention method. Some of the available intervention methods are (Schubert et al., 2004);

- **Capping:** This kill method is part of the surface intervention, and comprises of mechanically killing the blowout by closing-in the flow path release point at surface (Schubert et al., 2004). This makes it impossible for the uncontrolled flow of hydrocarbons to escape to surface, as it will be stopped by a barrier. There are numerous elements which may act as mechanical barriers, among others, special capping stacks, shear rams, ball valves or diverters. It should be mentioned that capping may include closing one or several valves in the well barrier system, such as the x-mas tree valves, BOP valves, ect. (Nilsen, 2014).

- **Bullheading:** This operation is also part of the surface intervention. Water, mud or brine are then circulated down the drillstring with a greater momentum than the unwanted flow of reservoir fluids coming up the borehole, forcing the formation fluids back into the formation (Schubert et al., 2004). This procedure aims to balance the reservoir pressure, and kill the well statically (Nilsen, 2014). According to (Schubert, 1995) this kill technique is simple and requires no or little planning.
- **Natural depletion:** This is a passive kill technique, that may occur due to changes in borehole conditions caused by a blowout. These changes to conditions like pressure and flow, may naturally result in the uncontrolled flow of hydrocarbons to cease completely, and thus cause the blowout to natural deplete (Nilsen, 2014).
- **Cement:** Fast-reacting cement can be injected into the well as a plug in order to kill the blowout, and thus provide full well control (Nilsen, 2014). This kill technique may be used as part of both surface and relief well intervention. An alternative approach would be to set a gunk plug, a mix of diesel and gel, into the borehole (Schubert et al., 2004).
- **Bridging:** This is a passive technique for killing a blowout. When a blowout occur, the downhole conditions may experience some changes. As a result, the formation around the wellbore may collapse, there may be obstruction of the flow through the well due to the accumulation of material, or there can be a caving-in of the borehole. Consequently, all these situations will seal off the flow path, causing a reduction of the blowout rate or a killing of the blowout (Schubert et al., 2004; Vandenbussche et al., 2012).
- **Relief well:** As mentioned before, this procedure is only conducted when surface intervention is impossible or impractical. This is mainly because this method is time-consuming and a costly operation. This kill technique comprises of drilling a relief well towards the bottom of the blowing well, which directly intersect with the blowing well well, deplete the target reservoir, and thus kill the blowout. If communication can be established between these two wells, well control can be regained with the use of dynamic kill or cementing techniques (Nilsen, 2014; Schubert et al., 2004). An example

of planned well paths for two relief wells to the target well, obtained from an Activity program - Drilling conducted by Equinor, can be seen in figure 2.3. According to Rinde et al. (2016) well-kill operations through a relief well is considered to be the most reliable and optimal method for killing a blowout.

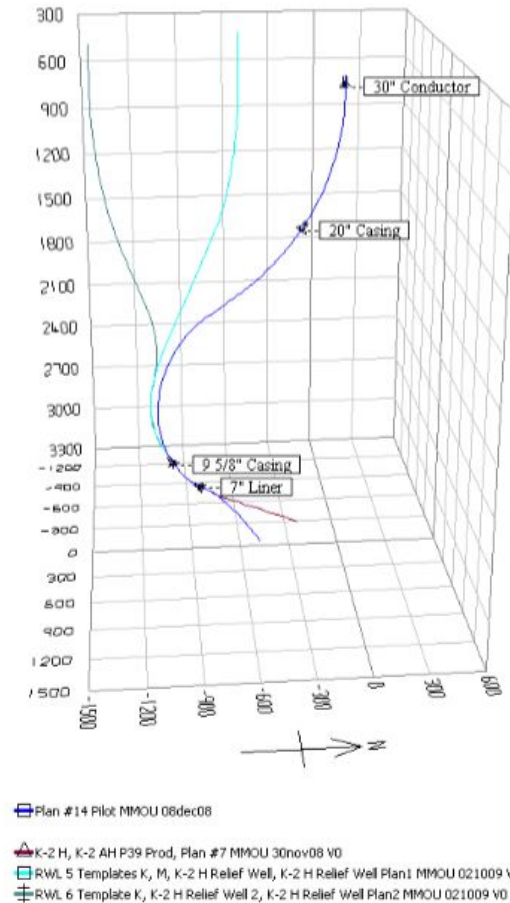


Figure 2.3: Example of planned well paths for two relief wells to the target well (Statoil, 2010).

- **Dynamic kill:** This intervention method is part of the relief well intervention. Kill mud is circulated into the blowing well at high pump rates, generating a high annular friction pressure (Schubert, 1995). This additional friction pressure loss makes a substantial contribution to the counter-pressure against the reservoir, which may kill the uncontrolled flow of reservoir fluids. As soon as the influx has been controlled, a weighted mud is circulated to statically control the well (Nilsen, 2014).

2.2.4 Oil Spill Preparedness Systems

In case of a blowout, it is crucial to manage the oil spill immediately to minimize the treat and possible damage to both humans and the environment (EPA, 1999). It is essential that an environmental analysis is conducted as soon as possible, no later than 48 hours after the pollution has been observed. The aim of such a survey is to identify and describe the possible damage to the surrounding environment (PSA, 2019b).

“Under the Pollution Control Act, operators are required to maintain a level of preparedness and response which is dimensioned to deal with acute pollution from their activities” (Regjeringen, 2016). This law states that essential measures to prevent and limit the damages and disadvantages of acute pollution have to be conducted by the responsible parties (LOVDATA, 1981). The oil spill contingency plan is an important part of this oil spill preparedness, and shall as a minimum include (IPIECA, 2015);

- Identification of possible damage
- Vulnerability analysis
- Risk assessment
- Response action

The contingency plan has to be in compliance with local regulations and framework. By having a well-planned, efficient and effective plan available, it is possible to reduce the impact of an oil spill on people and the environment significantly (PSA, 2019b; LOVDATA, 1981). Although, the action taken in case of a blowout varies depending on various circumstances, there are certain basic principles that applies for any kind of spill scenario. In simplicity, these principles can be described as the following (IPIECA, 2015);

- *Safeguarding the safety and health of people*
- *Stopping the source of the spill as quickly as possible*
- *Minimizing environmental impact*
- *Minimizing the risk of oil reaching the shore in offshore scenarios*

- *Minimizing the risk of oil entering watercourses or groundwater in onshore scenarios*

The initial step in oil spill preparedness is to identify the potential situations that may arise for a specific facility or operation. By using these situations, the operators have to define appropriate spill planning scenarios (IPIECA, 2015). Simulators can be utilized to determine and predict the behaviour of a potential oil spill caused by a blowout. The Oscar simulator and BlowFlow are two examples of tools used for spill calculations. These models will be described in section 2.3. The oil spill modelling form the basis for the emergency response analysis (Norsk Olje og Gass, 2013). Once different spill scenarios have been established, it is necessary to develop the optimum response strategy for each of the cases by employing different oil spill recovery techniques (IPIECA, 2015).

Although the contingency plan plays a vital role in the preparedness, it is important to ensure proper training of personnel and have access to suitable equipment for oil spill recovery. This is essential to ensure optimum oil spill response (IPIECA, 2015).

Oil Spill Recovery Techniques

After an oil spill has occurred, it is of high importance to implement actions to minimize the possible damage to the environment, and remove the oil in a safe and efficient way. Traditionally, there are four techniques available for dealing with oil spills, including mechanical recovery, chemical dispersion, biological decomposition and in-situ burning (SINTEF, 2010).

Depending on factors such as temperature, weather, type of oil, location and amount of oil spilled, the best recovery technique should be applied, or a combination of them. Although there has not been a major leap in the development of new spill containment equipments, the conventional techniques have been significantly improved. These techniques play a vital role in the oil spill recovery, removal and dispersal (EPA, 1999).

In general, *the mechanical oil spill recovery* consist of employing booms and skimmers. As seen in figure 2.4, the boom is a containment equipment used to capture the oil. This equipment control the spread of oil, and thus reduce the damage on the surrounding environment. Moreover, the boom concentrate oil in thicker layers, making the recovery process easier (EPA, 1999). After the oil has been contained, both skimmers and sorbents can be used to remove the oil from the surface. The latter being a material that soak up the oil either by absorption or adsorption, or a combination of both (EPA, 1999). A skimmer is a device put into the sea to separate oil from the waters surface, and then pump the oil into vessels for transportation (ITOPF, 2018). The approach of combining booms and skimmers is widely applied all over the world, but this specific recovery technique becomes less effective in case of bad weather and high waves (EPA, 1999).



Figure 2.4: *Boom deployed in an U configuration between two vessels to capture oil (ITOPF, 2018).*

Another technique used for dealing with an oil spill is *chemical dispersion*. This method use different chemicals to break oil into small droplets, making it possible for the oil to dissolve into water. As the oil is dispersed into water, natural processes like wind, waves and currents, may help to break the oil droplets further down. Because of the great negative affect on the environment, this oil spill recovery technique is not in general the first action taken by operators (EPA, 1999). It should be noted that the latest regulations from PSA allows the use of chemical agents during oil spill response operations (SINTEF, 2010).

The biological degradation is a slow, natural recovery process, where micro-organisms

breaks down the oil. This process is typically too slow to provide adequate environmental recovery. To speed up the process of degradation, there are different nutrients, enzymes or micro-organisms that can be used (SINTEF, 2010).

In-situ burning is a recovery technique applied to reduce the negative affect of oil spreading to the environment. With this technique, the oil is ignited and burned under controlled circumstances, usually close to the spill point (IPIECA, 2015).

It should be mentioned, that if the oil spill has reached beaches and shorelines, physical methods can be applied to clean up these areas. Physical methods include techniques like wiping with absorbent material, pressure washing and bulldozing (EPA, 1999).

2.2.5 Blowout Control

Blowout Contingency plan

According to Norwegian Pollution Control Act of 1981, §41: *"The pollution control authority may by regulations or individual decision lay down that contingency plans shall be submitted for approval for any activity that may result in acute pollution. The plan shall provide guidelines for the action to be taken in the event of acute pollution and shall be updated as necessary."* (LOVDATA, 1981).

To ensure sufficient blowout control, a predetermined blowout contingency plan should be in place for each installation and field. As a minimum, the plan has to address the following (NORSOK D010, 2013);

- *Field layout*
- *Well design*
- *Primary kill strategy in a blowout case*
- *A description of, or reference to, the emergency response organization*

It is necessary to perform a blowout and kill rate simulation study for each specific operation. In such a study it is essential to consider all possible blowout

scenarios that may occur during an operation (Yuan et al., 2014). In order for operators to apply for a drilling permit, they are required to calculate Worst Case Discharge (WCD) scenarios, describing in detail surface intervention methods to kill the flow, and demonstrate the ability to regain control of a blowing well. Such a WCD scenario should be based on discharge point at seabed with a hydrostatic water column, or at surface with atmospheric pressure. This leads to the risk of underestimating a blowout being reduced significantly (Liu et al., 2015).

According to Yuan et al. (2014), there are numerous simulators available with the purpose of studying blowout and kill rate. Some of these simulators will be described in section 2.3. Utilizing simulators in the planning stage of the well, is important for many reasons, including (Nilsen, 2014; Schubert et al., 2004);

- Minimize the risk of an unwanted situation
- Analysis of different well control events
- Estimate the most effective killing mechanism
- Study the hydraulics aspects associated with the killing operation
- Evaluating procedures

Therefore, advanced well control simulators, like the OLGAs computer software, have become important tools in the petroleum industry (Lage et al., 2006).

As mentioned earlier, the operators are required to develop a contingency plan, including a primary kill strategy. The kill strategy should as a minimum include a plan for both drilling a relief well and for capping (Yuan et al., 2014). According to (NORSOK D010, 2013), the plan for drilling a relief well shall comprise of number of relief wells needed, clear description of the killing method, simplified relief well path, etc. During a blowout kill operation through a relief well, depending on the technique, there are limitations that needs to be accounted for, to successfully kill a blowout. The mobile offshore rig used for drilling a relief well may have limits when it comes to pumping rates, available horsepower and storage capacity for kill mud (Rinde et al., 2016; Lage et al., 2006). In addition, it is important to optimize the kill mud density. In order to maintain the static balance in the blowing well, the kill mud density must be high enough. During a

kill operation with high pump rates, the friction pressure may be very high due to the frictional pressure loss in the relief well annulus and in the kill lines. With such high friction pressure, the pump capacity may be exceeded. In such cases, one of the following actions should be conducted (Yuan et al., 2014);

- Pumping down drillstring and annulus simultaneously
- Repositioning drillstring
- Considering different bottomhole assembly (BHA) and drill pipe configurations

Another approach would be to install a Relief-Well Injection Spool (RWIS) on the relief-well wellhead beneath the BOP. This device will provide additional flow connections into the wellbore, making it possible to deliver increased pump capacity. This may ensure a potential blowout to be killed by only one relief well, which is why RWIS is an important tool in blowout contingency planning (Oskarsen et al., 2016).

It is vital to wait with the intersection process between the target well and the relief well, until all the mud pumps and kill fluids are lined up and ready for the killing operation. In order to successfully control the blowout, it is important that the pump capacity and formation fracture pressure are not exceeded. Therefore, it is important to stage down the pump rate as the pump pressure is approaching the limit (Yuan et al., 2014). In addition, it is important to evaluate the mobilizing time for a relief well rig in the contingency plan, as the relief well drilling should start no later than 12 days after the decision of drilling a relief well was taken. In a similar manner, a plan for capping and containment of a blowing well should also be conducted (NORSOK D010, 2013).

Blowout control equipment

There are different well control equipment installed in a well to prevent and control a blowout. During the drilling operation, these include (Belayneh, 2018a);

- Changes in pit level is an indication of influx of formation fluids
- The BOP seals of the well in case of a kick

- The choke is used to control the well pressure
- The chokeline can be used to transport well fluids out of the well if the BOP is closed
- A separator is used to separate the gas from the mud

An illustration of the blowout control equipment usually installed in a well is shown in figure 2.5.

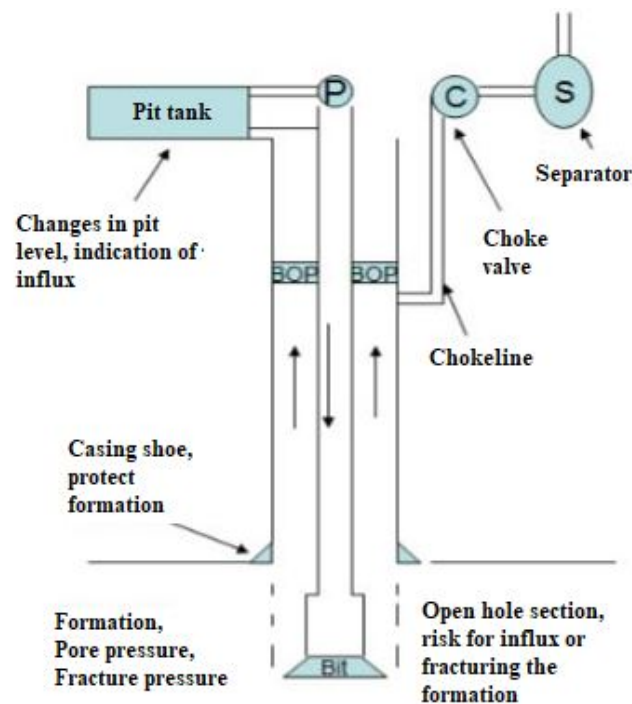


Figure 2.5: Well control equipment (Fjelde, 2016).

As mentioned earlier, the BOP is installed in a well with the purpose of acting as a secondary barrier. The BOP stack may comprise of two types of preventers, namely the ram BOP and the annular BOP (Belayneh, 2018b). The annular BOP is often closed first, and is more flexible on which pipe size it can close around. As shown in figure 2.6, the annular BOP is mounted at top of the BOP stack. The rams usually work as a backup in case of a failure in the annular BOP. There are various types of rams available, including pipe rams that close on a fixed pipe size, and the shear/blind rams that can close the hole without pipe as well as shear the string. The main difference between these two types of preventers, is that the

ram mechanically moves towards the center of the wellbore in order to restrict flow, while the annular type close around the drill string (Belayneh, 2018b).

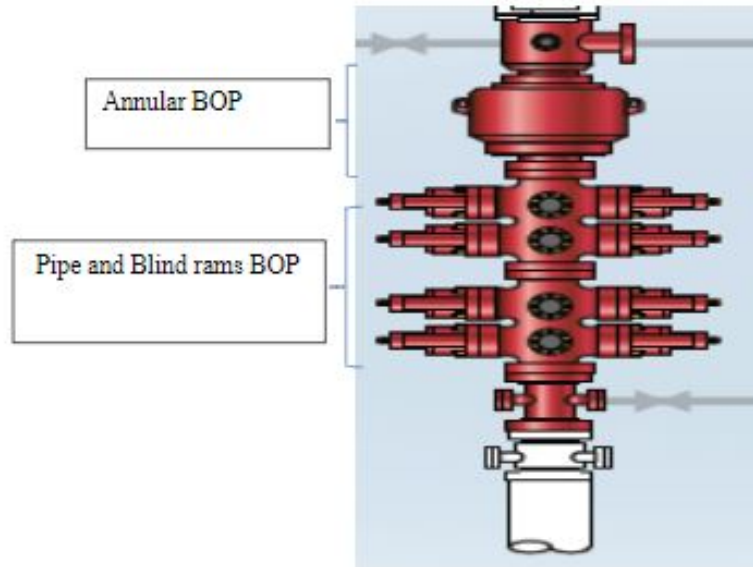


Figure 2.6: A schematic of a BOP (Belayneh, 2018b).

The PSA has specific regulations operators have to follow regarding well control equipment during a drilling operation. *The Facilities Regulations* section 49, states that well control equipment should be designed and capable of activation such that it ensures both barrier integrity and well control (PSA, 2019c). It is also stated in the same regulation, that the operators should have a contingency plan in place to divert uncontrolled flow of hydrocarbons away from the facility, if a BOP is not already installed in the well (PSA, 2019c). In order to fulfil the Norwegian barrier requirements, it is important to follow NORSOK D010 (2013) as a guide when planning a well. This is vital to ensure that all the necessary blowout control equipment are included in the installation. In general, operators in Norway, UK and US GoM, are focusing on the two-barrier principle, meaning that it should always be at least two well barriers active in a well (Holand, 2017).

2.2.6 Blowout Spill Consequences

Due to the severity of a blowout and its corresponding negative effects, blowout prevention has become a top priority in the oil and gas industry. This catastrophic event, can lead to large oil spills, causing severe damages to the environment,

give great financial loss, and even personnel injuries and casualties (Liu et al., 2015). The financial loss is associated with loss of valuable hydrocarbon reserves, unexpected cost related to the cleaning up process, and damages to equipments. As a consequence of a blowout, the credibility of an operator or the personnel may be harmed, as well as a potential time-delay for drilling operations in near area (Arild et al., 2008).

Environmental Risk Analysis, Oil Spill Response Analysis (OSRA), and Total Risk Analysis (TRA), are all examples of risk analysis operators on the NCS have to conduct, by law, in order to quantify and predict the risk of any petroleum activity (Karlsen and Ford, 2014b). According to Karlsen and Ford (2014b), a basic ERA consist of a combination of probabilities for oil spill scenario and corresponding blowout rates and duration, as well as potential environmental damages. The operators utilize such an analysis with the intention of determining if an activity is acceptable or not, by evaluating the potential environmental risk against their own acceptance criteria for risk (Nilsen, 2014). As mentioned earlier, the petroleum industry is regulated by laws. In Norway, these laws and regulations are controlled and supervised by PSA (PSA, 2019a).

An increasing focus on preserving and protecting the environment, in combination with the industry performing drilling operations in more challenging areas, reduces the margins within well control. A blowout represent one of the major treats associated with drilling, completion, maintenance and production of an oil field (Liu et al., 2015; Arild et al., 2008). Because of the many hazards this incident may cause, blowout represents a substantial component in an ERA to dimension the appropriate oil spill emergency preparedness (Nilsen, 2014). Calculations of potential blowout rates, volumes and duration are needed as input in such analysis. In fact, blowout calculations form the basis for oil spill drift forecast, giving reasonable indications of the amount of oil that will be present in the environment and the recovery time (Arild et al., 2008). Figure 2.7 shows a typical blowout risk analysis chain employed in the various risk analysis.



Figure 2.7: *Blowout risk analysis (Arild et al., 2008).*

According to Arild et al. (2008), the blowout risk related to petroleum activity can in simplicity be described as the following;

- *Blowout probability*
- *Blowout rate uncertainty distribution, including differentiation of sea bottom and topside releases*
- *Blowout duration uncertainty distribution*

Although blowouts have become a rare phenomenon due to advancement in drilling and well intervention technology, the consequences of a potential blowout are of too high magnitude to simply ignore. By looking at the BP's Macondo accident in the Gulf of Mexico April 2010, one clearly see the importance of preventing a blowout. In that specific case, a well control situation resulted in a surface blowout with 11 casualties and enormous damages to the environment. These consequences were a result of over 4.9 million barrels of oil spilled to the surroundings. It took BP several months to kill the blowing well, and regain control of the situation (National Commission, 2011). Similar consequences can be found from other accidents, which shows why it is of uppermost importance for all operators to prevent and minimize the risk of having an uncontrolled release of formation fluids to the surroundings.

2.2.7 Blowout Statistics

According to a report published by the UNEP Industry and Environment agency (UNEP, 1997), the probability of shallow gas blowouts in exploration wells were approximately one in every 200 wells. This statistic was based on data collected from USA, Gulf of Mexico and the North Sea (Oudemans, 2007), and demonstrate how rare phenomena a blowout is. In addition, SINTEF has created a database

recording blowouts from the US Gulf of Mexico and the North Sea, which is presented in figure 2.8.

AREA	Dev. drlg	Expl. drlg	Unk. drlg	Comp- pletion	Work- over	Production		Wire- line	Aband- oned well	Un- known	Total
						External cause*	No ext. cause*				
US GoM OCS	58	59	1	14	46	14	11	6	2		208
	27.9%	28.4%	0.5%	6.7%	22.1%	6.7%	5.3%	2.9%	1.0%	0.0%	
UK, and Norwegian waters	11	33	1	7	14	1	5	10	2		84
	13.1%	39.3%	1.2%	8.3%	16.7%	1.2%	6.0%	11.9%	2.4%	0.0%	
Total	69	92	2	21	60	15	16	16	4	0	292
	23.6%	31.5%	0.7%	7.2%	20.5%	5.1%	5.5%	5.5%	1.4%	0.0%	

* External causes are typical; storm, military activity, ship collision, fire and earthquake.

Figure 2.8: Amount of blowouts experienced during different petroleum activities (SINTEF, 2017).

The figure above presents an overview of blowouts occurrence by operational phase, and shows a total of 292 blowouts from 1 January 1980 to 31 December 2014 (SINTEF, 2017). From figure 2.8, one notice that blowouts are most frequent during drilling, and especially during exploration drilling. Although the statistics above shows that blowouts do not occur frequently, the possible consequences of such an event is of too high magnitude to simply ignore. This is the main reason for blowout modelling being such an important topic in the oil and gas industry. Hence, there is an increasing focus in the industry to develop tools with the purpose of simulating blowout scenarios.

2.3 Blowout Modelling

In oil production it is essential that the formation fluids flow vertically through the tubing. These fluids are initially present in a high pressure and porous reservoir. When the hydrocarbons are flowing upwards to the surface, the pressure decreases. As a result, the light hydrocarbons dissolved in the liquid gets released. In a high-pressure environment, gas preferentially dissolves in oil rather than in water. For this reason, the mixture of fluids in the reservoir may only contain liquid, like connate water and oil with dissolved gas. An oil production well forms

a complex multiphase flow system which can be predicted by using numerical simulators (Gomes, 2016).

In light of developing a new steady state flow model, it is necessary to study already existing simulators. There are generally two types of numerical simulations software available related to blowout modelling. One simulator focuses on killing a blowout, and how this should be done hydraulically. The second type of simulator focuses on estimating the rate, volume and duration of a blowout, hence studying the oil spill. The latter one, provides results that can be used in an ERA and in oil spill emergency response plan (Arild et al., 2008; Karlsen and Ford, 2014b).

When conducting blowout calculations, there are several factors to consider, including flow rate, release point, flow path and flow medium. All these parameters are unknown and come with a high degree of uncertainty (Karlsen and Ford, 2014b; Nilsen, 2014). Because of the wide variety of possible combinations of these parameters, all blowouts are assumed to be different and need to be treated as such.

A statistical-based model seeks to compare a blowout to one that has occurred in the past, and thus base blowout modelling on historical data. The quantity of the flow rate of formation fluids has a direct influence on the total amount released, and thus also a great impact on the potential damage of the environment (Nilsen, 2014). Conventionally, conservative numbers for uncertain reservoir parameters have been used for calculating blowout rates, consequently only introducing rates based on historical data. However, as every blowout scenario is to be considered unique, this model is not considered to be optimum. Another approach is to only address one or few conservative worst case scenarios, and calculate the WCD blowout based on this. These described methods may generate unrealistic scenarios, thus either overestimate or underestimate the risk of a possible blowout (Arild et al., 2008). For this reason, numerical simulators based on probability distributions, have been introduced for modelling potential blowout rates, duration and volumes (Karlsen and Ford, 2014b).

There are several other factors affecting the characteristics of a blowout. The source for the blowout, namely the reservoir, and its size, in combination with the duration of a blowout, determines the amount of fluids released. Whether the emission of fluids are oil, gas, condensate, water or a mixture of these, also has a great impact on the possible damage a blowout may cause (Nilsen, 2014). Furthermore, the flow path in which the uncontrolled hydrocarbons flow through from reservoir to discharge point, and restrictions in the flow path, also have an influence on the characteristic of a blowout.

As mentioned earlier, blowout calculations and simulations plays an important role in the risk analysis operators conduct before performing any activity offshore. It is essential to avoid such an catastrophic event, but also minimize consequences of a blowout if it occurs. This means taking all kinds of blowout scenarios into considerations (Nilsen, 2014). The blowout rate is a direct measure of the physical, economic and environmental harm caused by a blowout, as well as a great indicator for the amount of work required to regain control of the situation. This clearly shows the importance of developing simulators to estimate blowout parameters and possible consequences of oil spill, and the effort companies lays in this line of work.

There are currently no relevant international or national standardized methodology relevant for ERA in calculation of blowout rate, volume and duration. Therefore, in order to standardize nomenclature, procedure and documentation of blowout calculations, the Norwegian Oil and Gas Association (OLF) has established guidelines (Karlsen and Ford, 2014b; Nilsen, 2014). According to the OLF guidelines, the results should be presented in a probabilistic manner. This is vital in order to reflect the uncertainty in an ERA. Otherwise, the uncertainty will not be reflected in the final results, and the level of detail will be compromised (Nilsen, 2014).

2.3.1 Models for Analysing Blowouts

As of today, there are various software models available to predict the blowout parameters, calculate blowout kill parameters, and estimate the consequences of an oil spill. According to Yuan et al. (2014), these include Santos (2001), Lage et al. (2006), Oudeman (2007), and BlowFlow (Ford, 2012). Such models play an essential role in evaluating how blowouts can be controlled or for oil spill preparedness planning, depending on the objectives behind each model (Liu et al., 2015). These models have been developed with different intentions, and may be categorized depending on the purpose, which is presented in figure 2.9.

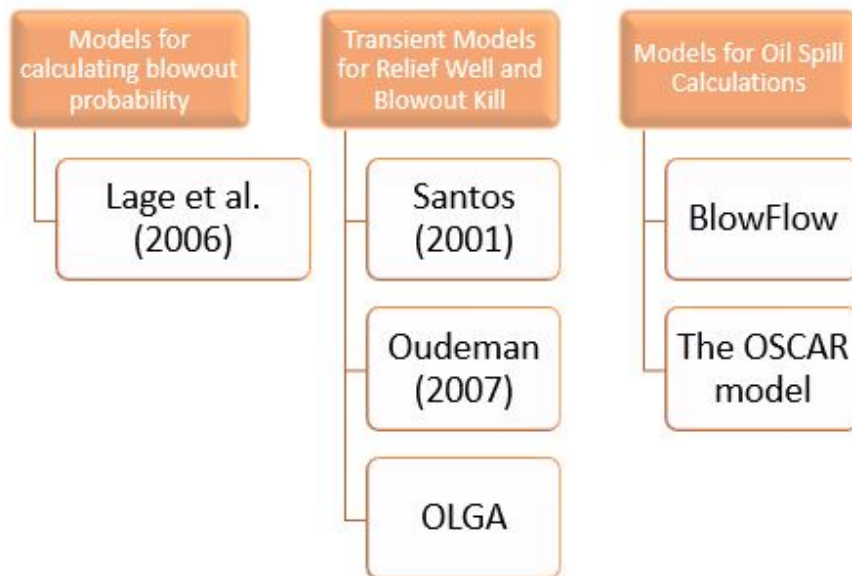


Figure 2.9: *Models for analysing blowout, categorized by their purpose.*

Models for calculating blowout probability

Lage et al. (2006)

Lage et al. (2006) developed a methodology to perform analysis of the risk of blowouts. In order to quantify the probability of having a blowout, the model is based on an innovative approach that uses relevant empirical data in combination with expert estimates. This is an extension of the Bayesian approach, which is widely used in the petroleum industry (Lage et al., 2006). The model comprise of an extensive Hazard and Operability analysis, including a Quantified Risk

Assessment (Yuan et al., 2014). In addition, Lage et al. (2006) used the OLGA software to simulate different flowing conditions with the purpose of analysing consequences of a blowout (Lage et al., 2006).

Transient models for relief well and blowout kill

Santos (2001)

This is a numerical model created with the purpose of analysing blowouts in ultra deep waters. The model simulates blowout rate and dynamic kill technique using a relief well, where the model is dependent of time (Yuan et al., 2014). Santos (2001) comprises of two mathematical models, the wellbore model and the gas reservoir model, respectively. These models predicts the well pressures and flow properties during a gas blowout by implementing a transient model that consider multiphase flow behaviour in the well (Santos, 2001). As the two models are linked together, it is possible to calculate the corresponding flow rate for a certain bottomhole pressure (Yuan et al., 2014). This transient model was implemented in the FORTRAN software, where simulations were performed to study different blowout scenarios (Santos, 2001).

Oudeman (2010)

Oudeman first developed a simulator in 1998, based on the nodal analysis for estimating the blowout rate by matching the inflow performance of the well to the vertical lift performance (VLP). However, the simulator had lack of accuracy in the calculated blowout rates (Oudeman, 2007). Therefore, an improved model was published in 2010, with the focus on considering tubular configuration as the flow path. In the modified model appropriate values for roughness were used instead of default values, making it possible to calculate blowout rates with higher degree of accuracy (Oudeman, 2010). This blowout simulator has been developed and validated with field data from the North Sea (Yuan et al., 2014).

OLGA Dynamic Multiphase Flow Simulator

This is a dynamic multiphase flow model utilized for simulating multiphase flow systems, developed in 1979 by the Institute for Energy Technology in Norway. In addition to being the first transient model develop for the petroleum industry, it

has also become an industry standard for modelling multiphase flow (Add Energy, 2018). This model and consequently software serves as a base for a variety of other software programs used in blowout analysis, and is currently being commercialized by Schlumberger (Schlumberger, 2019).

Models for oil spill calculations

The OSCAR model

This is a three-dimensional dynamic simulation tool for oil spill contingency and response, developed by SINTEF. This software presents an overview of hydrocarbon transport, oil spill and effects during a blowout, and can simulate the results of different response strategies (SINTEF, 2014).

BlowFlow

BlowFlow is a software tool and methodology developed by NORCE for risk-based evaluation of blowout scenarios in order to estimate blowout rates, volumes and duration. These calculations plays an important role in oil-spill preparedness planning (Yuan et al., 2014). Unlike the other described simulators, this model utilizes a stochastic modelling approach, e.i. Monte Carlo Simulations, where probability distributions for a certain number of inputs are used instead of fixed values (Karlsen and Ford, 2014a; IRIS, 2015). An illustration of the BlowFlow model framework is shown in figure 2.10. The output of the model are blowout rate, duration and volume, presented as statistical distributions. The software therefore takes into account the high uncertainty related to several reservoir input parameters (Karlsen and Ford, 2014b). This is one of the major reasons for why this specific simulator differs from other available models for analysing blowouts. The model is currently being commercialized by Oliasoft. As this thesis is carried out in cooperation with Oliasoft, the BlowFlow engine will be described in detail in chapter 3.

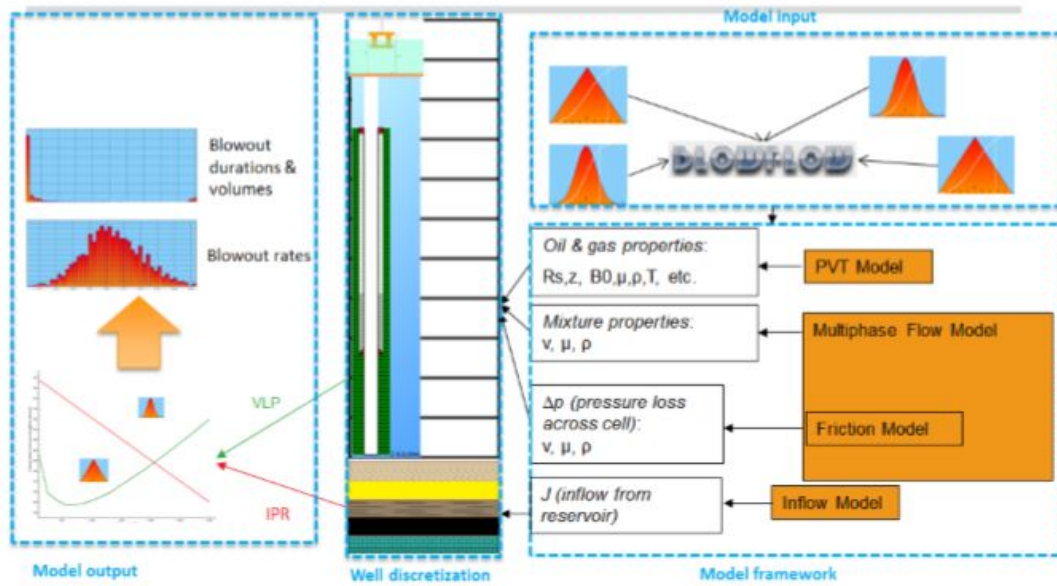


Figure 2.10: *BlowFlow model framework (Karlsen and Ford, 2014a).*

Computer programs for blowout modelling

OLGA Well-Kill

This is an upgraded version of the OLGA simulator, which focuses on well control. The simulator was created with the intention of comparing various kill scenarios for a blowout that occurred in the North Sea (Rygg et al., 1992). OLGA Well-Kill is a multiphase flow software designed to simulate dynamic kill operation as well as well intervention methods. The results from this simulator plays an important role in contingency planning, as well as in actual blowout situations (Rygg et al., 1992). OLGA Well-Kill is currently being offered exclusively by Add Energy, and has been widely used all over the world. The program has been applied on 70 live blowouts, including both the Macondo and Montara blowouts, and has been used in over 1200 blowout contingency plans (Add Energy, 2018).

Oliasoft Blowout Simulator

This simulator is built on the BlowFlow engine. The purpose of this program is to compute potential blowout rates, volumes and durations. As of today, the computer program represents the only solution capable of performing stochastic blowout calculations in accordance with the latest guideline from OLF and NOR-SOK D-010 (Nilsen, 2014). The outcome of such a simulator is vital in oil spill

preparedness planning as well as in actual blowout situations (Oliasoft, 2019). The blowout simulator is integrated as a module in the well planning software, Oliasoft WellDesign. This software include modules for well trajectory, casing design, tubing design and conductor analysis, which makes it possible for the operators to have control over every aspect related to the well planning (Oliasoft, 2019).

Drillbench Blowout Control

This blowout control software is also powered by the OLGA Dynamic Multiphase Flow engine. The simulator may be employed to perform dynamic analysis of possible blowout scenarios, as well as perform well kill simulations (Schlumberger, 2019). The software was in the past, before being commercialized by Schlumberger, referred to as OLGA Advanced Blowout Control (ABC). Yuan et al. (2014) conducted a study of WCD blowout scenarios in ultra deep waters by using the software OLGA ABC to simulate the dynamic wellbore temperature and calculate relief well hydraulic parameters. The study evaluated operational parameters during the kill process in order to optimize the blowout control without exceeding the operational window (Yuan et al., 2014).

These mentioned software engines are widely employed in the industry, either directly or as a core for other simulators. One example, is the well-known company Wild Well, which bases their well control modelling on the OLGA and Drillbench software engines (Wild Well, 2019). As mentioned above, Add Energy uses the OLGA Well-Kill software in their analysis and service. This clearly shows how frequent such simulators are used in the oil and gas industry today. In order to show how it is possible to use blowout modelling to perform oil spill calculations, the Oliasoft Blowout Simulator will in this thesis be used to present a realistic blowout simulation example, which is presented in chapter 4.

3. BlowFlow

As this thesis is carried out in cooperation with Oliasoft, this chapter will describe the BlowFlow model in more detail. The idea is to present one approach of blowout modelling, and show how it is possible to conduct simulations of blowout rate, volume and duration, for oil spill preparedness planning. The engine will be used in chapter 4 to present a simulation example.

BlowFlow is a software tool and methodology created by NORCE for risk-based evaluation of blowout scenarios, to measure blowout rates, durations and discharged volumes. The result from such an evaluation can be used to estimate the consequences and effects of a blowout, in dimensioning of oil spill preparedness planning as well as in emergency response planning. All in which plays an important part as input in an ERA (Arild et al., 2008).

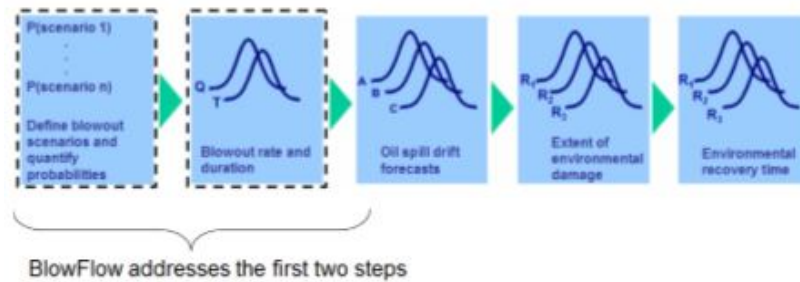


Figure 3.1: *BlowFlows role in an ERA (Karlsen and Ford, 2014a).*

BlowFlow addresses the first two steps in an ERA, shown in figure 3.1. The engine takes into account the uncertainty of the input parameters, and thus simulates a probabilistic blowout. As most of the available software engines regarding blowout analysis only focuses on deterministic simulation, where uncertainties are not taken into account, the development of BlowFlow has the possibility to make a great impact on the petroleum industry (Karlsen and Ford, 2014a).

3.1 Design Philosophy

The BlowFlow engine is based on some principles, which were used to guide the evolution of the methodology. According to Arild et al. (2008) these principles include;

- *Geological, technical and operational conditions that affect blowout rate and duration should be reflected in the analysis*
- *There should be a consistent way of capturing and handling of uncertainties*
- *There should be a pre-defined list of relevant background information that will be used in the analysis*
- *The presentation and communication of results should be simple and in non-expert format*
- *The results from the analysis should be transparent and provide guidance with respect to which factors are most important*

The main purpose of the software is to perform oil spill calculations. However, other important aspects of this methodology include enhancing the communication between different companies and give decision makers stronger confidence with respect to how to reduce the consequences of a potential blowout. In fact, the tool is meant as a cross-disciplinary tool for communication between people from different disciplines (Ford, 2012). The model aims to help standardize methodology, nomenclature and documentation related to blowout modelling (Arild et al., 2008). For these reasons, the BlowFlow engine meets the recommendations presented in the OLF report (Nilsen, 2014).

Unlike other described blowout simulators (see section 2.3.1), BlowFlow takes into account the high uncertainty related to numerous reservoir input parameters (Karlsen and Ford, 2014b). By utilizing a predictive Bayesian approach, which employs probability distributions for a certain number of inputs instead of fixed numbers, it is possible to express the uncertainty when calculating the blowout rates, volumes and duration (Arild et al., 2008; IRIS, 2015). Hence, the output of the model is presented as statistical distributions.

In order to include the relevant parameters regarding blowout analysis, the pressure, volume and temperature (PVT) model, the multiphase flow model, and the inflow model are implemented in the simulator as correlations (Karlsen and Ford, 2014b). This creates a complex system which needs to be dealt with numerically. To numerically solve these equations, a Monte Carlo Simulation is integrated in the framework of the model (Arild et al., 2008). The Monte Carlo simulation process can be seen in figure 3.2.

A stochastic modelling approach is utilized, and due to the uniqueness of every field, well and drilling operation, the majority of input variables are assessed based on expert judgement rather than historical data from other wells (Karlsen and Ford, 2014b). According to Karlsen and Ford (2014b), the use of probability parameters, based on expert assessment, is a unique feature, and has never before been successfully implemented in a software tool calculating blowout rates, duration and volumes.

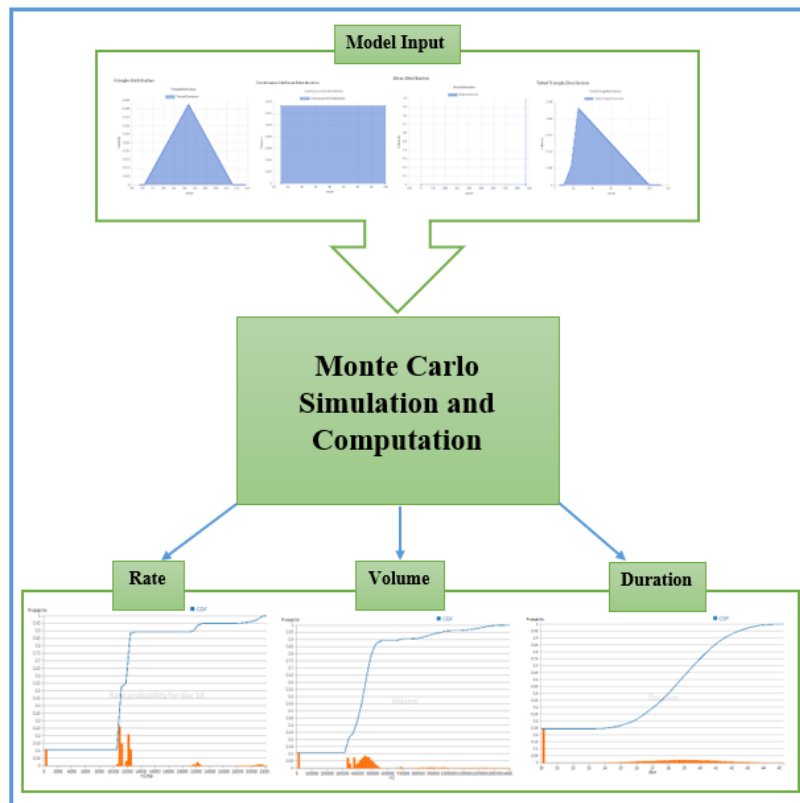


Figure 3.2: *The Monte Carlo Simulation process in BlowFlow.*

3.2 Model Structure

The BlowFlow engine is based on steady state conditions, where multiphase flow is considered. In order to increase the range of application, the engine has implemented a variety of models (Karlsen and Ford, 2014b). The figure 3.3 shows the model structure of the BlowFlow software. However, the software comprises of three main models (Ford, 2012), namely;

- **Blowout flow rate model**, based on the PVT Model, the inflow model and the outflow model
- **Blowout duration model**
- **Blowout discharge volume model**

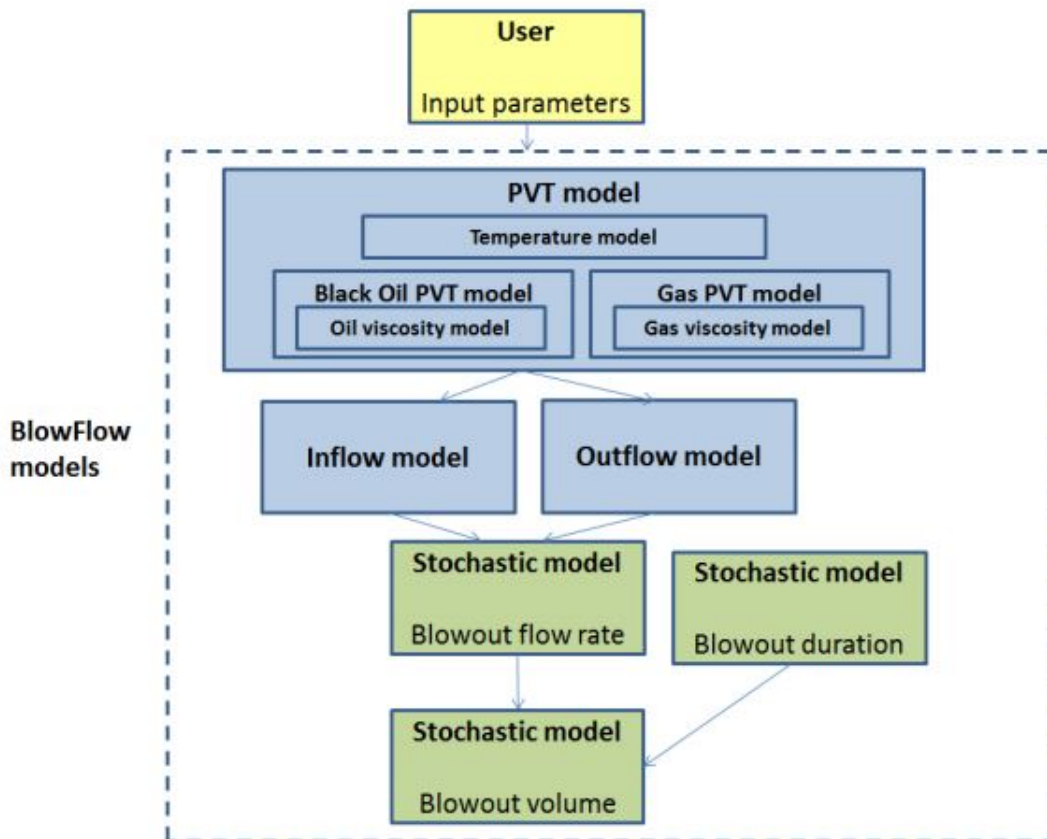


Figure 3.3: The BlowFlow model structure (Ford, 2012).

3.2.1 PVT Model

There are four available PVT models in BlowFlow, depending on different empirical correlations and the fluid type. The software uses a Black Oil PVT model to calculate the necessary fluid properties of oil. This PVT model is based on empirical correlations, including Vasquez-Beggs, Standing and De Ghetto (Ford, 2012). The Standing and Vasquez-Beggs correlations are employed for light and medium oils, while the De Ghetto model is used for heavy and extra heavy oils (Karlsen and Ford, 2014a). These PVT models contain equations for (Ford, 2012);

- Bubblepoint pressure, P_b
- Solution ratio, R_s
- Oil formation volume factor, B_o
- Oil compressibility, c_o

The other general oil properties, including oil density and gas-oil interfacial tension, are equal for all models. Moreover, there is only one PVT model available in the software to compute the essential fluid properties of gas. The Gas PVT model calculates the following parameters (Ford, 2012);

- Gas density, ρ_g
- Gas formation volume factor, B_g
- Gas isothermal compressibility, c_g
- Pseudocritical temperature and pressure, T_{pc} and P_{pc}
- Pseudoreduced temperature and pressure, T_{pr} and P_{pr}
- Pseudoreduced gas density, ρ_{pr}
- Gas compressibility factor, Z
- Gas-condensate interfacial tension, σ_{gc}

Although the oil and gas viscosity models are actually part of the Black Oil PVT model and Gas PVT model, respectively, the BlowFlow engine define them as separate models. This is done with the intention of increasing the flexibility in

calculating these parameters. There are four available oil viscosity models, including Vasquez-Beggs, Standing, De Ghetto and Egbogah, while there are two available gas viscosity models, namely Lee and Lee Modified (Ford, 2012). The author refers to Ford (2012) for additional information about these correlations.

Furthermore, a simple temperature model is integrated in the PVT model. This model converts measured formation temperatures into flowing well temperatures. It is therefore necessary to define the surface and seabed temperatures, as well as the geothermal temperature gradient. Because the BlowFlow software is based on steady state conditions, the model neglects temperature changes over time (Ford, 2012).

3.2.2 Inflow Model

The inflow model is based on a modified method of estimating the productivity index, presented by Larsen (2001). Stochastic inputs defined by the user of the software are sampled and processed by the reservoir model in order to produce the IPR curve for both oil and gas (Karlsen and Ford, 2014a). BlowFlow provide different expressions for the productivity index depending on the type of model chosen, including (Ford, 2012);

- **Oil-Basic:** Basic reservoir model, which is used if the productivity indices are not available. This model is only valid for oil inflow.
- **Oil-Fractured well:** Extended version of the Oil-Basic Model which may be applied for a fractured reservoir.
- **Explicit:** The simplest inflow model available in BlowFlow. Then the productivity index for the predefined penetration scenario is set directly as probability distributions. This inflow model works for both oil and gas.

In addition to the explicit model also working for gas, the software consist of a reservoir model for gas deliverability (Karlsen and Ford, 2014a). This is a model for single-phase gas or gas/condensate, based on pseudo pressures. It contains the same inputs as the Oil-Fractured model (Ford, 2012).

3.2.3 Outflow Model

The outflow model is a two-phase flow model based on steady state conditions, which may be applied for both oil and gas. The outflow model uses a nodal analysis technique to compute the blowout rates. The well is then discretized into nodes. As the surface pressure and temperature are known, an initial guess is made for those variables in the next cell. All necessary calculations are then performed for each of the segments (Ford, 2012; Karlsen and Ford, 2014b). Hence, the calculations are performed from the top of the well and downwards. Once performed for all cells throughout the well, and the computed pressure drop across the cells is equal to the initial guess within some margin, the VLP curve is established. By using the VLP curve in combination with the IPR curve produced from the inflow model, the flow rate may be estimated with the help of the intersection method (Karlsen and Ford, 2014a).

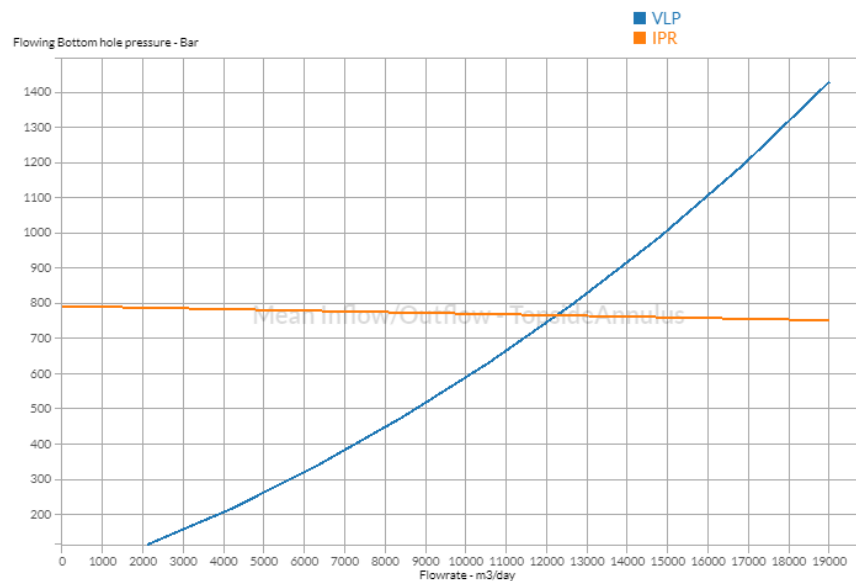


Figure 3.4: A VLP and IPR curve showing the outflow/inflow from annulus to surface and the intersection point.

There are three available models in BlowFlow for calculating the outflow. The multiphase flow correlations include Hagedorn-Brown for oil and gas in vertical wells, Beggs and Brill for oil and gas flow in horizontal or inclined wells, and Gray for vertical flow in gas-condensate wells (Ford, 2012).

3.3 The BlowFlow Analysis Process

The BlowFlow analysis process consist of three steps; Assessment of input data, BlowFlow analysis (model), and conducting a thorough evaluation of the results (Ford, 2012). These three phases make up the work process used in the tool, shortly described in figure 3.5.

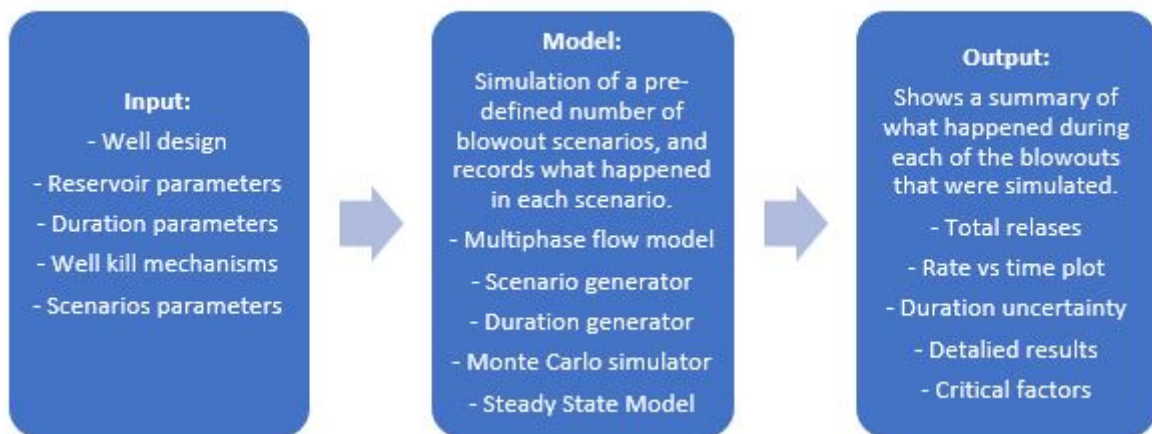


Figure 3.5: *The BlowFlow work process (Arild et al., 2008).*

3.3.1 Assessment of Input Data

The BlowFlow software requires input on a large number of variables. The first step in the BlowFlow analysis, which is also the most time-consuming part of the process, is to conduct a precise evaluation of the input data (Arild et al., 2008). Although many of the input parameters required in the simulator can be obtained from relevant documentation related to the drilling operation, most of the variables needs to be defined based on historical data or expert judgement, or a combination of both (Ford, 2012). An overview of the most essential input categories required in the BlowFlow simulator are presented in table 3.1.

Table 3.1: *Input parameters required in BlowFlow (Arild et al., 2008).*

Category	Sub-category
Reservoir	Fluid Temperature gradient Reservoir zones PVT models Multiphase flow models
Well Design	Platform Architecture Drill string Survey
Duration	Capping Relief well Bridging Natural cessation
Probabilistic scenarios	Blowout flow path Release point Penetration depth Bit location BOP opening

Input variables comprises of both certain and uncertain parameters, which may be implemented in the software by the user operating the tool. In general, one distinguishes between two types of inputs, namely probabilistic and deterministic parameters (Karlsen and Ford, 2014a). Probabilistic parameters are represented by single probability values or probability distributions in order to perform an assessment of uncertain parameters, while the deterministic inputs are parameters not connected to uncertainty (Ford, 2012). Typically, the deterministic parameters are related to the architectural and geometrical design of the well, and the formation temperature gradient (Karlsen and Ford, 2014a).

A large number of the input reservoir parameters are highly uncertain, and may have a great impact on the results from an analysis. To deal with the uncertainty related to many of the blowout parameters, a stochastic modelling approach is implemented in the model. Then, probability distributions for a certain number of reservoir inputs are used instead of fixed numbers, which increases the accuracy of the blowout analysis (Karlsen and Ford, 2014b).

Blowout killing mechanism is an important factor in determining the blowout duration, and thus has to be selected before running the simulation. The pre-defined duration models covered in BlowFlow are relief well, capping, natural cessation and bridging. The user may implement the probability of success as well as duration, for each killing operation (Arild et al., 2008).

When entering data into the model, the user must choose an appropriate distribution model, that is, the distribution model that best represents the data for the actual well and the scenario. BlowFlow offers a variety of distributions types, including;

- Continuous Uniform Distribution
- Dirac Distribution
- Exponential Distribution
- Gaussian Distribution
- Piece Wise Linear Distribution
- Triangle Distribution
- Weibull Distribution
- Trapezium Distribution
- Tailed Triangle Distribution
- General Continuous Distribution

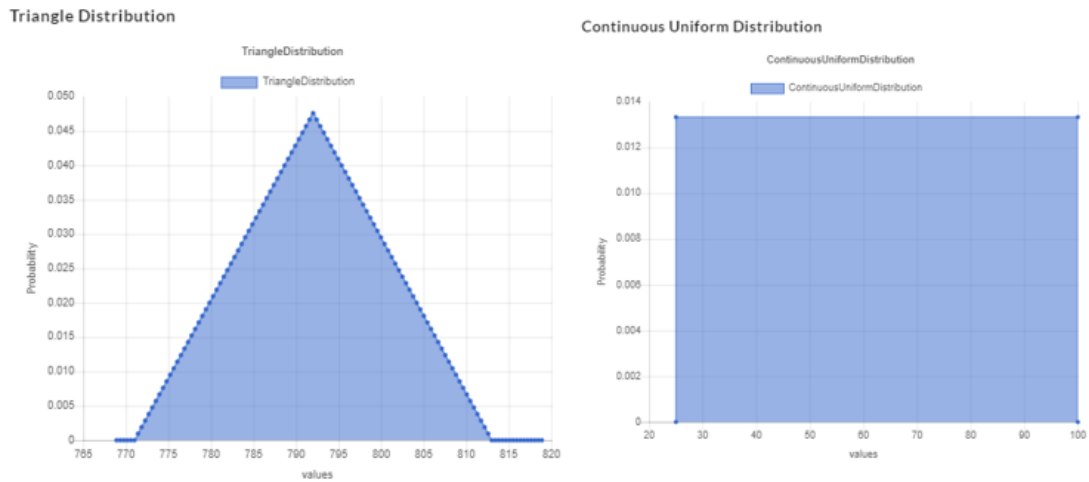


Figure 3.6: *Example of two types of distribution models available in BlowFlow. The first being a triangle distribution model, while the second is a continuous uniform distribution model.*

The author refers to Adams et al. (2010) and Newendorp and Schuyler (2000), for additional information regarding the various distributions models.

3.3.2 BlowFlow Analysis

After all the input parameters have been assessed, the next step in the process is to run the overall analysis, and generate all possible combinations of blowout rate, duration and volume (Arild et al., 2008). The basis for this analysis is the Monte Carlo Simulation, which is performed on a pre-defined number of blowout scenarios. The Monte Carlo process in BlowFlow is shown in figure 3.2. The result from each case is recorded and presented as a summary (Ford, 2012).

3.3.3 Evaluation of Results

The output of the simulation tool is a summary of each of the blowout scenarios expressed through probability distributions of rates, volumes and durations (Arild et al., 2008). The probability distributions are presented as density curves and cumulative distributions functions, where each value has an associated probability (Ford, 2012). In addition, the program presents a table of rates and volumes as mean, max, min, P10, P50 and P50.

- **Blowout rate:** Deterministic or stochastic values calculated for all defined

scenarios. This parameter is presented across time for the entire duration of the blowout.

- **Blowout duration:** Defined as the time until the blowout is successfully killed.
- **Blowout volume:** Estimate of the total volume of oil and gas released, calculated as the product of flow rate and duration.

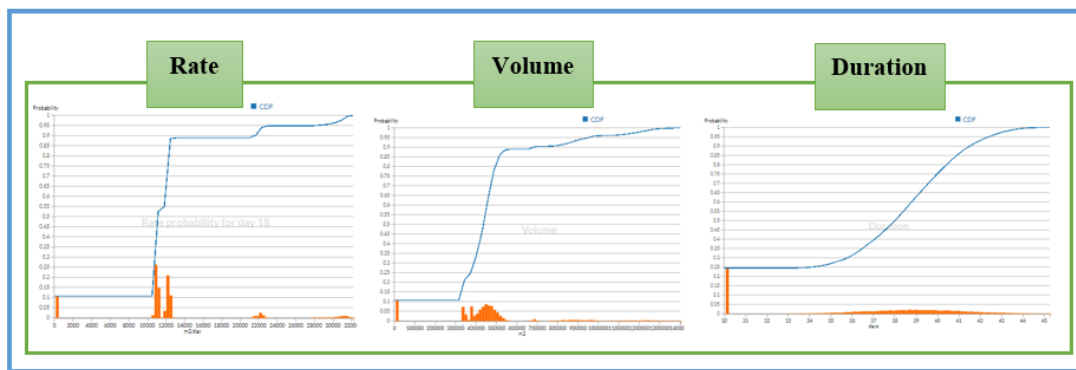


Figure 3.7: Example of result from the simulator, expressed through probability distributions of rates, volumes and durations.

The last phase of the BlowFlow work process consist of evaluating the results obtained from the BlowFlow analysis. An important part of this evaluation is to study the effect of risk-reducing measures, and use this study to adjust the input variables. Such re-analysis provides a basis for ranking and selection of candidate measures (Ford, 2012). It is these results of the simulation that will be used in oil spill preparedness planning as well as in actual blowout incidents.

4. Simulation in Oliasoft Blowout Simulator

This chapter will present a simulation example with the BlowFlow model as engine by using the Oliasoft Blowout Simulator. The case considers a vertical exploration well of 4400 m with a water depth of 975 m, under High-Pressure, High-Temperature (HPHT) conditions. All figures associated with this simulation example are obtained from the Oliasoft Blowout program.

4.1 Well Input

As described in chapter 3, the Oliasoft Blowout Simulator requires input on numerous parameters in order to perform the analysis. These properties must be carefully considered to be able to predict the possible blowout rate, volume and duration accurately. In order to present a realistic simulation example, the input data have been determined based on discussion with Kjell Kåre Fjelde, Gomes et al. (2015), Gabolde and NGUYEN (2006), and the Macondo Blowout in 2010 (Oldenburg et al., 2012).

4.1.1 Topside

The case is considering a subsea exploration well with water depth of 975 m. A drill floor elevation of 25 m is considered adequate. The wellhead is installed at the seabed, located 1000 m from the drill floor at the platform. For simplicity, the well trajectory is assumed to be vertical, mimicking an exploration well. The well is assumed to be 4400m deep. The figure 4.1 presents a schematic of the topside and water depth, shown in the program.

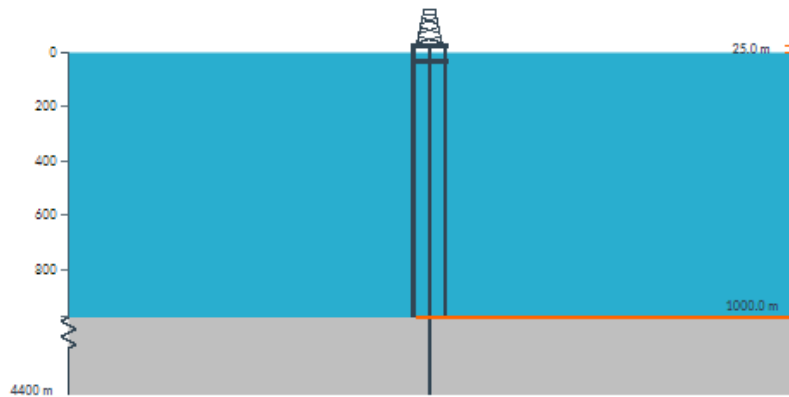


Figure 4.1: *Schematic representation of the platform and water depth.*

4.1.2 Formation

It is assumed that the drill floor temperature is 15 °C, and that the seabed temperature is 4 °C. These inputs are represented by single values. With a geothermal temperature gradient of 4.8 °C/100m, one may estimate the formation temperature for the well in question. This is calculated by the software, and presented as a graph, shown in figure 4.2.

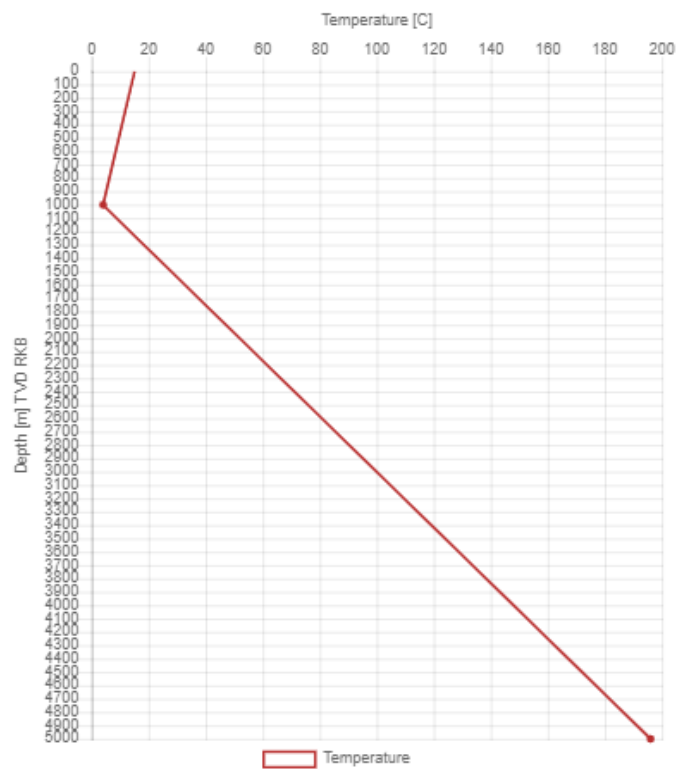


Figure 4.2: *Estimated formation temperature throughout the well.*

As explained earlier, the management of BHP is an important part of the drilling operation, and thus it is essential to study the pore and fracture pressure in a well. A plot of the pore pressure (outlined in blue) and the fracture pressure (outlined in yellow) gradients against depth are presented in figure 4.3. This figure also include the setting depth for the casings in addition to the mud weight used when drilling each section, which will be further elaborated in section 4.2.

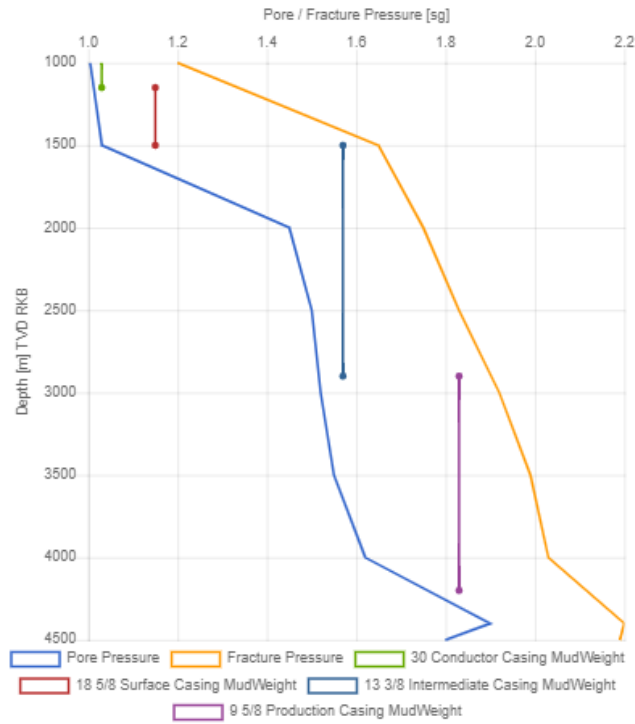


Figure 4.3: *The formation pressure profile, with corresponding casing setting depths.*

By studying the figure above it is reasonable to believe that there may be a reservoir present at approximately 4250 m. This assumption is based on the sudden increase in pore and fracture gradient at that depth. At this specific depth, the graph shows a pore pressure of 1.9 sg. This information can be used to calculate an estimate of the reservoir pressure, by applying equation 4.1.

$$P = \rho_f * g * h = 1.9 * 0.091 * 4250 = 792bar \quad (4.1)$$

where P is the pressure [bar], ρ_f is the formation density [sg], g is the gravitational constant and h is the well depth [m].

4.1.3 Drill String Data

It is necessary to define the drill string data in the program. For simplicity, one only consider drill bit and drill collar to be part of the bottomhole assembly. These components of the BHA and the drill pipe makes up the drill string program. Dimensions of the drill string components are presented in table 4.1. Although it is possible to define several properties regarding each drill string component, only the minimum required inputs will in this case be stated, including type, length, pipe body outer diameter (OD) and pipe body inner diameter (ID).

Table 4.1: *Drill string components and their dimensions.*

Type	Length [m]	Pipe body OD [in]	Pipe body ID [in]
Drill Pipe	4100	5	4.276
Drill Collar	99.5	6	3
Drill Bit	0.5	8.5	-

By using the average joint length and the total length of each component, the software calculates the number of drill string components needed in the well. However, as these are not required inputs in order to run a simple simulation, the program assumes one component of each type presented in the table above.

4.1.4 Reservoir Characteristics

The next step is to select a proper inflow model. The case is based on the inflow model, OilBasic, because there is no knowledge of the productivity index as well as this being the preferred model for vertical wells (Erichsen, 2019).

With the use of the OilBasic model, one need to define the permeability and the skin factor (Ford, 2012). These two factors are both crucial with respect to reservoir productivity. A skin factor of zero corresponds to no damage, and due to the high uncertainty related to this parameter, the well is considered to have little damage. Hence, the skin factor is set to 0.03, which is a default value from the software. In the light of the Macondo well, a permeability of 500 mD is considered

(Oldenburg et al., 2012). For simplicity, one consider the permeability to be the same regarding direction, and thus the kV/kH ratio is set to 1. This is also the value recommended by the Oliasoft Blowout Simulator user manual (Erichsen, 2019). Based on these reservoir input data, the BlowFlow engine calculates the corresponding productivity index of the reservoir.

The reservoir is assumed to comprise of both oil and gas, hence there will be multiphase flow in the well. The oil density for the well in question, is $870 \text{ kg}/\text{m}^3$, which yields an API grade of 31.14. According to figure 5.2, this is a characteristic black oil. The gas density, ρ_{gas} , is set to 0.919, while the air density, ρ_{air} , is assumed to be 1.225. The gas gravity, γ_{gas} , may be determined employing equation 4.2.

$$\gamma_{gas} = \frac{\rho_{gas}}{\rho_{air}} = \frac{0.919}{1.225} = 0.750 \quad (4.2)$$

This calculation yields a gas gravity of 0.750. In addition, the Gas Oil Ratio (GOR) is set to 600. These parameters are taken from the case study by Gomes et al. (2015). For simplicity, the presence of impurities in the reservoir, such as CO_2 , H_2S and N_2 , are assumed to be negligible. It is believed that the presence of small amounts of such gases will not have any major affect on the flow rate of uncontrolled fluids.

The reservoir area in this case is assumed to be equal to the BlowFlow default values, meaning that it is a rectangle-shaped reservoir with reservoir size (length and width) being set to 1000 m (Erichsen, 2019). In order for the OilBasic model to be valid, a rectangle-shaped reservoir is required (Ford, 2012). The reservoir pressure was calculated from equation 4.1 to be 792 bar. There is a high degree of uncertainty related to the reservoir pressure, which is why the pressure value is presented using a triangle distribution, T(771,792,813) bar. These values represents the assumed minimum, most likely and maximum reservoir pressure, respectively. The triangle distribution of the reservoir pressure is shown in figure 4.4.

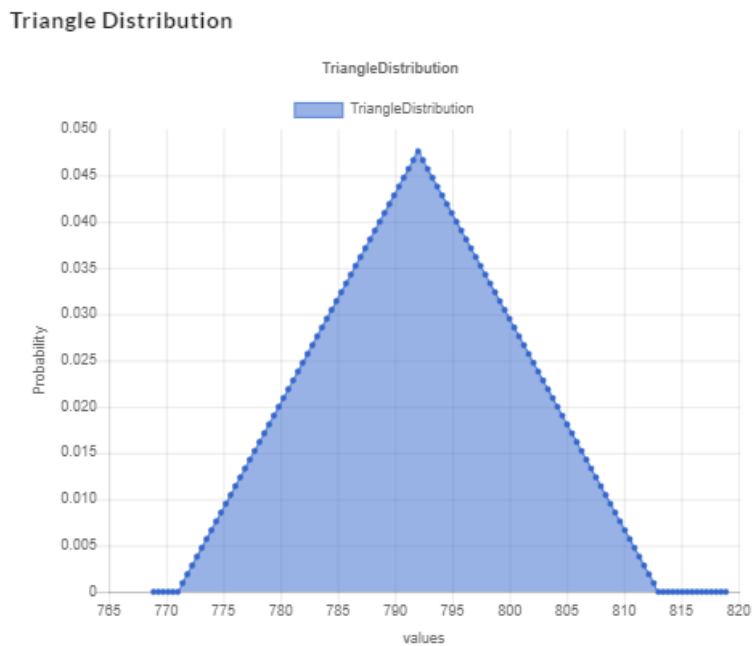


Figure 4.4: *Triangle distribution of the reservoir pressure.*

By studying the pressures throughout the well (see figure 4.3), one may expect the reservoir to be at a depth of approximately 4250 m. With the use of known surface temperature and seabed temperature, in combination with a geothermal gradient of 4.8 °C/100m, the reservoir temperature is estimated to be 167 °C. Such reservoir temperature, in combination with high reservoir pressure, yields a HPHT reservoir.

Although the total height of the reservoir zone may be an uncertain property, this parameter is presented as a dirac distribution. This yields a gross thickness of 65 m. Because the whole reservoir is assumed to contain hydrocarbons with no layers of shale, the net/gross ratio is set equal to one.

In order to give an overview of the input parameters regarding the reservoir, figure 4.5 summarize the input reservoir parameters used in this simulation example. Although, some of these variables are defined using probability distributions, such as the reservoir pressure, the most likely value is presented in the figure.



Figure 4.5: Reservoir zone properties with the use of OilBasic model.

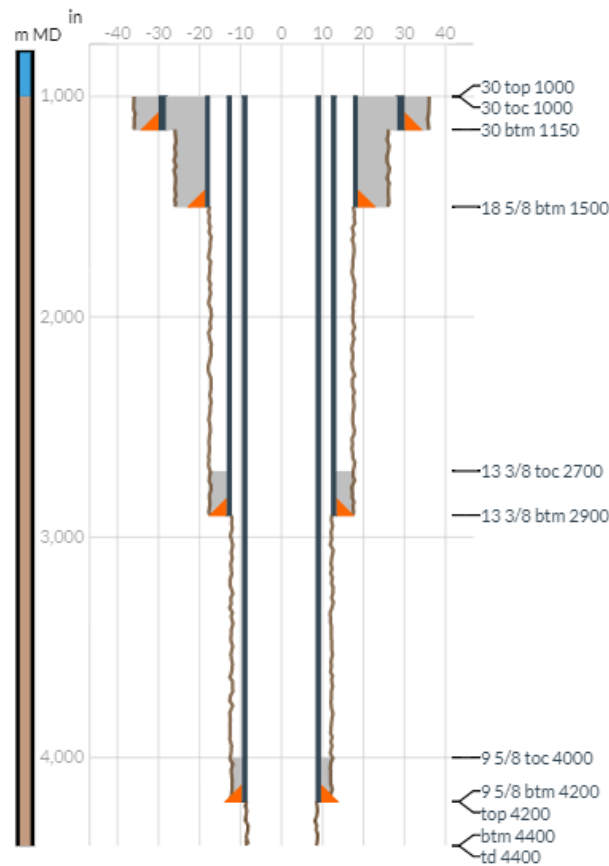
4.2 Casing Design

The casing program chosen for this well is presented in table 4.2. In addition, the software generates a schematic illustration of the wellbore, shown in figure 4.6. All casings are anchored from the wellhead at seabed, meaning that the top of each casing is at a depth of 1000 m. Both the conductor casing and the surface casing are cemented from casing shoe up to wellhead, while the intermediate casing and the production casing are cemented 200 m up from the casing shoe. Accurate size, nominal weight and grade of the casings are found using Gabolde and NGUYEN (2006). After the production casing has been set and cemented, one consider an open hole section of 200 m.

Table 4.2: *Casing program used as input in the Oliasoft Blowout Simulator.*

Hole section [in]	Casing	Size [in]	Setting depth [m]	Mud @ shoe [sg]	Top of cement [m]	Nominal weight	Grade
36	Conductor	30	1150	1.03	1000	309.7	X-56
26	Surface	18 5/8	1500	1.15	1000	97.7	K-55
17 1/2	Intermediate	13 3/8	2900	1.57	2700	77	C-90
12 1/4	Production	9 5/8	4200	1.83	4000	53.5	C-95
8 1/2	Open hole	-	4400	-	-	-	-

A riser with an OD of 24" and a ID of 22.5" is selected. The length of the riser is set equal to the wellhead depth, meaning that the riser is subjected from the platform with a length of 1000 m. The riser is attached to the top of the BOP system at the seabed.

**Figure 4.6:** *Wellbore schematic showing the casing program and open hole section.*

4.3 Trajectory

As mentioned earlier, a vertical exploration well is considered. Hence, the well trajectory is vertical with no inclination. The trajectory design with corresponding casings and riser is shown in figure 4.7.

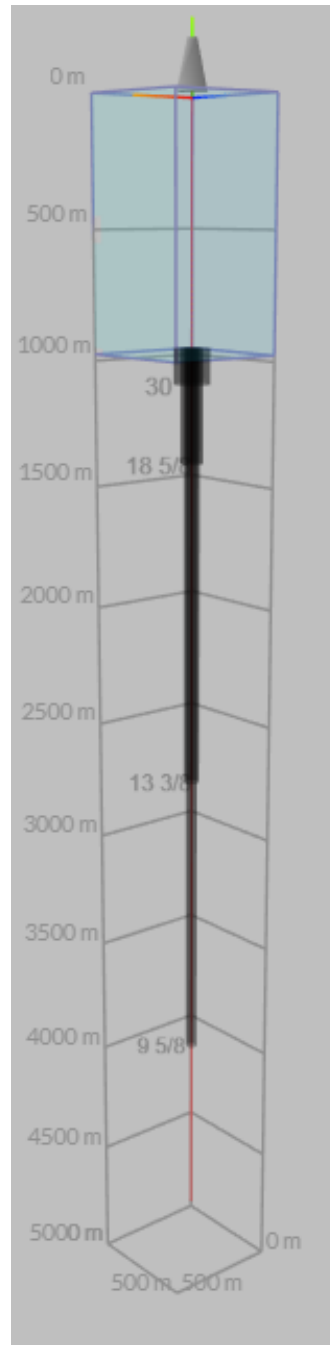


Figure 4.7: *Illustration of the vertical well trajectory.*

4.4 Blowout Simulation

4.4.1 Simulation Settings

As described in chapter 3, one need to specify which kind of empirical correlation models that should be applied in the simulation. In this specific simulation example, based on description from Vasques and Beggs (1980) and Erichsen (2019), the following correlations are considered;

- **Vasquez-Beggs PVT model:** Because we consider a medium oil with 31.14°API. This model is the preferred model for light and medium oil due to the model being based on results from more than 600 crude oil systems, and thus is applicable to a wider range of oil properties.
- **Hagedorn-Brown multiphase flow model:** Because we have a vertical well with both oil and gas flow. This model is the most widely used multiphase model for calculating VLP in the industry.
- **Vasquez-Beggs oil viscosity model:** Because we consider a medium oil with 31.14°API, and the Vasquez-Beggs PVT model is being used.
- **Lee Modified gas viscosity model:** Because this model has better performance for a greater range of gas viscosities.

It is possible to adjust the number of simulations, meaning number of Monte Carlo iterations performed. This number may be reduced to a low value (<1000), in order to check if the blowout simulation is valid. However, it should ideally not be lower than 10 000 when running a full simulation (Erichsen, 2019). Therefore, the number of iterations are set to 10 000 in this case.

4.4.2 Simulation Scenarios

Type of blowout scenario will vary depending on several factors, including blowout discharge point, the flow path, penetration depth, BOP opening and well kill mechanisms. As there is a great uncertainty related to which kind of blowout scenario that will occur, these parameters are defined as probability distributions in BlowFlow.

Blowout exit points and flow path

It is known that the blowout is highly affected by flow path and discharge point. These quantities are regarded as uncertain and thereby described by probability distributions.

The default probabilistic distributions related to exit points are set to 50% at surface and 50% at seabed, with a blowout duration of maximum 100 days. Moreover, both the topside and seabed blowout scenarios will depend on flow path of the uncontrolled fluids. In Oilsoft Blowout Simulator one may choose three possible flow paths;

- Blowout through drill string
- Blowout through annulus
- Blowout through an open hole

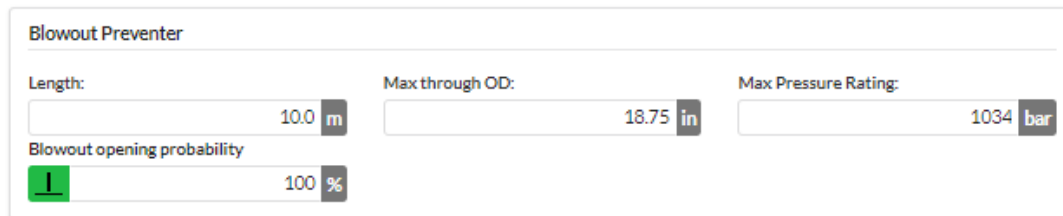
The default probabilistic distributions related to flow path are set to 11% through drill pipe, 78% through annulus, and 11% through open hole, regardless of release point. These default distributions are based on data from the SINTEF Offshore Blowout Database (SINTEF, 2017), and will therefore not be changed in this simulation example. The figure 4.8 summarize the flow path and discharge point probability distributions.

Blowout scenario	Probability [%]
Surface/Topside Blowout	50
Blowout through String	5.5 (11% of 50%)
Blowout through Annulus	39 (78% of 50%)
Blowout through Open hole	5.5 (11% of 50%)
Subsea Blowout	50
Blowout through String	5.5 (11% of 50%)
Blowout through Annulus	39 (78% of 50%)
Blowout through Open hole	5.5 (11% of 50%)

Figure 4.8: Probabilistic scenarios of blowout exit points and flow path.

Reservoir penetrations and restrictions

The flow rate of a potential blowout is also affected by the BOP opening. Even though a failure in closing the BOP may appear, a fully open BOP is not likely to be the scenario. According to OLF guidelines, a 95% closed BOP is considered reasonable due to the BOP representing a high-reliability system (Nilsen, 2014). However, as one should always prepare for a WCD scenario, a fully open BOP is considered as basis in this case study. Hence, the BOP opening probability is set to 100%. As for the other BOP parameters (see figure 4.9), including BOP length, maximum through OD and maximum pressure rating, these are set to the default values recommended by the program.



Blowout Preventer	
Length:	10.0 m
Max through OD:	18.75 in
Max Pressure Rating:	1034 bar
Blowout opening probability	100 %

Figure 4.9: *BOP settings used in the case study.*

In addition, the flow rate is affected by reservoir penetration depth. Although it is difficult to predict what penetration depth a potential blowout is most likely to occur at, Nilsen (2014) has proposed accurate penetration depth distributions;

- Blowout when drilled 5 m into the reservoir: 20%
- Blowout when drilled half way through the reservoir: 40%
- Blowout when drilled through full reservoir-zone: 40%

The software has 55% probability for blowout when penetrating top 5 m of the reservoir, and 45% probability for blowout when drilled through full reservoir, as default values for reservoir penetration depth. Unlike the proposed possibility of a blowout when drilled half way through the reservoir stated in Nilsen (2014), the software assumes that it is not likely for a blowout to occur at this penetration depth. This is shown in figure 4.10, and will be the penetration depth distributions used in this simulation example.



Figure 4.10: *Reservoir penetration depth distributions.*

Well Kill Mechanisms

Before running the simulation it is vital to set types of blowout stopping mechanisms, as well as their duration and probability of success. The intention of such mechanisms is to limit and halt a blowout. Because it is not possible to predict with certainty which of the well kill mechanisms that will lead to a cessation, the different well kill mechanisms are set as probabilistic distributions (Erichsen, 2019). In this dissertation the two killing mechanisms capping and relief well are considered, which is based on these two techniques being the standard in PSA (2019b).

Capping: The simulation assumes a 50% probability of a successful kill operation by capping subsea within 30 days.

Relief Well: Because there is a high possibility of success in killing a well with a relief well, the probability of killing a blowing well with a relief well is set to 100%. The relief well process comprises of several phases, including decision time, mobilization time, rig move time, drilling time, steer/control time and kill relief time. Each of these phases and corresponding estimated durations must be defined before running the simulation. The estimated duration for each of the phases, are based on Nilsen (2014) and comments from Kjell Kåre Fjelde.

- According to Nilsen (2014), the time it takes to mobilize a rig to the desired location is typically 14 days. It should be noted that this is the case for drilling a relief well by mobilizing a new rig. In most cases, it is possible to drill the relief well with the same rig that drilled the target well, thus the

mobilization time is set to zero days.

- The rig move time is represented by a triangle distribution, $T(2,3,4)$ days. This is according to Nilsen (2014) based on well control expert judgement.
- After mobilizing the rig at the accurate position, the drilling of the relief well may start. According to Nilsen (2014), the time needed to drill a relief well is highly uncertain, mainly due to the many obstacles that may occur during this process. Nilsen (2014) also recommend representing this parameter as a triangle distribution, namely $T(20,25,30)$ days. It is reasonable to believe that the drilling of a relief well may need even more time. Therefore, after discussion with Kjell Kåre Fjelde, a triangle distribution of $T(20,40,60)$ days was set as drilling time.
- After drilling the relief well, one need to steer the relief well into the blowing well. As mentioned before, it is crucial to hit the target well at the right location in order to enhance the probability of a successful kill operation. The time it takes to steer and control the relief well into the blowing well is set to 1 day (Nilsen, 2014).
- Finally, the time used to kill the blowing well, need to be defined. The time it takes to stop the uncontrolled flow is set to 1 day.

The time line representing the relief well kill mechanism is shown in figure 4.11. The figure shows the most likely number of days the different phases requires.



Figure 4.11: *The different phases of a relief well process, with corresponding estimated duration.*

For more information about these mentioned killing mechanisms, see section 2.2.3.

Summary of well input for this simulation example

Table 4.3: *Reservoir input data for the simulation.*

Parameter	Value	Unit
Reservoir pressure	771-792-813	bar
Depth of reservoir	4250	m
Oil density	870	kg/m ³
API grade	31.1	°API
Gas gravity	0.750	-
GOR	600	-
Permeability	500	mD
Skin factor	0.03	-
Gross thickness	65	m
Net/Gross ratio	1	-
Water depth	975	m
Reservoir temperature	167	°C

4.5 Blowout Summary

The output section of the program presents a summary of the results from each simulated blowout scenario. These results are expressed through probability distributions of flow rate, duration and volume. The probability distributions are presented as density curves, where each value has an associated probability. It should also be mentioned that the simulator presents the results as cumulative distributions functions. The program presents tables of rate and volume as mean, max, min, P10, P50 and P90, but our main focus will be on studying the mean results.

It should be noted that the program presents detailed information of the different parameters used in calculations of blowout rate, volume and duration, as well as cross-plots of the VLP and IPR curves for each of the flow path scenarios. However, this will not be further addressed in this thesis.

4.5.1 Flow Rate

The flow rate is represented both as a probability density curve function and as a cumulative distribution function. The probability is plotted against flow rate in m^3/day , shown in figure 4.12. The different columns of various height in the graph represents the probability for each specific flow rate.

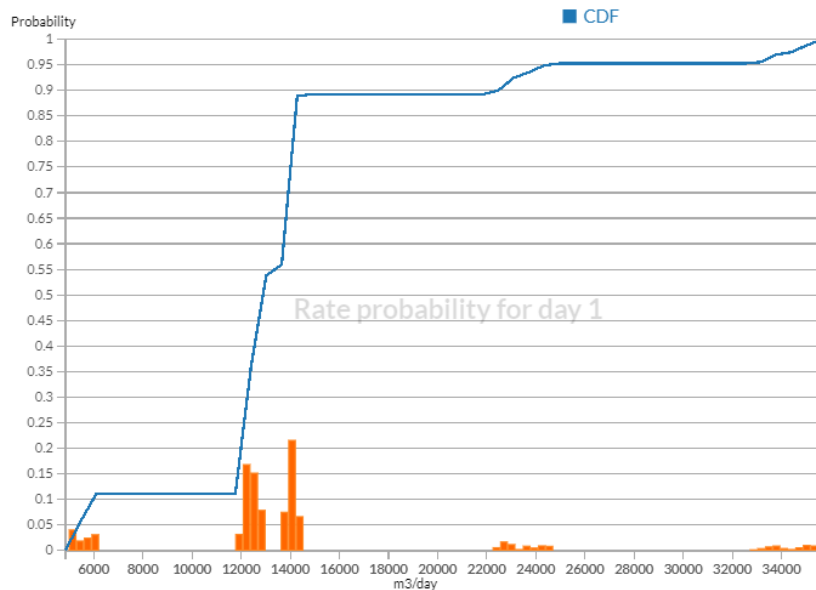


Figure 4.12: Probabilistic oil flow rate distribution at day 0.

The different columns in the graph above represent various blowout scenarios. By analysing the different rates at the various flow path scenarios (see table 4.4 and 4.5), one notice that the different grouping of columns corresponds to different flow path scenarios. The first group of columns shows the flow rate range for both surface and seabed blowout through drill pipe, which has a range from 0 to 6250 m^3/day . The next grouping of columns represents the potential rates from a blowout through annulus. This scenario has a rate range from approximately 11 800 to 14 500 m^3/day . As there is set a 78% probability of a blowout having this specific flow path, there is naturally a higher propability distribution of these columns in figure 4.12. It is believed that the two last grouping of columns corresponds to potential rates of a blowout to seabed and surface from an open hole, respectively. As seen from both the figure above and the tables representing the mean flow rates, there is a relatively low probability of such high blowout rates.

As mentioned earlier, the software present a table of flow rate results as mean, min, max, P10, P50 and P90. By studying both potential seabed blowout and surface blowout at the various flow path scenarios, one see that the oil flow rate ranges from a minimum of 4844 Sm^3/d to a maximum of 35703 Sm^3/day , while the gas flow rate ranges from a minimum of 2.91 SMm^3/d to a maximum of 21.4 SMm^3/d . The potential flow rate in case of a blowout can be any value within these ranges, depending on the flow path and release point. It should be noted that the cumulative distribution function shows a 95% probability of oil flow rate ranging between 0 to 24 000 m^3/day .

Table 4.4 shows flow rate distribution values for oil and gas for potential surface blowout with different flow paths. This is the mean values of the simulation, which represents the most likely blowout rate to occur at a potential surface blowout, depending on the various scenarios. Because the mean flow values are presented in tables 4.4 and 4.5, they do not necessarily match the distributions values in graph 4.12. According to table 4.4, the total weighted rates for a surface blowout are 14 044 Sm^3/d oil and 8.427 SMm^3/d gas.

Table 4.4: Mean potential surface blowout rate.

Flow path scenario	Distribution %	Oil rate [Sm^3/d]	Gas rate [SMm^3/d]
Drill pipe to surface	11	5052	3.031
Annulus to surface	78	13211	7.927
Open hole to surface	11	28943	17.366
<i>Total weighted rates for surface</i>	<i>100</i>	<i>14044</i>	<i>8.427</i>

Since one consider the possibility of a seabed blowout to occur, various scenarios have been constructed in order to estimate the flow rates in such cases. Table 4.5 shows the flow rate distribution values for oil and gas, for potential seabed blowout with different flow paths. These flow rates are also represented by the mean value from the simulation. The program yields total weighted rates for seabed of 13 696 Sm^3/d oil and 8.218 SMm^3/d gas.

Table 4.5: *Mean potential subsea blowout rate.*

Flow path scenario	Distribution %	Oil rate [Sm³/d]	Gas rate [SMm³/d]
Drill pipe to seabed	11	5825	3.495
Annulus to seabed	78	12853	7.712
Open hole to seabed	11	27547	16.528
<i>Total weighted rates for seabed</i>	<i>100</i>	<i>13696</i>	<i>8.218</i>

From the two tables above one notice highest flow rates in case of an open hole blowout. This is reasonable because an open hole flow path has no drill pipe present, e.i. has less friction, resulting in lower BHP, and thus larger inflow from the reservoir. As expected, blowout through drill pipe result in the lowest blowout rate. It is believed that the low rate is caused by the large friction inside the drill pipe, making it more difficult for the hydrocarbons to flow.

In most of the scenarios, surface blowout generates higher rates than seabed blowout, which is reasonable according to Liu et al. (2015). It should be mentioned that this is not always the case. Oliasoft assume that the only difference between a seabed and surface blowout, is the discharge point. When cross-plotting VLP and IPR curves, there are many factors that may affect the absolute open flow, e.i. the intersection point between those two curves. These factors include various outlet boundary conditions, total depth of the well, pressure and velocity. Often the surface rates are higher than the seabed rates, with the exception of cases with very high flow velocity towards the top of the well. This causes the friction pressure to be significantly higher than the gravity pressure, leading to a higher rate from a seabed blowout. This is most likely the case for blowout through drill pipe scenarios, where the rates are higher for a seabed blowout.

The program presents estimated density curves for potential flow rates as a function of time. Therefore, it is possible to show the potential flow rates for each day in the graph, within a maximum duration of 100 days. This makes it possible to notice how the different kill mechanisms affect the flow rates.

As there is a 50% possibility of the blowout being killed by capping within 30 days, there is a notable change in the rate distribution as one approaches 30 days on the graph. 32 days after the blowout was first noticed, see figure 4.13, one observe an increase in the probability of low flow rates, while a decrease in the probability of higher rates. The lowest flow rates corresponds to approximately $0 \text{ Sm}^3/\text{d}$. This result is expected, because it is reasonable to believe that the capping of a blowing well would most likely lead to a reduction of the blowout, not a complete ceasing. The flow rate distribution after 32 days, i.e. after the capping mechanism is applied, can be seen in figure 4.13.

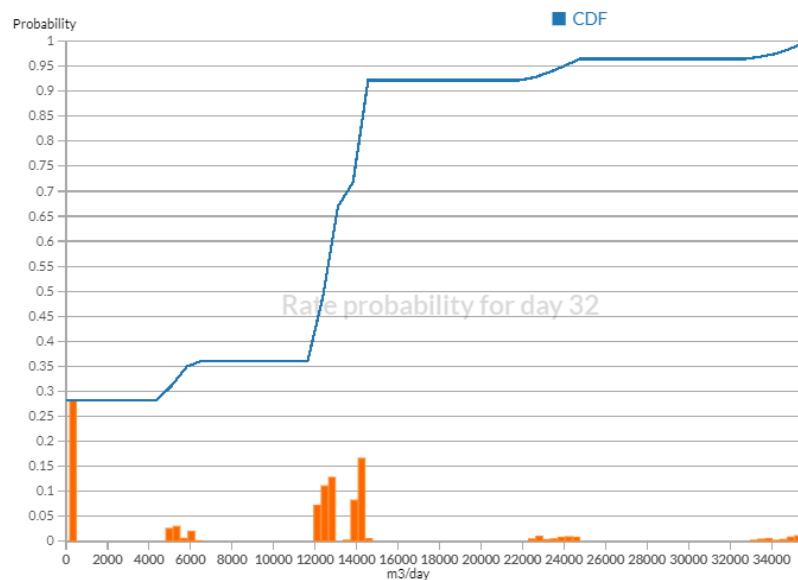


Figure 4.13: Probabilistic flow rate distribution at day 32.

Due to the application of a relief well killing technique, it is expected to observe a step change in the rate distribution from 30 to 60 days. This expectation is based on the input from section 4.4.2. As the second kill mechanism is applied, one observe an increase in the probability of low oil rates, while a decrease in the distributions of high oil rates. This effect continues, until the relief well has successfully killed the blowing well after approximately 65 days. Hence, the probability of zero rate increases, while the probability of other rates decreases, until the blowing well gets killed. This effect can be observed in the figure below. This result is reasonable, because the success rate of killing the blowout with a relief well is set to 100%.

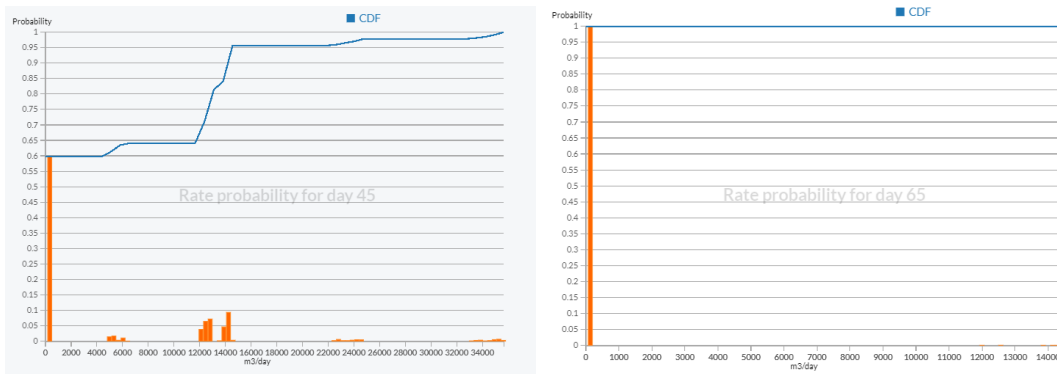


Figure 4.14: Probabilistic flow rate distribution at day 45 and 65, respectively.

4.5.2 Volume

The BlowFlow simulator estimates the total volumes of oil and gas that may be released depending on the various blowout scenarios. This is only an indication of total volume released until the well is killed after approximately 65 days. The volume is a function of the probability distribution of both blowout rate and duration, which is why also this parameter is presented as a density curve and cumulative distribution function. Figure 4.15 shows the blowout volume probability distribution for this specific example. From the figure one observe a maximum volume released during a blowout of 2 319 044 m^3 , while the minimum possible volume discharged is 124 077 m^3 .

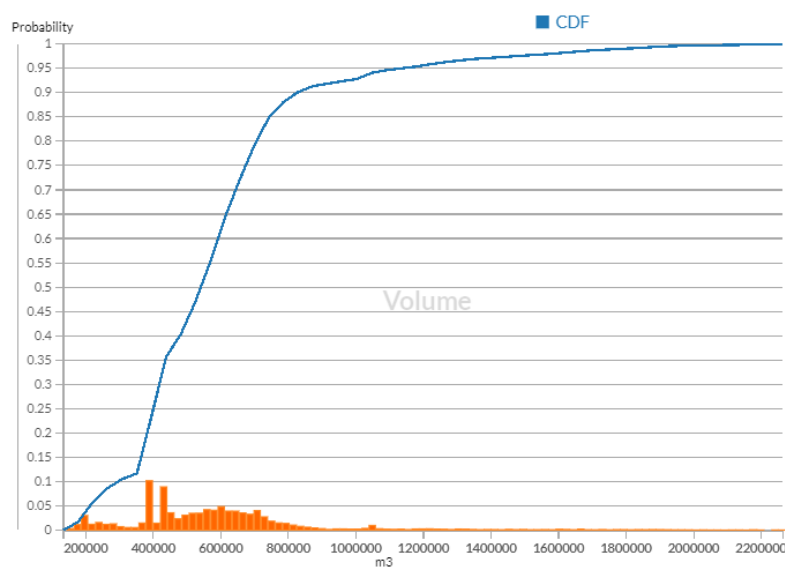


Figure 4.15: Probabilistic indication of total blowout volume released until the well is killed.

The total volume of released hydrocarbons will, as with the rate, also be affected by flow path scenario and discharge point. Similar to the flow rate graph, the various columns in figure 4.15, represent the different blowout scenarios. The first grouping of columns corresponds to a surface/seabed blowout through the drill pipe. In such scenarios the total volumes released have a range of approximately 120 000 to 300 000 m^3 . The next grouping of columns have a range of 300 000 to 900 000 m^3 , and corresponds to a blowout through annulus. According to the cumulative distribution function, there is a 92% probability that the total volume released will lay between 0 and 900 000 m^3 . The remaining columns correspond to the potential volume released from a blowout to seabed and surface from an open hole. The figure clearly shows that blowout through an open hole has the highest total volume discharged. However, there are a relatively low probability of such large volumes being released. These results are reasonable, due to the similar trend shown in the rate graph in figure 4.12.

The simulator presents a summary of the mean, min, max, P10, P50 and P90, potential volume released in case of a surface and seabed blowout. The mean potential volume discharged to surface and seabed, are shown in tables 4.6 and 4.7, respectively.

Table 4.6: *Potential mean blowout volumes in case of a surface blowout.*

Flow path scenario	Distribution %	Oil volume [Sm³]	Gas volume [SMm³]
Drill pipe to surface	11	229475	137.7
Annulus to surface	78	600108	360.1
Open hole to surface	11	1314877	788.9
<i>Total weighted volume for surface</i>	<i>100</i>	<i>637963</i>	<i>382.8</i>

From the table above one observe that it is most likely to have a surface blowout through annulus with a total release of 600 108 Sm^3 oil and 360.1 SMm^3 gas. In case of a seabed blowout, the table 4.7 shows that it is most likely to have a blowout through annulus with a total release of 489 904 Sm^3 oil and 293.9 SMm^3 gas.

Table 4.7: *Potential mean blowout volumes in case of a seabed blowout.*

Flow path scenario	Distribution %	Oil volume [Sm³]	Gas volume [SMm³]
Drill pipe to seabed	11	222046	133.2
Annulus to seabed	78	489904	293.9
Open hole to seabed	11	1049660	629.8
<i>Total weighted volume for seabed</i>	<i>100</i>	<i>522013</i>	<i>313.2</i>

As seen from these results, a surface blowout tend to lead to larger volumes being discharged, and is therefore usually of highest detrimental. According to Liu et al. (2015), a surface blowout usually result in a much higher gas fraction, much higher mixture velocity and much lower pressure at the bottom of the well compared to the reservoir. In case of a seabed blowout, there would be a backpressure for instance caused by the hydrostatic pressure of water. This backpressure has the potential to dampen the unloading significantly (Yuan et al., 2017). All these factors causes a more severe blowout if the release point is at surface. The result from this simulation example is therefore reasonable due to the statement from Liu et al. (2015).

4.5.3 Duration

The BlowFlow simulator estimates the duration of a blowout. This is an indication of how long it is going to take to regain control of, and kill the blowing well. Similar to the two other parameters, the duration is presented by a density curve and a cumulative distribution function, where the probability is plotted against time in days. The duration probability distributions are shown in figure 4.16.

The duration is a function of the different killing mechanisms considered. It will depend on the time of occurrence and the probability of a killing mechanism to successfully kill the blowout. In this conducted analysis one assume that the blowout gets killed by either capping or by drilling a relief well.

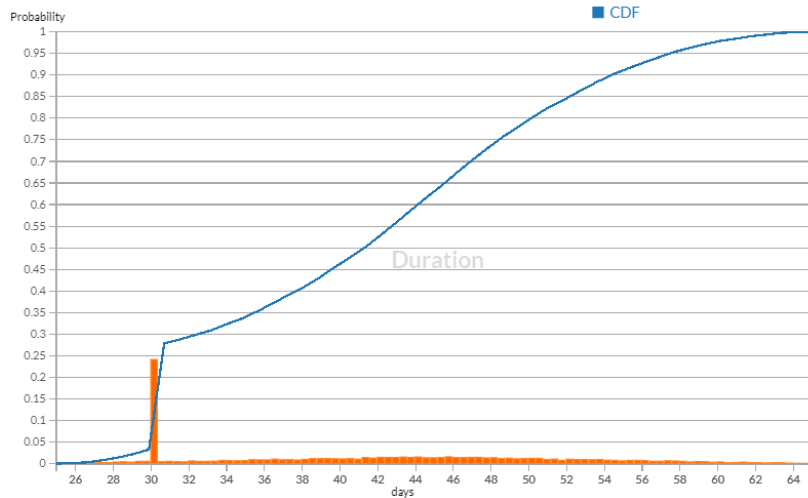


Figure 4.16: *Blowout duration probability distribution.*

The duration graph in figure 4.16 shows two peaks, namely after approximately 30 and 46 days. This is expected because the various kill mechanisms interfere at different times. The first peak is associated with the application of capping. According to the cumulative distribution function, there is a 10% chance of successful killing the blowout within 30 days. After 32 days the application of capping has taken place, and one notice a 29% probability that the blowout is killed by either capping or relief well. It should be noted that the application of relief well may begin before or during the capping mechanism, due to the triangle distribution for drilling time being set to $T(20,40,60)$. This is why the graph increases slightly before capping occurs.

If the blowout is not killed by capping, the well will continue to blow with full or halted rate until it is killed by the relief well. The kill operation by relief well is set to have a 100% probability of success. The time taken to kill a well with relief well is set as a continuous distribution, which is why it is difficult to determine the precise duration of the blowout from figure 4.16. This gives a continuous distribution of the columns with a range from 26 to 65 days. The distributions shows a minor peak at approximately 46 days. The longest possible blowout duration is 65 days, due to the assumption of successfully killing of the blowing well by a relief well. It should be noted that the columns are widely spread, which reflect the uncertainty related to the different killing mechanisms.

5. Mathematical Model for Steady State Flow

Multiphase flow models, like the steady state flow model, are widely used in the petroleum industry. One possible application of such a model, is to simulate a blowing well. During numerical modelling of blowout rate it is important to develop both mathematical and computational models, where the mathematical model form the base for the simulation. As the steady state flow model comprises of a complex system of equations, it will be solved numerically.

The purpose of this thesis is to develop a steady state flow model for a blowing well in Matlab, based on the code developed by Gomes (2016). The thesis aims to improve the model, by making it compatible with an annular geometry as well as implementing an inflow model. The latter being described in chapter 7. The following chapter will present the various calculations and models that will be integrated in the steady state flow model.

5.1 Conservation Laws

With respect to well flow, there are three fundamental laws that applies, namely conservation of mass, conservation of momentum, and conservation of energy (Fjelde, 2016). Multiphase flow models based on conservations laws are widely utilized in the oil and gas industry. Such models have a broad range of applications, and may be utilized to simulate blowouts, underbalanced drilling operations or flow assurance. One may categorize the multiphase flow models in two main groups, mainly transient models and steady state models. In a transient model, the flow and pressure are dependent of time, while these parameters are independent of

time in a steady state model (Danielson et al., 2000).

5.1.1 Steady State Model

If one consider steady state conditions, the model is independent of time, there will be no sonic waves propagating in the system, and the mass flow rate of each phase will be constant, regardless of position in the well (Fjelde, 2016; Danielson et al., 2000).

In order to apply the conservation laws for a pipe, the pipe has to be divided into cells, as shown in figure 5.1. The conservation laws then have to be solved for each of the cells by applying a shooting technique. The discretization process and the shooting method will be address in sections 6.2.1 and 6.2.2, respectively.

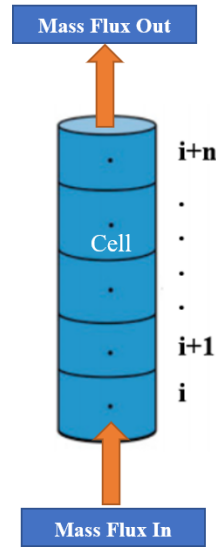


Figure 5.1: *Illustration of the conservation of mass in a discretized pipe.*

If the temperature gradient in the well is assumed to be constant, the conservation of energy can be neglected. The transient drift flux model can be used for modelling two phase flow, e.g. in Fjelde (2016). This transient model can be simplified for steady state flows. In terms of conservation of mass, one simply remove the time dependency of the basic conservation law (Fjelde, 2016).

Conservation of liquid mass:

$$\frac{\delta}{\delta z}(A\rho_l\alpha_l v_l) = 0 \quad (5.1)$$

Conservation of gas mass:

$$\frac{\delta}{\delta z}(A\rho_g\alpha_g v_g) = 0 \quad (5.2)$$

Furthermore, one may remove the acceleration term in the momentum equation to make it compatible with steady state conditions.

Conservation of momentum:

$$\frac{\delta}{\delta z}p = -((\rho_l\alpha_l + \rho_g\alpha_g)g + \frac{\Delta p_{fric}}{\Delta z}) = -(\rho_{mix}g + \frac{\Delta p_{fric}}{\Delta z}) \quad (5.3)$$

Table 5.1: *Definition of variables used in the conservation laws.*

Variable	Unit
A - Area	m^2
ρ_l - Liquid density	kg/m^3
ρ_g - Gas density	kg/m^3
v_l - Liquid velocity	m/s
v_g - Gas velocity	m/s
p - Pressure	Pa
g - Gravity constant	$9.81 m/s^2$
α_l - Liquid volume fraction	-
α_g - Gas volume fraction	-
ρ_{mix} - Mixture density	kg/m^3
Δz - Vertical displacement	m
Δp_{fric} - Frictional pressure drop	Pa

Equations 5.1, 5.2 and 5.3, defines the steady state model for multiphase flow in a pipe. Because there are usually multiphase conditions in a well, one has to take into consideration the mixture properties of a flow, meaning a mixture of liquid and gas flow. Additional closure laws are needed to close the model, including models for friction, gas slippage and PVT.

The conservation laws presented above only consider liquid and gas flow without

mass transfer between the phases. In most practical cases, the oil contain dissolved gas, and thus the black oil model should be considered (Coats et al., 1998; Pettersen, 1990). This is a model that in fact employs the conservation laws, but with another formulation, in combination with taking the mass transfer between phases into account.

5.2 Black Oil Model

Petroleum reservoirs are often categorized in terms of their fluid type, and thus the fluids PVT parameters. Figure 5.2 shows some characteristics of the main petroleum fluids (Petrowiki, 2015c).

Characteristic	Oils			Gases	
	Heavy Oils and Tars	Black Oils	Volatile Oils	Gas Condensates	Wet and Dry Gases
Initial fluid molecular weight	210+	70 to 210	40 to 70	23 to 40	<23
Stock-tank-oil color	black	brown to light green	greenish to orange	orange to clear	clear
Stock-tank oil-gravity, °API	5 to 15	15 to 45	42 to 55	45 to 60	45+
C ₇ -plus fraction, mol%	>50	35 to 50	10 to 30	1 to 6	0 to 1
Initial dissolved GOR, scf/STB	0 to 200	200 to 900	900 to 3,500	3,500 to 30,000	30,000+
Initial FVF, B_{oi} , RB/STB	1.0 to 1.1	1.1 to 1.5	1.5 to 3.0	3.0 to 20.0	20.0+
Typical reservoir temperature, °F	90 to 200	100 to 200	150 to 300	150 to 300	150 to 300
Typical saturation pressure, psia	0 to 500	300 to 5,000	3,000 to 7,500	1,500 to 9,000	—
Volatile-oil/gas ratio, STB/MMscf*	0	0 to 10	10 to 200	50 to 300	0 to 50
Maximum vol% liquid during CCE**	100	100	100	0 to 45	0
OOIP, STB/acre-ft (bulk)	1,130 to 1,240	850 to 1,130	400 to 850	60 to 400	0 to 60
OGIP, Mscf/acre-ft (bulk)	0 to 200	200 to 700	300 to 1,000	500 to 2,000	1,000 to 2,200

*At bubblepoint pressure. **Constant composition expansion of reservoir fluid.

Figure 5.2: *Petroleum fluids and their characteristics (Petrowiki, 2015c).*

There are mainly two models used to specify the mass transfer between liquid and gas phases, namely the black oil model and the compositional model. The compositional model is complex due to the large number of components, and its use is restricted to highly volatile oil systems (Peaceman, 1977). In the black oil model one disregards the composition of oil, and define it as a phase in the

system. This system may in addition to oil, contain water and gas (Pettersen, 1990). Hence, the black oil model is compatible with a three phase flow regime if desired.

The black oil PVT model has wide acceptance in the industry. This model is associated with oils with API degree lower than 40 and which experiences relatively small changes in composition within the two phase envelope (Gomes et al., 2015; Brill and Mukherjee, 1999). For simplicity, these small changes in composition are neglected, and it is assumed to be no mass exchange between the water phase and the other phases (Peaceman, 1977). Furthermore, the model assumes that oil may absorb and release gas, while gas cannot do the same for liquid (Pettersen, 1990).

The black oil model is generally employed to find various properties of each of the different phases present in a pipe. The most important parameters defined in the black oil model are presented in figure 5.3, and will be further explained in section 5.2.3. Such fluid properties may be measured in a laboratory by conducting PVT analysis or they may be determined by a wide range of empirical correlations (Singh and Hosein, 2012).

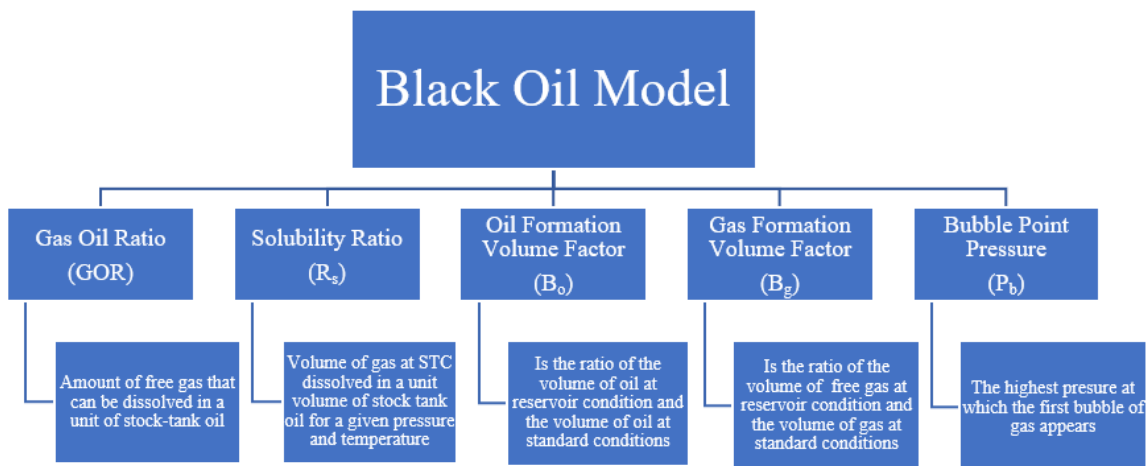


Figure 5.3: *Essential variables defined in the black oil model (Gomes, 2016).*

The relationship between GOR and R_s are shown in figure 5.4. As the pressure increases, more gas get dissolved into the liquid phase. For conditions where $p < P_b$, the solubility ratio is generally proportional to the pressure, e.i. an

increasing linear function. Above bubble point, the oil contain no free gas, and thus the solubility ratio is constant (Pettersen, 1990). In fact, above the bubble point $R_s = \text{GOR}$.

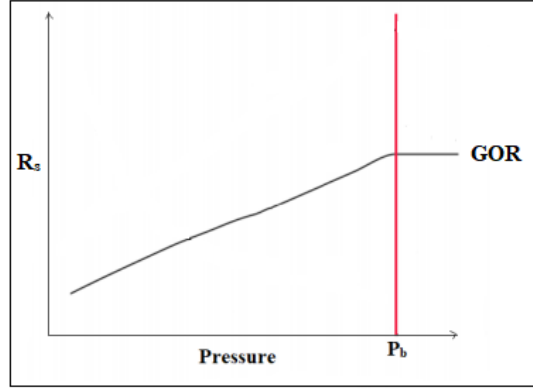


Figure 5.4: *The relationship between R_s and GOR (Pettersen, 1990).*

5.2.1 Required Initial Parameters

When using the black oil model there are several input variables that need to be defined physically in the model in order for it to work. These inputs are presented in table 5.2. It should be mentioned that the model developed by Gomes (2016) has here been modified to consider blow in annuli instead of a tubing.

Table 5.2: *Initial parameter needed to be defined in the black oil model (Gomes, 2016).*

Symbol	Parameter	Unit
d_o	Outer diameter of annulus	m
d_i	Inner diameter of annulus	m
e	Inner rugosity	m
GOR	Gas-Oil Ratio	scf/STB
γ_o	Oil gravity	-
γ_g	Gas gravity	-
M_{air}	Air molar mass	g/mol
ρ_{air}	Air density	lbm/ft ³
μ_o	Oil viscosity	cP
μ_g	Gas viscosity	cP
ρ_w	Water density	lbm/ft ³

Although it is possible to include oil viscosity model and gas viscosity model in the program to estimate the viscosity of the different phases, they are in this specific case defined as fixed values. These parameters are in combination with the other variables presented in the table above, declared inside the code in Matlab. For simplicity, the model only consider a mixture of gas and oil flow, hence does not include water flow.

5.2.2 Preliminary Calculations

In addition to the self-defined input variables listed in table 5.2, there are some preliminary calculations that need to be integrated in the black oil model in order for the model to determine the various PVT properties. The preliminary calculations, based on Gomes (2016), are presented in equations 5.4 to 5.10.

An important aspect of the model is that all variables included in the model should be given at surface conditions and in field units. This is vital because the black oil model utilizes the known flow rate at surface to calculate fluid properties at downhole conditions. Therefore, all the parameters will be defined at Standard Conditions (SC) or Stock Tank Conditions (STC) (Pettersen, 1990), which refers to temperature of $60^{\circ}F$ and pressure of 14.7 psi.

Solubility ratio at bubble point in Scf/STB:

At bubble point all the gas is dissolved in the liquid, hence

$$R_{sb} = GOR \quad (5.4)$$

Oil flow rate at standard conditions:

As water is neglected in the flow, the oil flow rate at standard conditions, Q_{ost} , will be equal to the total liquid flow at surface, Q_l . Both are presented in, ft^3/s .

Gas flow rate at standard conditions:

$$Q_{gst} = GOR * Q_l \quad (5.5)$$

where Q_{gst} is the gas flow rate at surface in ft^3/s

Relative roughness:

$$K = \frac{e}{d_o - d_i} \quad (5.6)$$

Hence, relative roughness, K , is a dimensionless variable.

Dead oil density in lbm/ft^3 :

$$\rho_{do} = \gamma_o * \rho_w \quad (5.7)$$

Gas density at standard conditions in lbm/ft^3 :

$$\rho_{gst} = \gamma_g * \rho_{air} \quad (5.8)$$

API grade:

$$\gamma_{API} = \frac{141.5}{\gamma_o} - 131.5 \quad (5.9)$$

Flow area in in^2 :

$$A = \frac{\pi * (d_o - d_i)^2}{4} \quad (5.10)$$

5.2.3 Empirical Correlations

According to Yahaya and Gahtani (2010), empirical correlations are defined as mathematical relations based on experimental data. Correlations for fluid properties such as solution gas/oil ratio (R_s), bubble point pressure (P_b) and oil volume formation factor (B_o), are presented as functions of pressure, temperature, gas gravity and oil gravity (Gomes, 2016).

Over the last decades, numerous empirical correlations have been established with the purpose of estimating pressure drop and various fluid flow characteristics during multiphase flow (Brill and Mukherjee, 1999; Yahaya and Gahtani, 2010). The Standing correlation (Standing, 1947), developed in 1947, is one example of such an empirical correlation. This correlation comprises of empirical relations for bubble-point pressures, solubility ratio and oil formation factor. Although the correlation was developed from limited data, it is one of the best known and

widely used method for calculating these parameters in the petroleum industry (Vasques and Beggs, 1980; Standing, 1947). For these reasons, the Standing correlation will be employed in the flow model to calculate the properties of each phase as well as the mixture properties.

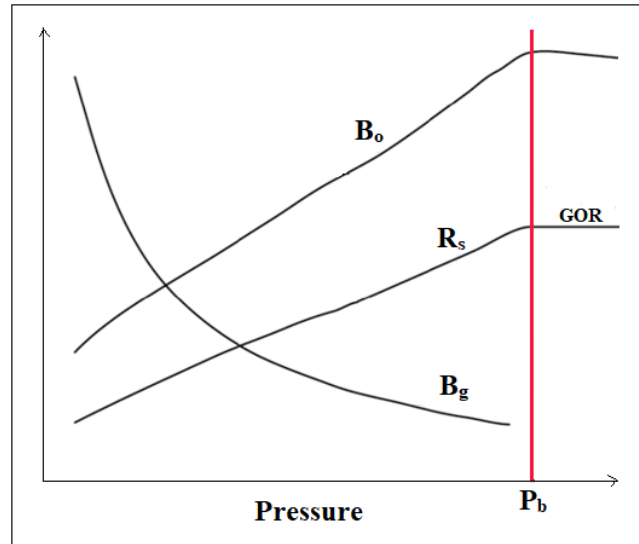


Figure 5.5: Typical response of the important parameters in the black oil model (Pettersen, 1990).

Figure 5.5 shows typical response of the essential parameters in the black oil model. The behaviour of the R_s is discussed earlier. The oil formation volume factor will increase with increasing pressure, because more and more gas gets dissolved in the oil. At bubblepoint, there is no free gas in the oil, and thus there will be a small decrease in the function, since the oil will be compressed for higher pressures. In an opposite way, the gas formation volume factor will decrease due to the same phenomena. As B_g approaches the bubble point pressure, it will get closer to zero (Pettersen, 1990).

Bubble point pressure

The Standing correlation can be employed to estimate the bubble pressure in psi, which is defined as the highest pressure at which the first bubble of free gas appears in a multiphase system (Beggs, 1987):

$$P_b = 18 \left(\frac{R_{sb}}{\gamma_g} \right)^{0.83} 10^{y_g} \quad (5.11)$$

Here R_{sb} is the dissolved gas oil ratio at bubble pressure, calculated by equation 5.4 as part of the preliminary calculations. The internal variable, y_g , is defined by equation 5.12.

$$y_g = 0.00091T - 0.0125\gamma_{API} \quad (5.12)$$

where T is the temperature in $^{\circ}F$, and γ_{API} is the API grade calculated from equation 5.9, in the preliminary calculations.

PVT properties are highly affected by the bubble point pressure. If $P_{wf} < P_b$, then the solubility ratio increases with increasing pressure, whereas if $P_{wf} > P_b$, the solubility ratio is constant. This may be utilized to determine if the flow in a pipe is multiphase or single-phase. If the pressure is below the bubble point pressure, then there is a two-phase oil/gas system. If the pressure is above the bubble point pressure, then there is no free gas, and only unsaturated oil is flowing in the pipe (Ford, 2012; Pettersen, 1990).

Solubility ratio

The parameter solubility ratio defines the volume of gas at standard conditions dissolved in a unit volume of stock tank oil for a given pressure and temperature condition (Brill and Mukherjee, 1999). The solubility ratio can be calculated from empirical correlations or determined experimentally. By using the Standing correlation, which is developed on basis of a regression line, the solubility ratio in Scf/STB can be defined by equation 5.13 (Standing, 1947).

$$R_s = \gamma_g \left[\frac{p}{(18)(10^{y_g})} \right]^{\frac{1}{0.83}} \quad (5.13)$$

where p is the pressure at downhole conditions in psi. It should also be mentioned that for $p > P_b$, the pressure in the equation 5.13 will be replaced by the bubble point pressure. As mentioned in the preliminary calculations, the solubility ratio at bubble point is equal to GOR.

Oil formation volume factor

The volume of stock-tank oil at standard conditions is generally smaller than the volume of in situ oil. This difference is mainly caused by the dissolved gas being released from the oil when oil is transported to surface. The formation factor for oil is defined as the ratio of the volume of oil plus its dissolved gas at downhole conditions, V_o , and the volume of oil at standard conditions, V_{ost} (Peaceman, 1977).

$$B_o = \frac{V_o}{V_{ost}} \quad (5.14)$$

B_o in bbl/STB can be obtained by applying the Standing empirical correlation, defined in equation 5.15 (Standing, 1947; Sutton and Farshad, 1990).

$$B_o = 0.972 + 0.000147F^{1.175} \quad (5.15)$$

where F is an internal variable, defined as:

If $p < P_b$: saturated oil

$$F = R_s \left(\frac{\gamma_g}{\gamma_o} \right)^{0.5} + 1.25T \quad (5.16)$$

If $p > P_b$: undersaturated oil

$$F = R_{sb} \left(\frac{\gamma_g}{\gamma_o} \right)^{0.5} + 1.25T = GOR \left(\frac{\gamma_g}{\gamma_o} \right)^{0.5} + 1.25T \quad (5.17)$$

Here R_{sb} is calculated by using equation 5.13, setting $p = P_b$. Hence, above bubble point $R_s = R_{sb} = GOR$. Because the Standing correlation is only compatible for cases where $p < P_b$, one need to include the Vasquez-Beggs correlation for cases above the bubblepoint pressure (Sutton and Farshad, 1990). The Vasquez-Beggs correlation for B_o is defined by equation 5.18.

$$B_o = B_{ob} e^{-c_o(p-P_b)} \quad (5.18)$$

where c_o is the isothermal compressibility factor of oil in psi^{-1} , defined by Vasquez-

Beggs as (Sutton and Farshad, 1990);

$$c_o = \frac{-1433 + (5 * R_{sb}) + (17.2 * T) + (-1180 * \gamma_g) + (12.61 * \gamma_o)}{p * 10^5} \quad (5.19)$$

In order to ensure a smooth transition between saturated and undersaturated flow, the Standing correlation is integrated inside the Vasquez-Beggs formula, and thus the formation volume factor for oil at bubble point pressure, B_{ob} , is determined by applying equations 5.17 and 5.15 (Gomes, 2016).

Gas formation volume factor

The formation factor for free gas can be obtained in a similar manner as for the oil formation volume factor. B_g is defined as the ratio of the volume of free gas at downhole conditions, V_g , and the volume of the gas at surface in standard conditions, V_{gsc} (Gomes et al., 2015; Petrowiki, 2015a);

$$B_g = \frac{V_g}{V_{gsc}} \quad (5.20)$$

If we assume real gas, we get:

$$\frac{V_g}{V_{gsc}} = \frac{\frac{ZnRT}{p}}{\frac{Z_{sc}nRT_{sc}}{p_{sc}}} \quad (5.21)$$

T is the temperature, T_{sc} is the temperature at standard conditions, p is the pressure, p_{sc} is the pressure at standard conditions, n is the number of moles of gas, and R is the universal gas constant. The Z is the gas compressibility factor. At standard conditions $Z=1$, assuming an ideal gas. The parameters n and R cancels out due to them being the same regardless of conditions (Petrowiki, 2015a). Hence, equation 5.21 can be simplified as;

$$B_g = Z \frac{T p_{sc}}{p T_{sc}} \quad (5.22)$$

At standard conditions, p_{sc} corresponds to 14.7 psia, and T_{sc} is 520 °R. T can be expressed as input in °F, thus one need to include a conversion factor in the

equation in order to get the temperature in rankine. Hence, B_g is expressed in ft^3/scf .

$$B_g = \frac{14.7}{520} Z_{gas} \frac{T + 460}{p} \quad (5.23)$$

In such cases one have to use the calculated Z_{gas} to determine the gas formation volume factor (Petrowiki, 2015a).

Gas compressibility factor

In order to determine B_g , one first need to calculate the gas compressibility factor. First the following quantities must be defined (Gomes, 2016);

- **The pseudo critical pressure**

$$p_{pc} = 702.5 - 50\gamma_g \quad (5.24)$$

- **The pseudo critical temperature**

$$T_{pc} = 167 + 316.67\gamma_g \quad (5.25)$$

- **The pseudo reduced pressure**

$$p_{pr} = \frac{p}{p_{pc}} \quad (5.26)$$

- **The pseudo reduced temperature**

$$T_{pr} = \frac{T}{T_{pc}} \quad (5.27)$$

There are various correlations available for determining the compressibility factor for gas, Z . In this specific case the implicit, iterative approach Dranchuck, Purvis and Robinson correlation (Dranchuk et al., 1973), will be considered. The equation for pseudo reduced gas density is;

$$\rho_{pr} = \frac{0.27p_{pr}}{T_{pr}} \quad (5.28)$$

$$Z_1 = 1 + \left(\frac{A_1 + A_2}{T_{pr}} + \frac{A_3}{T_{pr}^3} \right) \rho_{pr} + \left(\frac{A_4 + A_5}{T_{pr}} \right) \rho_{pr}^2 + \left(\frac{A_5 A_6 \rho_{pr}^5}{T_{pr}} \right) + \left(\frac{A_7 \rho_{pr}^2}{T_{pr}^2} \right) (A_8 \rho_{pr}^2) e^{(-A_8 \rho_{pr}^2)} \quad (5.29)$$

where $A_1 = 0.31506237$, $A_2 = -1.0467099$, $A_3 = -0.57832720$, $A_4 = 0.53530771$, $A_5 = -0.61232032$, $A_6 = -0.10488813$, $A_7 = 0.68157001$ and $A_8 = 0.68446549$.

$$Z = \frac{Z_1 + Z}{2} \quad (5.30)$$

$$Z_{gas} = Z \quad (5.31)$$

5.2.4 Phase Properties Calculations

The preliminary calculations in combination with the Standing empirical correlations can be applied to compute the different phase properties.

Gas-oil interfacial tension

The gas oil interfacial tension is used in the multiphase flow model to calculate the liquid holdup, which will be described in section 5.3.1. The equation for interfacial tension between the phases, σ , in dyn/cm, is according to Baker and Swerdloff (1956) given by the following expression;

$$\sigma = C * \sigma_{(T)} \quad (5.32)$$

where C is a correction factor defined as;

$$C = 1.0 - 0.024p^{0.045} \quad (5.33)$$

$\sigma_{(T)}$ is the tension between the liquid and gas phase for any temperature in the range between 68 and 100 °F, given by equation 5.34.

$$\sigma_{(T)} = \sigma_{68} - \frac{(T - 68)(\sigma_{68} - \sigma_{100})}{32} \quad (5.34)$$

One should use the formula for $C\sigma_{68}$ if the temperature is less than 68 °F, and the formula for $C\sigma_{100}$ if temperatures are higher than 100 °F (Baker and Swerdloff, 1956).

$$\sigma_{68} = 39 - 0.2571\gamma_o \quad (5.35)$$

$$\sigma_{100} = 37.5 - 0.2571\gamma_o \quad (5.36)$$

In situ liquid flow rate in ft^3/s

The oil flow rate, q_o , at downhole conditions is defined as

$$q_o = Q_{ost} * B_o \quad (5.37)$$

In situ gas flow rate in ft^3/s

The gas flow rate, q_g , at downhole conditions is defined as

$$q_g = (Q_{gst} - Q_{ost}R_s)B_g \quad (5.38)$$

If the gas flow rate is calculated to be less than zero, all free gas is dissolved in the oil. Hence, if q_g is less than zero, this parameter is set equal to zero in the calculations to prevent an unphysical situation with negative flow.

Liquid superficial velocity, v_{SL} in ft/s

$$v_{SL} = \frac{q_o}{A} \quad (5.39)$$

Gas superficial velocity, v_{SG} in ft/s

$$v_{SG} = \frac{q_g}{A} \quad (5.40)$$

Mixture velocity in ft/s

$$v_{mix} = v_{SL} + v_{SG} \quad (5.41)$$

Oil density in situ [lbm/ft^3]

$$\rho_o = \frac{\rho_{do} + R_s\rho_{gst}}{B_o} \quad (5.42)$$

Gas density in situ [lbm/ft^3]

In situ gas density is defined as the mass of the gas divided by the volume of gas at downhole conditions. Therefore, ρ_g can be determined from the real gas law

(Petrowiki, 2015a);

$$\rho_g = \frac{p * \gamma_g * M_{air}}{Z * R * T} \quad (5.43)$$

5.3 Multiphase Flow Model

When liquid and gas flow simultaneously in a pipe, the gas will flow at a higher velocity compared to the liquid phase, which leads to the liquid and gas phases occupying different cross-sectional areas of the tubing. This phenomena occur because gas has significantly lower density and viscosity than liquid (Economides et al., 1994). The parameter that define the liquid fraction within a cross-sectional area is called liquid holdup, H_L (Gomes et al., 2015; Gomes, 2016). The liquid holdup is correlated to the gas slippage, and this parameter play a vital part in the computation of the total pressure drop for a pipe (Cacho, 2015).

By employing a mechanistic model to solve for the liquid holdup as a function of various fluid properties, including liquid density, gas density, liquid superficial velocity, surface tension, oil viscosity, gas viscosity, gas superficial velocity and diameters, one obtain a closed steady state flow model (Gomes et al., 2015). A mechanistic model is based on physical principles, and an example is given in Lage and Time (2000). However, in this case, we will utilize a correlation model developed based on experimental data and with the use of regression techniques. The multiphase flow model follows the principles in Gomes (2016) and Economides et al. (1994), but is modified to apply for an annular geometry.

5.3.1 Calculation of Liquid Holdup

$$H_L = Hagedorn\&Brown(d_i, d_o, p, \rho_l, v_{SL}, v_{SG}, \sigma, \mu_o, v_{mix})$$

Because we are not considering different flow regimes in the flow model, the modified Hagedorn & Brown correlation is included in the model to evaluate H_L (Hagedorn and Brown, 1965). The following procedure of computing the H_L is based on Economides et al. (1994) and Ford (2012).

1. Calculate the liquid holdup without considering the slippage between gas

and liquid

$$\alpha_g = \frac{v_{SG}}{v_{mix}} \quad (5.44)$$

$$\alpha_l = 1 - \alpha_g \quad (5.45)$$

2. Calculate the inherent to the method, L_B ,

$$L_B = 1.071 - 0.2218 \left(\frac{v_{mix}^2}{d_o - d_i} \right) \quad (5.46)$$

If $\alpha_g < L_B$, then there is a bubble flow, and the Griffith correlation, given by equation 5.47, is applied to obtain the liquid holdup.

$$H_L = 1 - 0.5 * \left[1 + \frac{v_{mix}}{v_s} - \left(\left(1 + \frac{v_{mix}}{v_s} \right)^2 - 4 * \frac{v_{SG}}{v_s} \right)^{0.5} \right] \quad (5.47)$$

$$v_s = 0.8 \text{ ft/s}$$

If the flow regime in the pipe is not bubble flow, the original Hagedorn & Brown correlation is used to obtain H_L (Hagedorn and Brown, 1965), described in the following steps (Number 3 to 9).

3. Calculate the dimensionless numbers N_{vl} , N_{vg} , N_d and N_l .

$$N_{vl} = \sqrt[4]{\frac{\rho_l}{g\sigma}} \quad (5.48)$$

where N_{vl} is the liquid velocity number, and σ is the interfacial tension calculated from equation 5.34.

$$N_{vg} = v_{SG} \sqrt[4]{\frac{\rho_l}{g\sigma}} \quad (5.49)$$

where N_{vg} is the gas velocity number.

$$N_d = (d_o - d_i) \sqrt{\frac{\rho_l g}{\sigma}} \quad (5.50)$$

where N_d is the diameter number.

$$N_l = \mu_l \sqrt[4]{\frac{g}{\rho_l \sigma^3}} \quad (5.51)$$

where N_l is the viscosity liquid number.

- The viscosity number coefficient, C_{NL} , is determined by using the curve presented in figure 5.6.

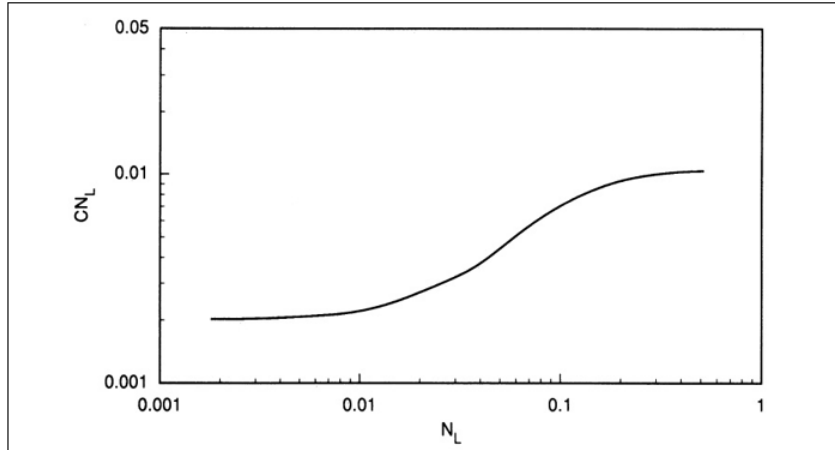


Figure 5.6: The curve used to determine C_{NL} (Economides et al., 1994).

- Calculate

$$\frac{N_{vl} P^{0.1} C_{NL}}{N_{vg}^{0.575} P_{atm}^{0.1} N_d} \quad (5.52)$$

where P_{atm} is the atmospheric pressure.

- The dimensionless number $\frac{HL}{\psi}$ is determined by using the plot presented in figure 5.7.

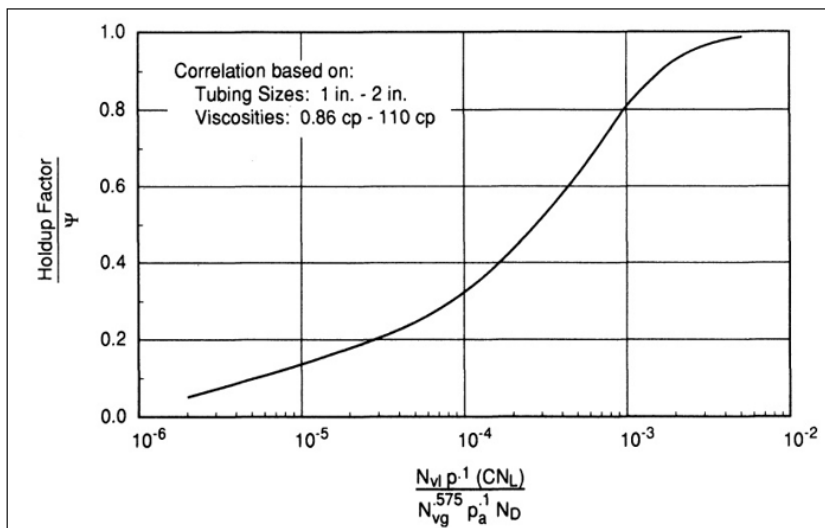


Figure 5.7: The plot used to determine $\frac{HL}{\psi}$ (Economides et al., 1994).

7. Calculate

$$\frac{N_{vg} N_l^{0.38}}{N_d^{2.14}} \quad (5.53)$$

8. Determine ψ by using the curve shown in figure 5.8

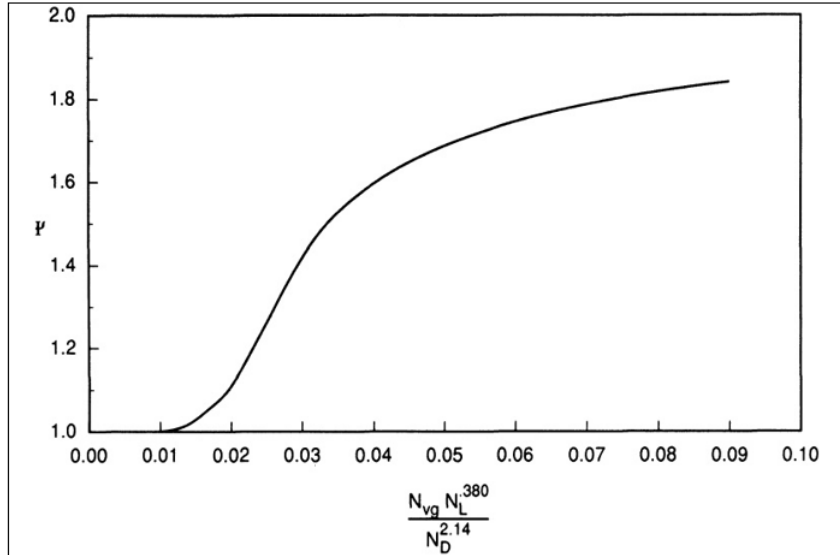


Figure 5.8: The graph used to determine ψ (Economides et al., 1994).

9. The final step is to calculate the liquid holdup, H_L , by using the following expression:

$$H_L = \frac{H_L}{\psi} * \psi \quad (5.54)$$

After determining the liquid holdup, the gas holdup can be found easily from equation 5.55.

$$H_G = 1 - H_L \quad (5.55)$$

After determining the phase properties and the liquid and gas holdups, it is possible to compute the remaining mixture parameters of the flow. This is done by applying equations 5.56 and 5.57.

- **Mixture density:**

$$\rho_{mix} = \rho_l * H_L + \rho_g * H_G \quad (5.56)$$

- **Mixture viscosity:**

$$\mu_{mix} = \mu_l^{H_L} * \mu_g^{H_G} \quad (5.57)$$

The mixture properties may be used to determine the Reynolds number, friction factor, as well as the frictional component of the total pressure drop. It should also be noted that the phase velocities now can be found by applying the liquid and gas holdups in combination with the superficial velocities.

5.3.2 Pressure Drop

At this stage, the fluid properties and flow parameters have been determined. The next step is to include a model for the pressure drop. When performing blowout calculations, it is of high importance to distinguish between laminar and turbulent flow regime, as different flow patterns yields different computation of the friction factor (Fjelde, 2016).

To distinguish between these two flow patterns, one may use the Reynolds number, Re , defined in equation 5.58.

$$Re = \frac{\rho_{mix} v_{mix} (d_o - d_i)}{\mu_{mix}} \quad (5.58)$$

For Reynolds number larger than 3000, one consider turbulent flow, and if Re is less than 2000 the flow is considered to be laminar (Fjelde, 2016). After determining the Reynolds number, there are various available friction factor formulas that may be applied to calculate the friction factor. If the flow regime is laminar, then the fanning friction factor in an annulus is defined as (Fjelde, 2016);

$$f = \frac{24}{Re} \quad (5.59)$$

However, if the flow regime is turbulent, the friction factor can be determined from among others, the Chen equation (Chen, 1979), the Blasius equation (Blasius, 1913) or the Colebrook function (Colebrook and White, 1937). One thing these formulas have in common is that they consider a rough pipe, which strongly affect the frictional pressure loss in a pipe. The Colebrook formula is expressed as (Colebrook and White, 1937);

$$\frac{1}{\sqrt{f}} = -2.0 * \log \left(\frac{K}{3.7} + \frac{2.51}{Re * \sqrt{f}} \right) \quad (5.60)$$

Because this implicit function can be solved for friction factor in the transitional zone, as well as for turbulent flow, the formula is recommended to use. In fact, this is the formula used to describe the friction factor for turbulent flow in the BlowFlow model (Ford, 2012). However, the Colebrook function must be solved by iteration. This can be eliminated by employing explicit functions, like Chen or Blasius. The Blasius equation is defined as (Blasius, 1913);

$$f = 0.052 * Re^{-0.19} \quad (5.61)$$

The friction factor can also be obtained from the Chen equation (Chen, 1979).

$$f = \left(\frac{1}{-4 * \left[\log\left(\frac{K}{3.7065} - \frac{5.0452}{Re} * \log\left(\frac{K^{1.1098}}{2.8257}\right) + \left(\frac{7.149}{Re}\right)^{0.8981}\right) \right]} \right)^2 \quad (5.62)$$

Relative roughness, K , is defined in the preliminary calculations by equation 5.6. This parameter is included in the Chen equation for friction factor, because we are not considering a smooth pipe.

Because the Colebrook function must be solved by iteration, the explicit equation by Chen will be employed in this thesis. This is also the model used in the original code by Gomes (2016).

Blowout rate calculations are highly sensitive to the friction pressure drop model. Gomes (2016) does not consider a transition zone between the two flow patterns in her code. In reality, there will be a transitional zone between laminar and turbulent flow. It is vital to consider this phenomena, and ensure a smooth transition between these two flow patterns, where the Reynolds number ranges between 2000 and 3000. This is solved in Matlab by interpolation, shown in Appendix A.2.6. This is of importance to ensure that the bisection method does not obtain stability problems, since it is based on having continuous functions. The bisection method is part of the calculation approach for steady state flow mode, and will be addressed in section 6.2.3

With known friction factor it is possible to calculate the frictional component

of the pressure loss by using a simple friction model defined in equation 5.63 (Fjelde, 2016).

$$\Delta p_{fric} = \frac{2f\rho_{mix}v_{mix}^2}{d_o - d_i} \quad (5.63)$$

The hydrostatic pressure gradient component of the pressure drop is simply obtained through,

$$\Delta p_{hyd} = \rho_{mix}g \quad (5.64)$$

Hence, the total pressure drop gradient in a pipe becomes;

$$\Delta p = \Delta p_{hyd} + \Delta p_{fric} \quad (5.65)$$

The momentum equation can be used to compute the pressure drop between two positions in a well moving upwards, thus:

$$p_2 - p_1 = -\rho_{mix}g\Delta z - \Delta p_{fric}\Delta z \quad (5.66)$$

Here the Δz is the vertical displacement between two points in a well. The approach for calculating fluid and flow properties as well as pressure drops for all cells simultaneously, will be elaborated in the next chapter.

6. Calculation Approach for Steady State Flow Model

The steady state flow model developed for modelling a blowing well, is based on the calculations and models presented in chapter 5, as well as the original code from Gomes (2016). After defining all relevant calculations, the model must be implemented in Matlab and solved numerically. The calculation approach applied to solve the flow model will be addressed in the following chapter. Modifications made to the original code will be highlighted in this chapter, as well as in chapter 7. The improved code is presented in Appendix A.2.

6.1 Model Description

The steady state flow model is based on two-phase flow in a pipe, covering oil and gas. Unlike the code from Gomes (2016), our model does not consider water flow. The model assumes a vertical well with steady state conditions, no time variations and constant viscosity. It should also be mentioned, that we in this case are considering an annular flow path with a drill pipe, rather than a tubing configuration used in the code developed by Gomes (2016).

The purpose of this model is to compute the correct BHP for certain known oil flow rate at surface. In this computation it is essential to take both the hydrostatic and friction pressure losses into consideration when calculating the total pressure drop. The flow model is built on the black oil model for calculations of PVT properties, a multiphase flow model for calculations of holdups and phase velocities, and a simple pressure loss model. As we do not have experimental PVT analysis available, the fluid properties will be determined by empirical correlations.

The Standing correlation will be employed for PVT consideration, while the Hagedorn & Brown correlation is used for calculating holdups and phase velocities. We can look upon the black oil model as a mass conservation principle comparing surface condition with the specific downhole condition under consideration. The black oil model correlations replaces the conservation laws for mass discussed in the previous chapter. Because the black oil model is applied, it is vital that all parameters used in the model are defined in field units.

6.2 Computational Method

The combination of black oil model correlations and closure equations in a steady state model result in a set of complex equations that are rather difficult to solve analytically. Therefore, the flow model is solved numerically and implemented in a software tool. Matlab will be applied for computational purposes in this thesis, and the computational approach will be described in the following section.

6.2.1 Discretization Process

As the mathematical method is determined from the previous chapter, the next step in the development of a steady state flow model for a blowing well, is to develop a computational procedure that simulates the vertical flow behaviour in a well. The conservation laws compose a system of non-linear ordinary differential equations. In order to apply these set of equations in combination with closure laws, one need to discrete the well into a certain number of cells of equal size. This is referred to as the discretization process (Fjelde, 2016). An illustration of the discretization process of a vertical well with corresponding nodes are presented in figure 6.1.

The flow parameters in each node are assumed to be constant. To ensure validity of this assumption, the cells have to be small enough (Gomes et al., 2015). The discretization process will be more precise with an increased number of cells, which will make the computed solution more accurate. A more refined discretization process requires more computing power, and thus also increased computational time (Fjelde, 2016). Thus, it is important to evaluate and choose an adequate

number of nodes, to ensure a refined solution with minor computational power required.

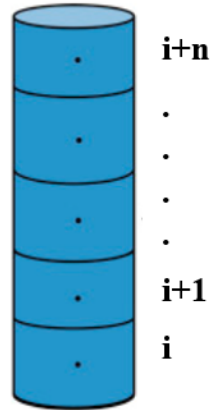


Figure 6.1: *The discretization process in a vertical well.*

For each segment of the well, there are a number of calculations that needs to be solved. These calculations have to be done simultaneously for all nodes, which gives rise to a large set of equations to be solved (Fjelde, 2016). The phase properties have to be determined by using the black oil model and to take care of mass conservation principles. In addition, the Hagedorn & Brown can be used to evaluate the liquid holdup, which again can be used to determine phase velocities and different mixture properties. At last, one need to calculate the total pressure drop as part of the multiphase flow model. The computation is complete, when these calculations have been performed for all the cells in the well and the boundary condition at surface has been met.

6.2.2 Shooting Method

According to Fjelde (2016), there are various methods available for solving the conservations laws for all segments after the discretization process. The simple shooting technique, which is an iterative algorithm, will in this case be employed. After the well has been discretized into a specified number of boxes, one will start at the bottom of the well, where the initial flow variables are known, and calculate cell by cell until the outlet is reached. The outlet act as the last cell, where the pressure is defined as P_N . Hence, numerical integration will be performed from the bottom of the well until the outlet is reached at surface. This specific shoot-

ing approach of calculating from the bottom of the well and up differs from the procedure used in both the BlowFlow engine and in Gomes et al. (2015), where the numerical calculations starts at surface and are performed cell by cell until the bottom of the well is reached.

In order for this application of the shooting method to work, it is necessary to make an initial guess of the bottomhole pressure, P_{guess} , which is the pressure in node 1. At the outlet, we know that the real physical pressure is equal to atmospheric pressure, P_{atm} . This will act as a boundary condition. Our computed solution should match this outlet boundary condition if the solution should be correct (Fjelde, 2016). Hence, one end up solving the following expression;

$$f(P_{guess}) = P_N - P_{atm} = 0 \quad (6.1)$$

If a choke is present in the well, the known outlet pressure, and thus the boundary condition, will be the desired choke pressure, rather than the atmospheric pressure. It should also be mentioned that if a seabed blowout occur, there may for instance be a backpressure caused by the hydrostatic pressure of seawater. However, the computational method utilized is the same regardless of chosen outlet boundary condition.

If the outlet pressure does not equal the boundary condition within a specified tolerance, a new initial P_{guess} has to be guessed for and the calculations have to be repeated in a similar manner. This process is repeated until the difference between the computed outlet pressure and the outlet boundary condition is less than a specified tolerance (Gomes, 2016). In the search for the correct BHP, the bisection method is applied, which will be described in the next sub section.

6.2.3 The Bisection Method

The bisection method is an important part of the computational approach to solve the problem. It is a numerical method employed to find a root of a given function (Gerald and Wheatley, 2004). The method is based on the intermediate value theorem, and is therefore often referred to as the interval halving method.

This means that the search interval is divided in two, and the method finds in which half the root lies. The process is repeated with the endpoints of the smaller interval. If the function is continuous and changes signs at these two values, there must be one root present between these values (Gerald and Wheatley, 2004).

To illustrate the bisection process, figure 6.2 is included. The x_1 and x_2 specify the search interval, while the black dot represent the root of the corresponding function. It should be noted that this specific function is only given for illustration purpose. In this case, we are interested in finding the root in the specified search interval. We must ensure that the starting points satisfy $f(x_1) \times f(x_2) < 0$, and make sure that there is only one root in the search interval. After the root is determined, one proceeds with finding the midpoint, $x_3 = \frac{1}{2} * (x_1 + x_2)$, and continues the process with the new interval (x_1, x_3) , where the function still changes sign. The bisection process is repeated as long as the function changes sign within the search interval. In this case, the bisection method is employed to calculate the actual BHP of a well based on an initial guess of the BHP and a specified search interval.

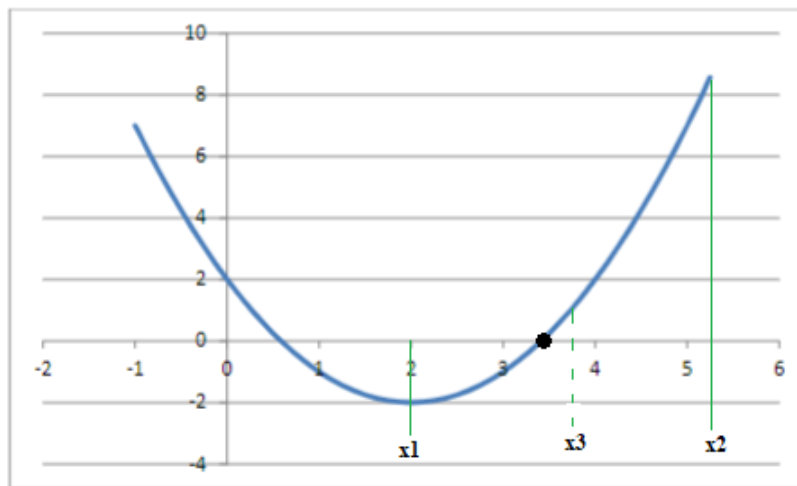


Figure 6.2: Calculation procedure of the bisection method (Fjelde, 2017b).

The iteration is stopped when the root is found with a certain accuracy $|f(x_3)| < ftol$, where the parameter $ftol$ is specified prior to running the simulation. The smaller tolerance, the more accurate the solution.

6.2.4 Calculation Procedure

Inputs and pre-calculations

As discussed in the previous chapter, it is of high importance to define the parameters GOR, R_s , B_o , B_g and P_b , as well the oil rate at surface conditions, in the steady state flow model. This is essential in order for the black oil model to work properly. In addition to the mentioned variables above, the following parameters must be defined in the model prior to running the simulation;

- Inner/outer diameter of pipe, flow area and well depth
- Fixed temperature at top and bottom of the well
- Phase densities and viscosities at surface conditions
- Inner rugosity and relative roughness
- Water fraction

Calculation procedure from bottom to top

The calculation procedure from bottom of the well to top in the steady state flow model utilized to calculate the bottomhole pressure is shown in figure 6.3.

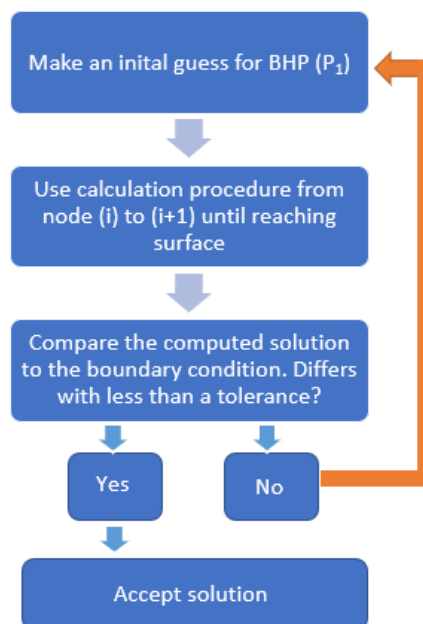


Figure 6.3: Calculation procedure from bottom to top in the steady state flow model.

Calculation procedure from node (i) to (i+1)

The calculation procedure in the steady state flow model applied to calculate BHP from cell (i) to (i+1) is based on the mathematical method presented in chapter 5. A short summary of this procedure is presented in figure 6.4.

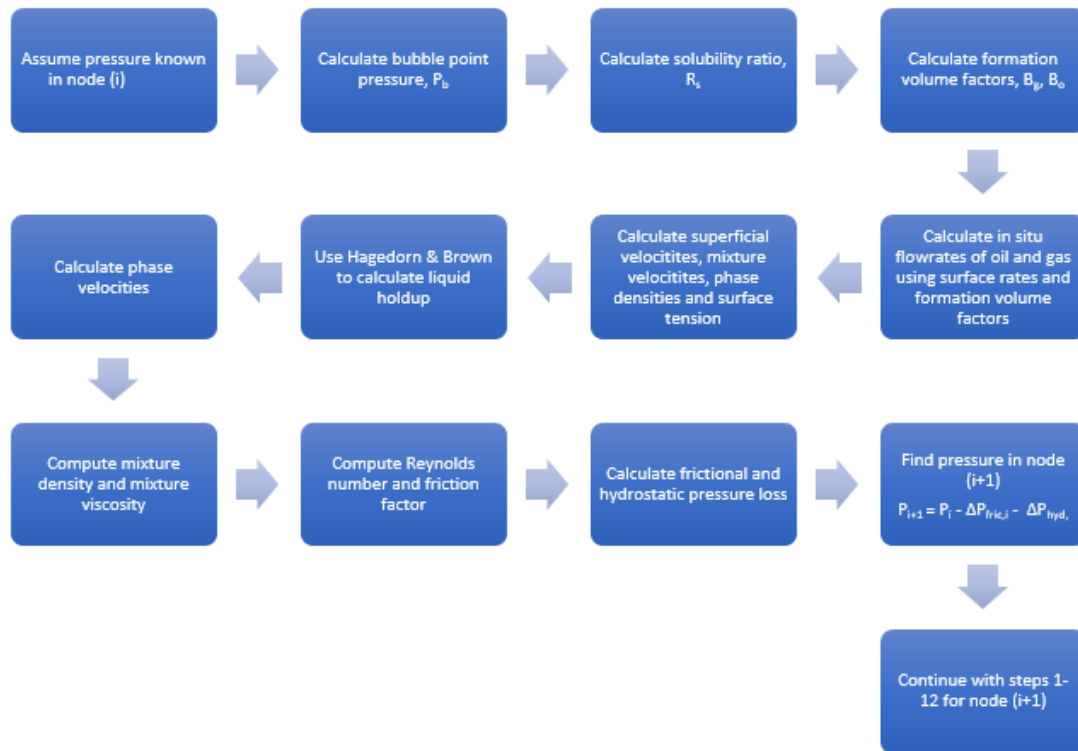


Figure 6.4: Calculation procedure from node (i) to (i+1).

When the pressure is assumed known at a certain point, the black oil correlations are used to calculate the in situ oil flow rates. In addition, these calculations will determine whether there is free gas present in the reservoir, or if the gas is fully dissolved in the liquid phase. The multiphase flow model based on the Hagedorn & Brown method, is used to determine liquid and gas fraction, while the pressure drop model accounts for pressure differences in a well caused by both hydrostatic and friction pressure. The procedure is repeated for cell (i+1) until the outlet is reached.

6.3 Code Structure

The simulator comprises of various scripts with different purposes. The core scripts for the program are main.m, itsolver.m and wellpressure.m, which is shown in figure 6.5. These scripts run the overall simulation.

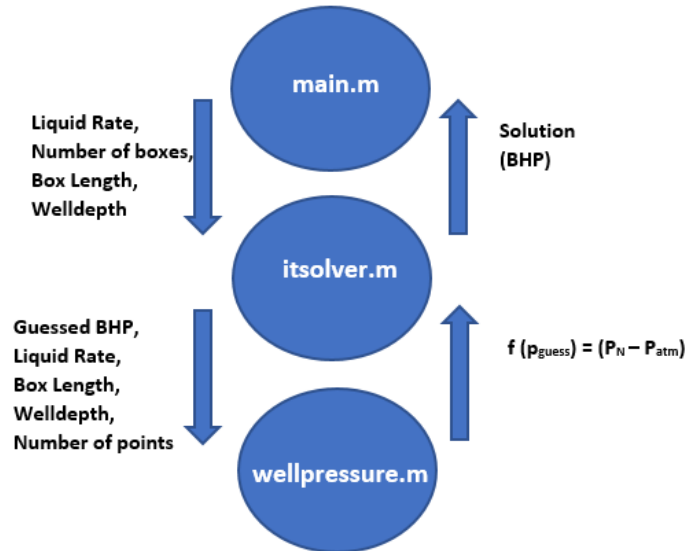


Figure 6.5: Base code structure.

In addition to scripts mentioned in the base code structure, the steady state flow model comprises of a number of other functions used to define important parameters in the model. These additional functions are associated with the black oil model, the multiphase flow model and the pressure loss calculations. All relevant functions are shown in the Matlab code presented in Appendix A.2.

6.3.1 Main.m

The main script run the simulation, provide some of the inputs to the simulation, and presents the final solution. In this script it is important to specify the vertical depth of the well, the number of cells the well is discretized into, as well as the assumed liquid rate at surface conditions. The liquid rate in this case is in fact the oil rate. Based on these inputs, the script calculates the appropriate length of each cell and the number of nodes associated with number of boxes. Table 6.1 shows the input parameters for the main script. The main file calls the function itsolver and returns the correct bottomhole pressure as output in psi.

Table 6.1: *Input parameters for the main program.*

Input parameter	Definition	Unit
welldepth	Depth of the well	m
nobox	Number of boxes the well is divided into.	-
nopoints	Number of nodes associated with number of boxes.	-
boxlength	The length of each of the boxes the well is divided into.	m
liquidrate	Liquid rate at surface	ft^3/s

6.3.2 Itsolver.m

This script contain the numerical solver of the model, which in fact is the bisection method described earlier. The solver is included in the program to solve the expression below.

$$wellpressure(pbot) = 0 \quad (6.2)$$

However, as it is not likely to find an exact match for equation 6.2, the itsolver has included a specified tolerance, $ftol$. As long as the $wellpressure(pbot)$ is less than the tolerance, one is satisfied with the answer. It should be noted that a smaller tolerance provides a more refined solution.

In addition to $ftol$, one must specify the initial guess of the bottomhole pressure and the search interval, both in which have the unit psi. In general, a good starting point for the iteration, is to use the hydrostatic pressure of liquid in the well as an initial guess of BHP. This is not necessarily correct, since there may be gas or friction effects present in the well. The search interval may also be adjusted to help the model to find a solution in case the bisection method does not find a root in the given interval.

6.3.3 Wellpressure.m

In this script one need to specify the boundary condition of the model, namely the outlet pressure. In general, there are two options available for choosing boundary condition. The first option is to set the boundary condition equal to the real surface pressure, e.i. 1 atm or 14.7 psi. The second option is to set the outlet pressure to a desired backpressure. If there is a choke present, the outlet pressure will be equal to the specified choke pressure. In case of a blowout, it is not likely to be a choke connected to the well at surface. If we have a seabed blowout, there may be a backpressure for instance caused by the hydrostatic pressure of seawater.

In the original code by Gomes (2016), the depth of the well must be specified in the wellpressure file. As the *welldepth* parameter is an input in the main script, it should be possible to make the wellpressure function extract this parameter from the main program. In order for the wellpressure function to be a function of the welldepth, and thus make it easier to run the simulation if changes are made in the depth of the well, the wellpressure script now after the modification receive this input variable directly from the main.m rather than needing to adjust it manually. Hence, the welldepth parameter is added as an output from both the itsolver and main scripts. It should be noted that this parameter reflect the true vertical depth (TVD) of the well.

The base code by Gomes (2016) is considering a tubular geometry, and is therefore only considering the outer diameter in the simulation. The code was therefore extended to include an annular configuration with a drill string. Hence, both the inner and outer diameter must be defined as inputs in the wellpressure script. Moreover, the formulas for relative rugosity, flow area, the Reynolds number, pipe diameter number, and the pressure loss due to friction, have been modified to apply for a blowout scenario with flow path through annulus. It is now perfectly fine to consider a tubular geometry if desired, one only need to define the inner diameter as zero.

Because the black oil model is implemented in the code, the variables in the

code must be defined in field units. Gomes (2016) expressed the different input variables in SI units, and had conversion factors added in the code for making the end result in field units. This has been changed in this improved code, and the input variables are now defined in field units directly. Therefore, the conversion factors are removed from the different equations in the wellpressure function, making the equations more similar to the formulas described in chapter 5. The improvements made to the wellpressure function, are shown in Appendix A.2.3. A summary of the changes made to the input variables units in both main.m and wellpressure.m are presented in table 6.2. Additional input variables remains with the same unit as in the original code by Gomes (2016).

Table 6.2: *Adjustments made to the units of the input variables.*

Variables	SI unit (base code)	Field unit (new code)
Surface liquid rate, Q_l	m^3/s	ft^3/s
Outer diameter, d_o	m	in
Inner diameter, d_i	m	in
Inner roughness, e	m	in

It is vital to include a temperature model inside the wellpressure function, to model the temperature changes from the bottom of the well up to the surface. When checking the original code by Gomes (2016), it was found that the temperature model implemented in the code was not sufficient. The code was considering a temperature gradient of $0.03 \text{ }^\circ F/ft$, which is more likely if we are considering a temperature gradient of $0.03 \text{ }^\circ C/m$. Numerical stability problems were obtained when trying to make the well deeper. The temperature profile in the well was based on providing the bottomhole temperature, and using the gradient to calculate temperature upwards in the well. This caused problems when the well was made deeper, causing negative temperatures in the well. Therefore, to handle deeper wells, the temperature model was replaced with an alternative temperature model, namely;

$$T(i + 1) = T(i) + tempgrad \quad (6.3)$$

where the temperature gradient, $tempgrad$, is expressed as;

$$tempgrad = \frac{T(nopoints) - T(1)}{(nopoints - 1)} \quad (6.4)$$

Here, $T(nopoints)$ refers to the surface temperature and $T(1)$ is the temperature in the first node, both defined in $^{\circ}F$. The user of the simulator has to specify the temperature on top and bottom of the well, and the temperature gradient is calculated based on that. This can then be used to calculate the fixed temperature profile in the well, such that each box has a fixed temperature. It is believed that this specific temperature model makes the simulation result more accurate.

`Wellpressure.m` calls upon input parameters from the `itsolver` script, including guessed BHP, liquid rate, number of points, well depth and box length. In this script the majority of inputs are declared, which are summarized in table 6.3.

Table 6.3: *Input parameters for the wellpressure function.*

Input Parameter	Definition	Unit
d_i	Inner diameter	in
d_o	Outer diameter	in
e	Inner roughness	in
GOR	Gas-Oil Ratio	Scf/STB
f_w	Water fraction	-
γ_g	Gas relative density	-
γ_o	Oil relative density	-
ρ_w	Water density	Lbm/ft ³
M_{air}	Air molar mass	g/mol
ρ_{air}	Air density	Lbm/ft ³
T(1)	Bottomhole temperature	$^{\circ}F$
T(nopoints)	Surface temperature	$^{\circ}F$
μ_w	Water viscosity	cP
μ_o	Oil viscosity	cP
μ_g	Gas viscosity	cP
P_{surf}	Real pressure at surface	psi

Because we are considering only gas and oil flow, $f_w = 0$. In addition to the input parameters in table 6.3, the function wellpressure performs the necessary preliminary calculations, and then utilizes the black oil model, the multiphase flow model including the pressure loss model, to calculate box by box from bottom of the well to surface. The approach of calculating from the bottom of the well and up differs from the procedure used in both the BlowFlow engine and Gomes et al. (2015), where the calculations starts at surface and are performed cell by cell until the bottom of the well is reached. When shooting from the bottom it is possible to integrate an inflow model directly in the model. Including an inflow model directly in the wellpressure function makes it possible to determine the blowout flow rate without plotting the IPR and TPR curves. The number of times one need to call upon the wellpressure script will then depend on how quickly the bisection method converges. Hence, the next chapter will focus on trying to implement an inflow model directly in the steady state flow model.

7. Blowout Flow Rate Model

Numerical simulators with their broad uses, have become important tools for the oil and gas industry. Models for performing oil spill calculations represents one of the numerical simulators available on the market. The purpose of blowout flow rate modelling is to determine the initial blowout rate for a defined scenario, e.i. do oil spill preparedness planning.

With the flow model developed in the previous chapter as a core for the simulation, there are two alternative approaches to model the inflow from reservoir, and thus simulate the actual flow rate of a blowing well and its corresponding downhole pressure. The first alternative approach is based on cross-plotting the IPR and TPR curves. The simulation is then run with different assumed surface rates, without making any changes to the code from chapter 6. After running the simulation for a specified number of rates, the IPR and TPR curves are estimated, and the correct BHP and surface flow rate are determined. A possible way of improving the steady state flow model, is to model the inflow from the reservoir directly, rather than defining the liquid flow rate at surface as a fixed input in the main script. This inflow model will then depend on the guessed bottomhole pressure in the bisection method, and the inflow will vary in the iterations being performed.

These two mentioned procedures of computing the blowout rate, will in this chapter be presented and tested. The main goal is to develop a program that provides the actual flow rate and corresponding BHP directly from the simulation, for both saturated and undersaturated reservoirs. The fact that the shooting technique is applied from bottom of the well and upwards, can make it possible to include an inflow model directly in the flow model.

7.1 Inflow Model

The purpose of an inflow model is to estimate the flow rate of fluids from the reservoir to the wellbore. The inflow performance relationship is given by the inflow model, and is defined as the relation between the bottomhole flowing pressure and the production rate at surface conditions (Schubert et al., 2004). In general one distinguish between two types of inflow model used to simulate the inflow from reservoir, depending on if there are single-phase or multiphase conditions present in the reservoir. These include the simple inflow model and the empirical inflow model.

7.1.1 Simple Inflow Model

According to Fetkovich (1973), the simple inflow model requires production of ideal homogeneous liquid obeying Darcy's law. Hence, in order for this model to be valid, it is essential that the reservoir pressure is higher than the bubble point pressure. In other words, one assume the reservoir to be located below the bubble point, and that there is single-phase inflow present (Ford, 2012). For cases where this condition holds, it is, according to Vogel (1968), expected to obtain a straight line of the IPR curve. The straight line relationship is given by the productivity index (PI) equation 7.1 (Ford, 2012).

$$q_o = J(P_{res} - P_{wf}) \quad (7.1)$$

Here, q_o is the inflow from reservoir at standard conditions [STB/day], J is the productivity index [STB/day/psi] describing the wells ability to produce (Petrowiki, 2016), P_{res} is the average reservoir pressure [psi], and P_{wf} is the bottomhole pressure [psi]. It is crucial that the productivity index is known, or computed prior to the calculation of the inflow rate. It should be noted that q_o is the rate at surface conditions (Petrowiki, 2016).

Although it is possible to apply this simple inflow model to simulate the inflow of a reservoir, it is important to notice that this specific model is only valid for cases where the reservoir pressure is above the bubble point, e.i. only for single-phase

inflow. As there can be multiphase conditions present at the reservoir, one would ideally include a model in the code to simulate for such cases.

7.1.2 Empirical Inflow Models

Only empirical correlations are available for modelling the inflow of multiphase reservoirs. According to Guo et al. (2008), some of these models include Vogel (1968), Standing (1968) and Fetkovich (1973). Although, there are a number of various correlations available for use, the Vogel equation for computation of inflow rates is most widely adopted in the petroleum industry (Guo et al., 2008). This is why the Vogel (1968) will be applied in this thesis.

Vogel (1968) was the first to present an adequate method for determining production rates or in some cases, flow rates of a blowing well. He pointed out that a straight line relationship between the bottomhole pressure and the flow rates does not hold in situations where two-phase flow is present in the reservoir (Vogel, 1968). The standard Vogel correlation, defined by equation 7.2, requires the bubble point to be above the reservoir as well as the BHP being lower than the bubble point pressure (Vogel, 1968).

$$q_o = q_{o,max} * \left(1 - 0.2 \left(\frac{p_{wf}}{p_{res}} \right) - 0.8 \left(\frac{p_{wf}}{p_{res}} \right)^2 \right) \quad (7.2)$$

Here, the inflow rate has the unit STB/day. For this model to work, it is necessary to have knowledge about the productivity index, the average pressure in the reservoir, and the BHP of the well (Petrowiki, 2015d). Consequently, it is important to apply the shooting technique from the bottom to the top. When the productivity index is known, it is possible to calculate the maximum rate, $q_{o,max}$, by utilizing equation 7.3 (Vogel, 1968; Ford, 2012).

$$q_{o,max} = \frac{J * p_{res}}{1.8} \quad (7.3)$$

The standard Vogel inflow equation is only valid if both the pressure in the reservoir and the BHP are below the bubble point pressure. Therefore, it is essential to include another expression to account for other conditions. In cases

where two-phase flow is present and the reservoir pressure is above the bubble point pressure, the inflow may be estimated using a combination of the standard Vogel equation and the straight line relationship described by the simple inflow model. Hence, the inflow can be expressed by the modified Vogel equation 7.4 (Ford, 2012).

$$q_o = J(P_{res} - P_b) + \frac{JP_b}{1.8} \left(1 - 0.2 \frac{P_{wf}}{P_b} - 0.8 \left(\frac{P_{wf}}{P_b} \right)^2 \right) \quad (7.4)$$

7.2 Modelling Procedures

As discussed earlier, there are two methods available for determining the blowout flow rate, and thus also the point of intersection between the IPR and TPR curves. These two approaches will be addressed in this section. There will be conducted three case studies in this thesis, which considers the two approaches of finding the correct flow rate of a blowing well and the corresponding BHP.

- **Case study #1:** Manually calculate inflow rate for various bottomhole pressures, and compare with assumed surface rates and bottomhole pressures calculated by the flow model. Hence, find a solution from the intersection point between the IPR and TPR curves.
- **Case study #2:** Include a simple inflow model directly in the flow model.
- **Case study #3:** Extending the code to be valid for both multiphase and single-phase inflow, by implementing both empirical inflow models and simple inflow model in the steady state flow model.

These case studies are built on a vertical well with depth of 4000 m, which corresponds to 13 123 ft. The simulations are based on a well experiencing a seabed blowout with an annular flow path. The blowing well is discretized into 200 boxes, each with a length of 20 m. A 8.5" casing and a 5.0" drill pipe are selected as configuration. The model assumes no water fraction, and one only considers oil flow from the reservoir. A backpressure of 250 psi is assumed applied on top of the well. Normally, there would be atmospheric pressure at the outlet, but if the blowout takes place below the sea, there will be a backpressure from the hydrostatic pressure of water. It should also be mentioned that there have been

developed technologies to dampen the unloading of risers by applying backpressure on top of the riser. Therefore, the parameter P_{surf} in this case corresponds to the pressure at seabed.

A downhole temperature of $302^{\circ}F$ and a surface temperature of $100^{\circ}F$ are employed to calculate the corresponding temperature gradient. This will be used to calculate the fixed temperature profile of the well.

The remaining parameters needed as input in the model, are obtained from the case study by Gomes (2016). The input parameters for the simulations, which are identical for all the case studies, are presented in table 7.1. It should be noted that these variables are defined inside the wellpressure function, see Appendix A.2.3.

Table 7.1: *Input parameters for the case studies.*

Input parameter	Definition	Value	Unit
d_i	Inner diameter	8.5	in
d_o	Outer diameter	5.0	in
e	Inner roughness	0.000288	in
GOR	Gas-Oil Ratio	600	Scf/STB
f_w	Water fraction	0	-
γ_g	Gas relative density	0.750	-
γ_o	Oil relative density	0.870	-
ρ_{water}	Water density	62.4	Lbm/ft ³
M_{air}	Air molar mass	29	g/mol
ρ_{air}	Air density	0.0765	Lbm/ft ³
T(1)	Bottomhole temperature	302	°F
μ_w	Water viscosity	1	cP
μ_o	Oil viscosity	12	cP
μ_g	Gas viscosity	0.01	cP
P_{surf}	Pressure at seabed	250	psi
P_{res}	Reservoir pressure	5000	psi
J	Productivity index	1	STB/day/psi

7.2.1 Case Study #1

The first alternative approach for finding the blowout flow rate, is to find the solution manually. This is the approach utilized by Gomes (2016) in her original code. The main principle is to vary the surface liquid rate in the main script, and read of the corresponding BHP. By cross-plotting the IPR and TPR curves, the intersection point may be used to obtain the correct blowout rate. This procedure is shown in figure 7.1.

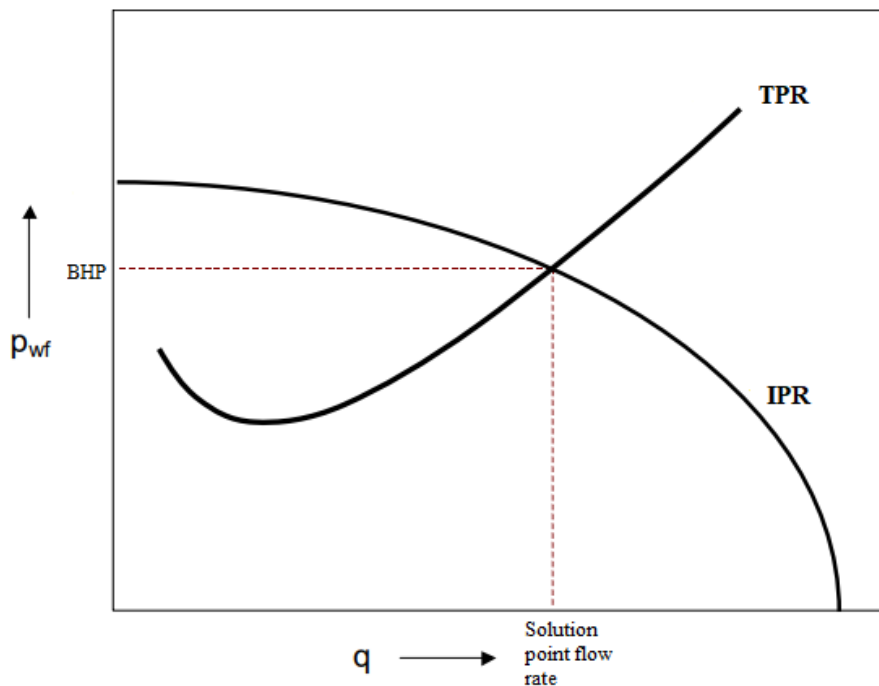


Figure 7.1: Plot used to determine the actual flow rate and corresponding BHP.

The TPR curve is obtained by assuming different rates at surface, and based on these rates, corresponding bottomhole pressures are calculated by the flow model. The IPR curve is determined by using the estimated BHP in combination with the inflow model, to determine the amount of hydrocarbons flowing from the reservoir at surface conditions. A solution is found at the point of intersection between these two curves. This means that a solution may be determined when the assumed rate at the surface provide a BHP which corresponds to an inflow equal to the assumed surface rate. Hence, one end up solving equation 7.5 at surface conditions (Ford, 2012).

$$q_{IPR} = q_{TPR} \quad (7.5)$$

The intersection point between these curves produce the unique BHP that will give a match between assumed surface rate in the flow model and the corresponding surface rate calculated by the inflow model.

The simulation is performed for a number of various rates. After extracting the BHPs from different surface rates, the numerous values of bottomhole pressure may be used to calculate the corresponding inflow rates, q_o , applying the simple inflow model from equation 7.1. Hence, case study #1 assumes single-phase inflow from the reservoir. It should be mentioned that in this case study the average reservoir pressure and the productivity index are not declared inside the simulator. They are only used in the calculations performed in Excel.

The first case study was performed with the approach described above. No adjustments were made to the code developed in the previous chapter. By using the parameters in table 7.1, simulations were performed several times, modifying only the surface liquid rate. The oil rate was varied from 1.5 to 5000 STB/day. The flowing downhole pressure ranging from 3072 to 4482 psi, extracted from the program for various surface rates, was then used to generate the TPR curve of the well. The IPR curve was obtained by using the different BHPs in combination with the simple inflow model, to calculate the corresponding inflow liquid rates, q_o . These calculations are performed in Excel, shown in Appendix A.1. After the computation for a desired number of scenarios, the various inflow rates (IPR) were cross-plotted with the outflow rates (TPR). The curves are plotted against BHP, as shown in figure 7.2. The point of intersection between the IPR and TPR curves is then detected, which yields the correct flow rate and BHP of a blowing well.

By studying the results from the simulation plotted in figure 7.2, the actual flow for the well in question is approximately 1600 STB/day, at a BHP of 3390 psi. Figure 7.2 shows that the IPR curve is a straight line. According to Vogel (1968), this is expected for single-phase flow, and is mainly due to the fact that the productivity index is independent of the rate above the bubble-point pressure (Guo et al., 2008).

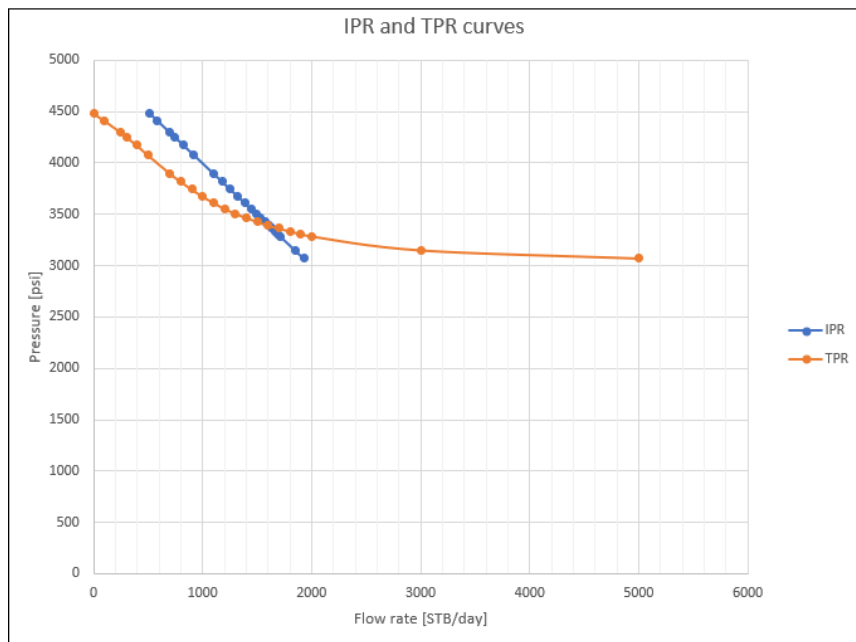


Figure 7.2: *IPR and TPR curves plotted in Excel.*

The approach employed in case study #1 is in fact a combination of techniques used in BlowFlow, Gomes (2016) and Gomes et al. (2015). Even though the liquid rate at surface is defined in the main program prior to running the simulation, the steady state flow model uses a shooting technique from the bottom and up by employing the bisection method to determine the corresponding BHP. Although this alternative way of finding the blowout flow rate is accurate, it is time-consuming, and it is believed that the program is not used at its full potential. A shooting technique from bottom to top makes it possible to implement an inflow model directly in the steady state flow model. Therefore, the next case studies will focus on including inflow models directly in the simulator.

7.2.2 Case Study #2

Secondly, an alternative approach of computing the blowout rate was investigated. The concept of this procedure is to model the inflow from reservoir directly by including an inflow model inside the wellpressure script, as shown in Appendix A.2. The procedure then uses a given initial guessed BHP to search for the matching blowout rate and downhole pressure. With this approach, the program numerically computes the correct flow rate of a blowing well, making it possible to extract the solution point flow rate of a blowing well directly from the program,

without conducting any calculations or plotting of curves manually, like in case study #1. The fact that we calculate from bottom to top makes it possible to integrate the inflow model directly in the steady state flow model.

The first step in developing a program that provides the correct flow rate of a blowing well, is to try implementing a simple inflow model in the base code. The inflow model used in this case consider single-phase flow, namely oil. The model integrated in the code is therefore only valid at undersaturated oil reservoirs conditions. Case study #2 focuses on testing the simple inflow model for the same simulation example as in case study #1, and thus comparing the two different approaches of determining the blowout flow rate.

Modifications made to the original code

This section will provide the modifications made to the original code in order for the simulation to run with an implemented inflow model.

As described earlier, the main script provide initial parameters to the simulation. These inputs remain the same as for the steady state flow model developed in chapter 6. As seen in Appendix A.2.1, the variable *rate* is now included as an output to the main script, in addition to the variable *pbot* from the original code. These output parameters are delivered to the main script from the *itsolver* function. It can be mentioned that the input parameter *liquidrate* will now no longer be in use as explained below. Hence,

$$[pbot, error, rate] = itsolver(nopoints, boxlength, welldepth, liquidrate)$$

It is in the *wellpressure* function the main adjustments are made. The changes made to this script, are shown in Appendix A.2.3. The first modification made, was to include the *rate* as an output parameter of the *wellpressure* function, in addition to the $f(P_{guess})$ kept from the original code. In this way, the two parameters are sent back to the main script. The code structure of the improved program is presented in figure 7.3. From the figure below, one may notice that the *liquidrate* parameter is no longer included in *main.m*. This is related to this

parameter no longer being used, e.i. it is a dead parameter, as the rate in the new modified code is declared inside the wellpressure function.

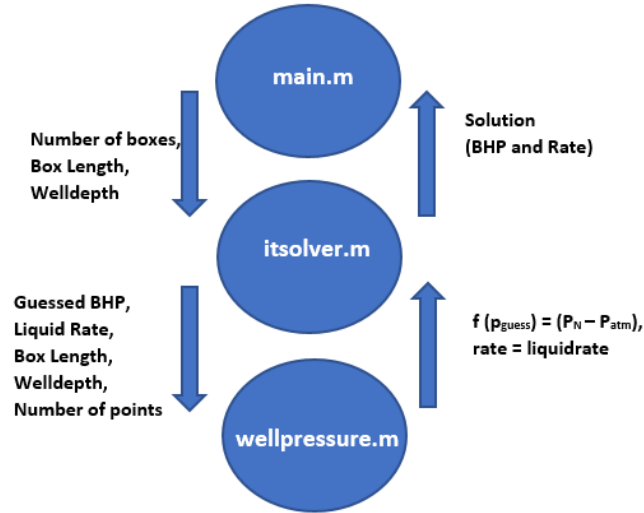


Figure 7.3: *New code structure of the improved model.*

The next step in the modification process, was to include a reservoir model, namely a PI model in the wellpressure script. As this case study is based on single-phase inflow of undersaturated oil, the simple inflow model is employed, defined in wellpressure as;

$$liquidrate = prodinx * (Pres - pbotguess);$$

Here liquidrate is q_o in STB/day, prodinx is the productivity index in STB/day/psi, and the reservoir pressure, Pres, and the guessed bottomhole pressure, pbotguess, are in psi. It should also be mentioned that the PI model operates with liquid flow rate at surface conditions (Petrowiki, 2016). Hence, if the correct BHP is guessed for, liquidrate will be the correct surface rate. Both the BHP and the rate have to be transferred back to the main program.

The inflow model is implemented in Matlab as an if-else statement, meaning that the model is only valid under specified conditions. If the guessed BHP is less than the average reservoir pressure, then the simple inflow equation may be used. Otherwise, the program set liquidrate equal to zero, to prevent an unphysical situation with negative inflow.

In order for the modified simulator to work, it is essential that new parameters such as productivity index and average reservoir pressure, are declared inside the code prior to running the simulation. These additional parameters are defined inside the wellpressure function.

Because the rate determined from the PI model has the unit STB/day, one must include a conversion factor to obtain the rate in ft^3/s . This is essential for the simulation to work, because the calculations requires rates in field units, e.i. ft^3/s . Furthermore, in the end of the wellpressure script, one need to specify that rate = liquidrate. This is vital in order for the wellpressure script to store this parameter, and transfer the found solution back to the itsolver script, and then back to the main program.

A list of new parameters in the wellpressure function after the modifications is presented in table 7.2. It should be noted that the temperature gradient added in wellpressure does not have any connection to the implementation of an inflow model. This parameter is added inside the core as part of the additional improvements made to the code, described in section 6.3.3.

Table 7.2: *New parameters declared in wellpressure.m for case study #2.*

New parameters declared inside the code for case study #2	Unit	Description
prodinx	STB/day/psi	The productivity index
Pres	psi	The average reservoir pressure
tempgrad	F/box	Temperature gradient/box
rate	ft^3/s	The final liquid rate returned

In should be noted that if the water fraction is equal to zero, like in this case study, the final liquid rate will be equal to oil rate.

In addition to the modifications made in the wellpressure function, some adjustments were made to the itsolver function. Although, the structure of the

bisection method is kept the same as in the original code, it was necessary to include the rate as an output from the itsolver function. Moreover, because the rate is added as an output of the wellpressure function, one need to include the rate as an output parameter in all the calls for the wellpressure function inside the itsolver function. The modifications associated with the itsolver script are shown in Appendix A.2.2.

The PI model is only valid at undersaturated oil reservoir conditions, and only when the downhole pressure is lower than the reservoir pressure. For these reasons, in the modified code, the *xguess* was adjusted to a lower value in the itsolver script. In the original code 1000 was used instead of 500, corresponding to a water filled well. As there is no water fraction in the reservoir, the *xguess* is adjusted to fit an oil and gas reservoir. This is not necessarily correct, but it might be a good starting point for the iteration. Therefore,

$$xguess = 500 * 9.81 * welldepth * 0.000145038;$$

It should also be noted that different values of the search interval were tested, in order to determine an appropriate interval and help the bisection method to find a solution. However, one ended up using a search interval of 725 psi in this case study, thus $xint = 725$. When calculating from bottom to top, one must be careful with choosing the correct search interval, because this can lead to stability problems in the simulator. Adjustment to the specified tolerance value in the itsolver was also made. It is believed that finding a solution giving a result within 1 psi error is accurate. The solution is acceptable if $f(P_{guess}) < 1$ psi, hence

$$ftol = 1$$

Result from the simulation

After implementing the inflow model in the program, and conducting all necessary modifications to the original code, a simulation was performed. The program with a simple inflow model gave a solution point flow rate of $0.1057 \text{ ft}^3/\text{s}$, corresponding to 1626.56 bbl/day. The solution was found at a BHP of 3390.7

psi. In addition to the correct rate and BHP, the program also presents various plots of the behaviour of some of the most important parameters in the code, including pressure drop, B_o , B_g , oil density, gas density and liquid holdup. These parameters are plotted against depth, and will be presented in the following.

The first parameter to study is the total pressure drop. Figure 7.4 presents the pressure drop profile in the well. As expected, the pressure at the top of the well is 250 psi, which represents the backpressure defined in the wellpressure script. Moreover, an increase in pressure as we move further down the well is also reasonable. From the figure, one see that the BHP is approximately 3400 psi at the bottom of the well, which is a reasonable result due to the BHP of 3390,7 psi corresponding to the solution point blowout flow rate of 1627 STB/day.

From figures 7.4 and 7.5, one observe that the well is not deep enough for all the gas to be dissolved in the oil. Therefore, it may be small amount of free gas present at downhole conditions. This is reasonable due to the downhole pressure only being approximately 3400 psi. Hence, an empirical inflow model should ideally be applied for such conditions.

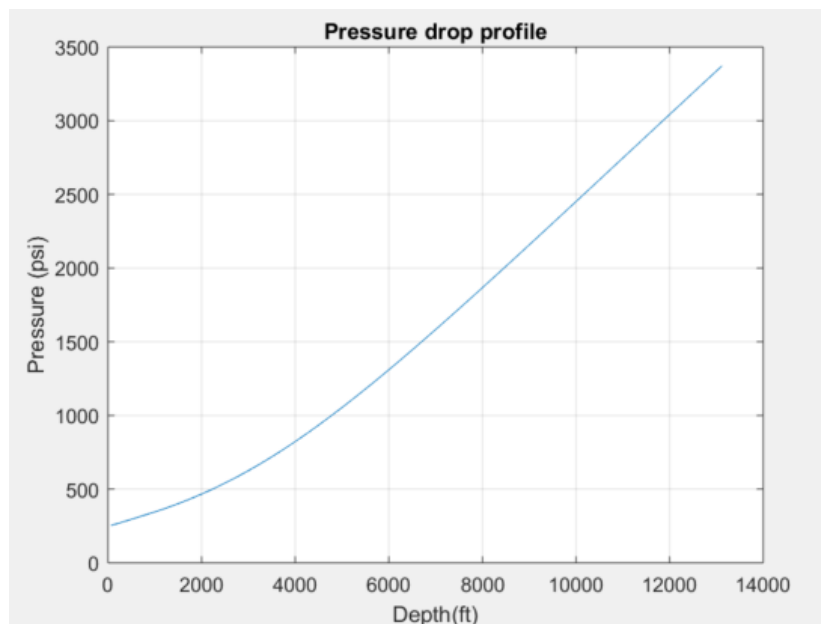


Figure 7.4: *Pressure drop profile in the well.*

The oil formation volume factor profile is provided in figure 7.5. At surface,

the B_o is approximately 1.003 bbl/STB, and at the bottom of the well it is 1.41 bbl/STB. This is reasonable due to the assumption of black oil conditions (see figure 5.2), which shows a characteristics response of B_o for black oil ranging from 1.1 to 1.5 scf/STB. This parameter will increase with depth, since more gas gets dissolved. As the oil move upwards in the well, more and more gas boils out from the fluids, because of the decrease in pressure. This phenomena will cause a decrease in the oil volume as one approaches surface. Therefore, it is natural to experience an increase in oil formation volume factor with depth. The oil formation volume factor profile in our case follows a typical response of such a parameter, compared to expected result in figure 5.5. However, it should be mentioned that we in this case has not reach the point at which all the gas is dissolved in the fluid. At that point it would be expected to notice a minor decrease in B_o . This support our assumption that there is multiphase inflow from the reservoir.

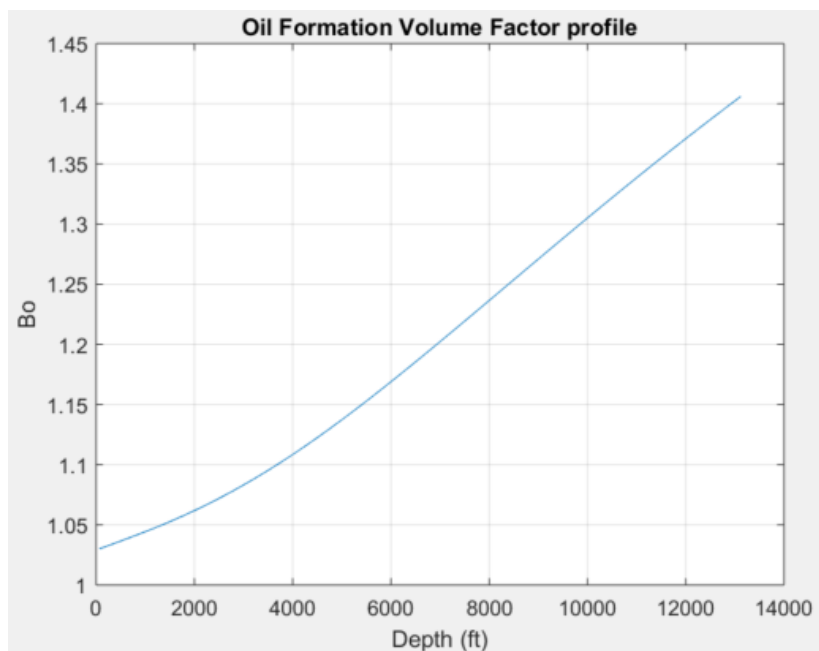


Figure 7.5: *Oil formation volume factor profile.*

The gas formation volume factor profile is presented in figure 7.6. The B_g at surface is 0.06. The figure shows, as expected, that the gas formation volume factor decreases with depth. This trend is general in an oil well, because the free gas gets more compressed the longer down in the well we move. This causes a decrease in the gas volume. From figure 7.6 one notice that the factor gets

closer to zero as one approaches the bottom of the well. Therefore, at downhole conditions B_g is approximately 0.006. This result emphasize our assumption that there is some free gas present at the bottom of the well. Similar to the B_o factor, the gas formation volume factor profile follows the anticipated trend of such a parameter, shown in figure 5.5.

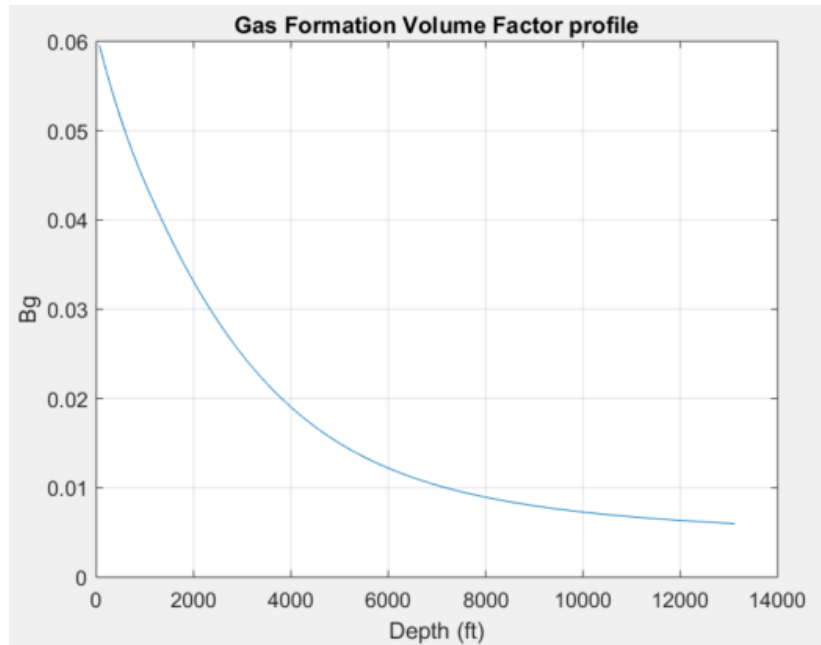


Figure 7.6: Gas formation volume factor profile.

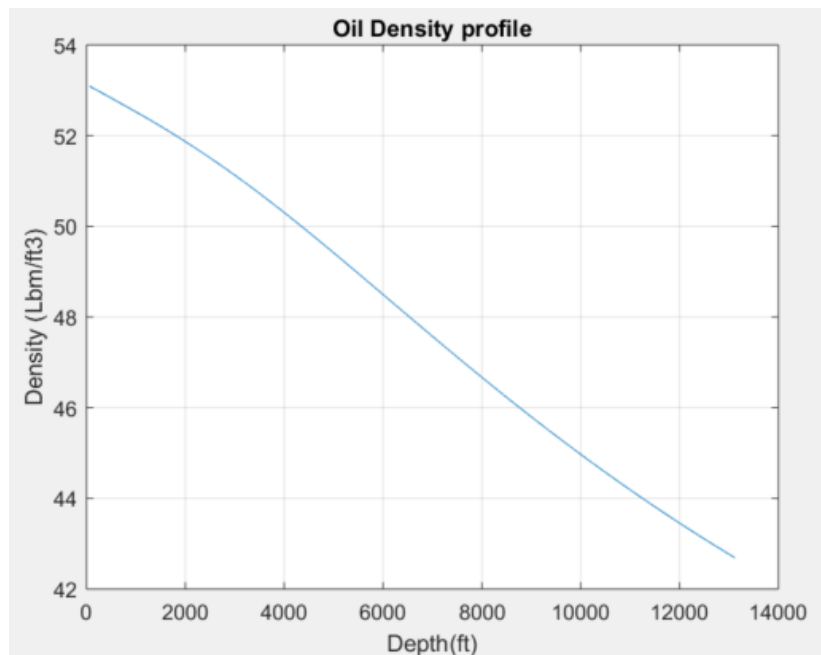


Figure 7.7: Oil density profile.

Figure 7.7 shows the oil density profile for the simulation example. The profile yields an oil density at surface of approximately $53 \text{ lbm}/\text{ft}^3$, and an oil density at downhole conditions of $42.5 \text{ lbm}/\text{ft}^3$. The result is reasonable, due the density being affected by, among others, both temperature and pressure. As one approaches the bottom of the well, both the temperature and pressure increases significantly. Both the increase temperature and pressure causes dissolution of gas, which contributes to a reduction in the density with depth. It is therefore reasonable to observe a decrease in oil density as one move further down the well.

The gas density profile for the simulation example is presented in figure 7.8. The gas density at surface can be obtained from the figure as approximately $0.90 \text{ Lbm}/\text{ft}^3$, while the gas density at the bottom of the well is $8.5 \text{ lbm}/\text{ft}^3$. As discussed above, the density is affected by an increase in both temperature and pressure. This causes the gas to get more compressed deeper down in the well. Therefore, it is reasonable to gain an increase in the gas density with depth.

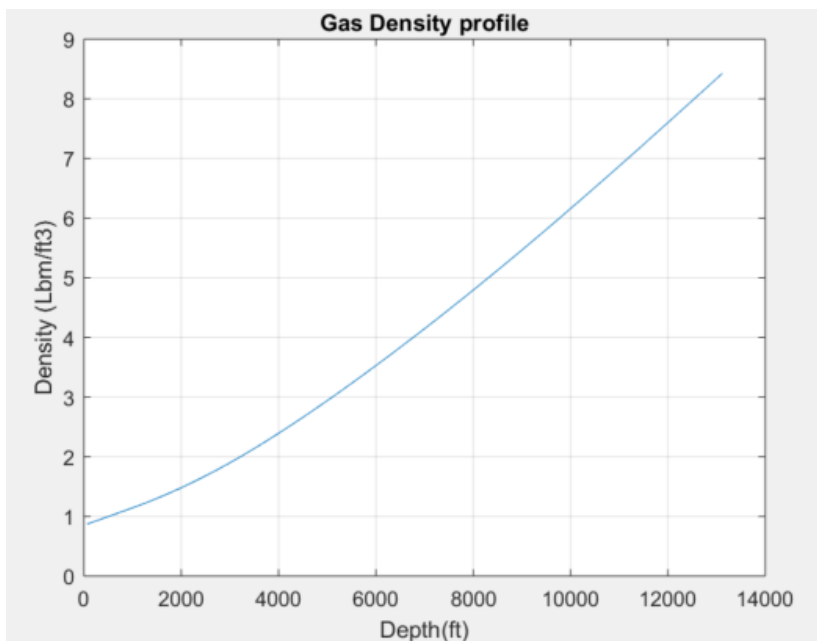


Figure 7.8: *Gas density profile.*

The liquid holdup profile is shown in figure 7.9. At the bottom of the well, the liquid fraction represents approximately 99% of the mixture fluid. This is expected due to the assumption of an undersaturated oil reservoir at this point, where almost all the gas is dissolved in the liquid phase. The figure shows the

presence of small amount of free gas at the bottom of the well, which means that it is on the verge of being correct to assume single-phase inflow. At surface, the liquid holdup is 24%, meaning that approximately 76% of the outlet flow will be gas. This result is reasonable, as it is expected that the gas will boil out of the oil and expand as one approaches the top of the well. It should also be noticed, that the liquid rate is equal to the oil rate, due to the assumption of the water fraction being set to zero. There may be discontinuity in the steady state flow model, causing the strange behaviour of this parameter at a depth of approximately 1000 m. This error may be caused by the wide use of empirical correlations in the model, and regarding the calculation of liquid holdup, namely the Hagedorn & Brown correlation.

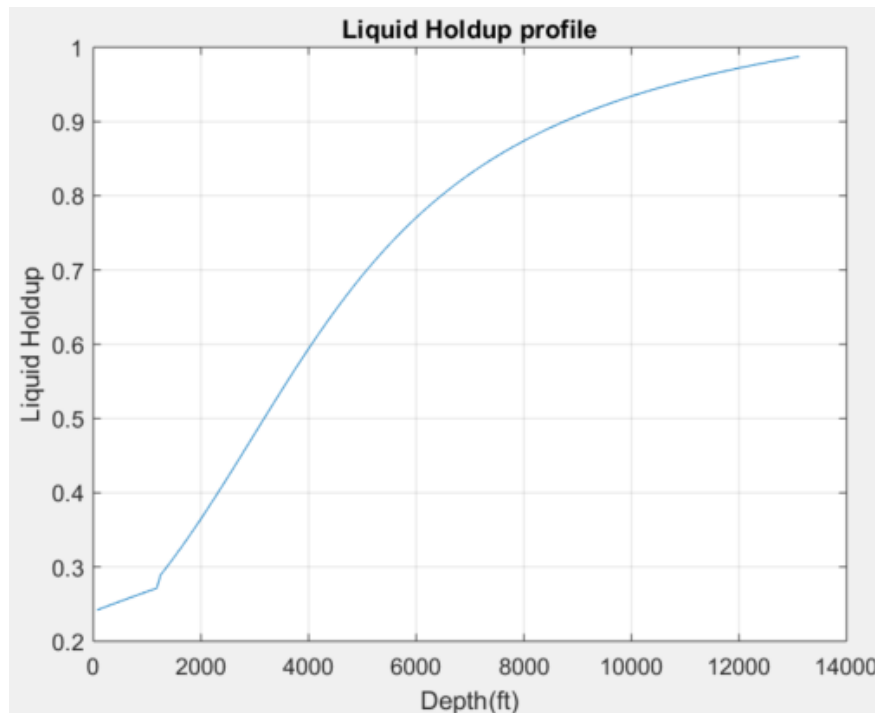


Figure 7.9: *Liquid holdup profile.*

After studying the various plots from the simulation it was found that the inflow from the reservoir in fact is at multiphase conditions. The different graphs show an inflow from the reservoir containing small amounts of free gas. It is believed that the transition between multiphase and single-phase flow occurs at some point between the reservoir and the wellbore. Therefore, the case should ideally be run with an implemented empirical correlation valid for multiphase inflow conditions.

7.2.3 Case Study #3

Finally, an attempt was made to extend the blowout flow rate model to being valid for multiphase inflow cases, as well as for cases with single-phase inflow. As described earlier, only empirical correlations are available for modelling the IPR of multiphase reservoirs. If one successfully include an empirical inflow model, like Vogel (1968) or Fetkovich (1973), in the steady state flow code, it may be possible to simulate inflow at multiphase conditions. Adjustments made to the code in case study #2 are kept unchanged, aside from the simple inflow model being replaced by an inflow model to account for both undersaturated and saturated conditions. In this case study the focus will be on implementing the Vogel equations, as these are most widely used in the petroleum industry. Hence, the goal of this last case study is to include the following conditions and corresponding inflow models inside the wellpressure script.

Condition 1: Single-phase flow, $P_{res} > P_b$ and $P_{wf} > P_b$

$$q_o = J(P_{res} - P_{wf}) \quad (7.1)$$

Condition 2: Multiphase flow, $P_{res} < P_b$ and $P_{wf} < P_b$

$$q_o = q_{o,max} * \left(1 - 0.2 \left(\frac{P_{wf}}{P_{res}} \right) - 0.8 \left(\frac{P_{wf}}{P_{res}} \right)^2 \right) \quad (7.2)$$

Condition 3: Multiphase flow, $P_{res} > P_b$ and $P_{wf} < P_b$

$$q_o = J(P_{res} - P_b) + \frac{JP_b}{1.8} \left(1 - 0.2 \frac{P_{wf}}{P_b} - 0.8 \left(\frac{P_{wf}}{P_b} \right)^2 \right) \quad (7.4)$$

The modifications made to the wellpressure script in case study #3 are shown in Appendix A.2.3. Similar to case study #2, the inflow models are implemented in Matlab as if-else statements, meaning that the models are only valid under specified conditions.

As the conditions for multiphase flow are affected by the bubble point pressure, it was necessary to define the bubble point pressure function before adding the

inflow models. Therefore, the inflow models were moved to after where the bubble point pressure function is called upon in the wellpressure script. Since bubble point pressure calculation is independent of flow rate, this was easily possible. However, the three parameters, oil, gas and water flow rate at surface, as part of the preliminary calculations, have to be conducted after the liquid rate has been defined, and they were therefore moved to after where the inflow models are called upon in the script. As the standard Vogel equation 7.2 is a function of maximum inflow rate, this additional parameter is declared inside the wellpressure script. Similar to case study #2, it is necessary to define the productivity index and the average reservoir pressure, prior to where the inflow models are called upon. Parameters declared in wellpressure.m for case study #3 are summarized in table 7.3.

Table 7.3: *Parameters declared in wellpressure.m for case study #3.*

Parameters declared inside the code for case study #3	Unit	Description
prodinx	STB/day/psi	The productivity index
Pres	psi	The average reservoir pressure
rate	ft^3/s	The final liquid rate returned
qmax	STB/day	Maximum inflow rate

No changes, aside from the ones made in case study #2 were necessary in the main script or in the itsolver function. To test the extended code, three simulation examples were run to check if all the conditions and corresponding inflow models work sufficiently and provide reasonable results.

Example 1: Condition 3

The first simulation example was conducted with the same inputs as the previous case studies. Because it was found from case study #2 that there must be small amounts of free gas present at the bottom of the well, one consider multiphase inflow from the reservoir. Because the pressure in the reservoir is higher than the bubble point pressure, as well as the BHP being lower than the bubble point pressure, an empirical model should ideally be employed. In fact, at condition

3, the modified Vogel inflow model, express by equation 7.4, may be used. The parameters in example 1 are presented in table 7.4.

Table 7.4: *Parameters in example 1.*

Parameter	Value	Unit
P_{res}	5000	psi
J	1	STB/day/psi
GOR	600	scf/STB
P_b	3565.8	psi
p_{wf}	3390.7	psi
rate	1622	STB/day

This would, if the model works correctly, give approximately the same results as in case study #2, because these two studies are based on the same simulation approach. The simulation was performed, presenting a blowout flow rate of $0.1054 \text{ ft}^3/\text{s}$, which corresponds to 1622 STB/day. The solution was found at a BHP of 3391 psi. The result from this example differs by a small value compared to the results in the other case studies. This minor variation is expected due to case study #2 assuming single-phase inflow, when it in fact is multiphase flow from the reservoir. Because of multiphase inflow conditions, the oil rate is slightly lower. The difference between these cases are however negligible, due to the deviation being less than 1%. From the simulation one observe that the program in fact utilizes condition 3 with equation 7.4, e.i. a combination of the simple inflow model and the standard Vogel equation, to calculate the inflow liquid rate. This can be seen by implementing a breakpoint in the simulator inside the inflow model prior to running the simulation.

Example 2: Condition 2

The next test was to see if the modified model is valid for cases where the bottomhole pressure is lower than the bubble point pressure as well as the reservoir pressure being lower than the well pressure, e.i. condition 2. In order to match these conditions, it was necessary to adjust some of the input parameters. Because the bubble point pressure is a function of relative gas density, temperature, API

and GOR, these variables need to be adjusted to ensure that $P_b > P_{res}$. In this example, the GOR was increased, causing an increase in bubble point pressure. For simplicity, the reservoir pressure is kept unchanged, to fit the conditions for the standard Vogel equation. Parameters applied in example 2 are given in table 7.5.

Table 7.5: *Parameters in example 2.*

Parameter	Value	Unit
P_{res}	5000	psi
J	1	STB/day/psi
GOR	1500	scf/STB
P_b	7611.9	psi
p_{wf}	1780.9	psi
rate	2301	STB/day

The simulation was performed, presenting a blowout flow rate of $0.1495 \text{ ft}^3/\text{s}$, which corresponds to approximately 2301 STB/day. The correct solution was found at a BHP of 1781 psi. This result is reasonable for multiphase inflow from the reservoir, as it is expected to notice a drop in well pressure as there is most likely more free gas present in the fluid. This pressure drop leads to a larger pressure difference between the reservoir and the well, causing an increase in the inflow from the reservoir, compared to example 1. From the simulation one notice that the blowout flow rate model in fact uses the standard Vogel equation to calculate the inflow liquid rate. This can be seen by implementing a breakpoint in the program inside the inflow model prior to running the simulation.

Example 3: Condition 1

The final test was conducted to see if the blowout model is valid for cases with single-phase inflow from the reservoir, e.i. condition 1. In such cases the well pressure is higher than the bubble point pressure, while the bubble point pressure is less than the average reservoir pressure. As learned from example 2, increase in GOR causes an increase in bubble point pressure. To ensure single-phase flow it was necessary to run the simulation with a lower GOR value, compared to

those in example 1 and 2. The reservoir pressure is kept unchanged. Hence, the parameters employed in example 3 are presented in table 7.6

Table 7.6: *Parameters in example 3.*

Parameter	Value	Unit
P_{res}	5000	psi
J	1	STB/day/psi
GOR	300	scf/STB
P_b	2012.3	psi
p_{wf}	4573.8	psi
rate	432	STB/day

The simulation was performed, which gave a blowout oil rate of $0.0281\text{ft}^3/\text{s}$, corresponding to 432 STB/day. The solution was found at a BHP of 4573.8 psi. By implementing a breakpoint in the simulator inside the inflow model, one observe that the simulator in fact uses the simple inflow model to compute the solution. In order to check if the inflow from reservoir is single-phase, one may extract the liquid holdup profile for this simulation example, presented in figure 7.10. From the figure one notice that the liquid fraction is equal to one at the bottom of the well, meaning that the reservoir and lower parts of the well are at undersaturated conditions. Free gas is present in the well at 4000 ft and up.

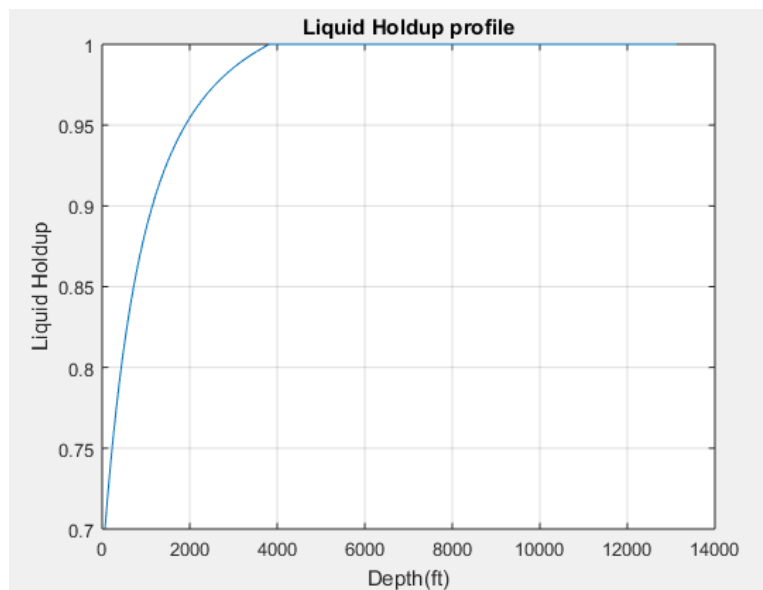


Figure 7.10: *Liquid holdup profile for example 3.*

7.3 Sensitivity Analysis

Various sensitivity studies have been conducted in order to study the effect some of the input parameters have on the blowout oil flow rate. These studies will be presented in this section, and will include analysis of the impact of friction model, GOR, productivity index and the application of backpressure. The sensitivity analysis are based on the input from table 7.1, and is run with the extended code developed in case study #3.

7.3.1 Friction Model

A brief sensitivity study was performed with the intention of analysing how the choice of friction factor model would affect the results. A simulation with input variables as in case study #3 example 1, was therefore performed with the Blasius equation (eq. 5.61) for turbulent flow, rather than the Chen equation (eq. 5.62). Thus, the Chen equation is replaced with the following expression;

$$f = 0.052 * Re^{-0.19} \quad (5.61)$$

Adjustments made to the friction pressure loss function are shown in Appendix A.2.6.

With the purpose of only analysing the impact of friction model, the other parameters were kept unchanged. A simulation with the Blasius equation provided a solution point flow rate of $0.1044 \text{ ft}^3/\text{s}$, which corresponds to 1607 bbl/day. Unlike the other case studies, the solution was found at a BHP of 3399.5 psi. Hence, the change of friction model provided a decrease in blowout rate, while consequently an increase in BHP. However, the differences in results between these two friction factor models are relatively small for this simulation case. The author therefore conclude that it is sufficient to employ the Chen expression for the simulation considered here. However, for other geometries and rates, the choice of friction factor should be investigated further.

7.3.2 GOR

As discussed earlier, the bubble point pressure is highly affected by the gas-oil ratio. It was noticed that an increase in GOR caused an increase in P_b . Because of the large impact of this specific parameter, it would be interesting to study how the GOR would influence the oil flow rate of a blowing well. In this sensitivity study, all the variables are kept as in case study #3 example 1, except for variations in the GOR parameter. The result from this analysis are shown in figure 7.11. The figure shows that an increase in GOR value causes an increase in blowout flow rate of oil. This trend is reasonable because a higher bubble point pressure in the well will lead to more free gas in the well, reducing the bottomhole pressure, which consequently leads to more inflow from the reservoir.

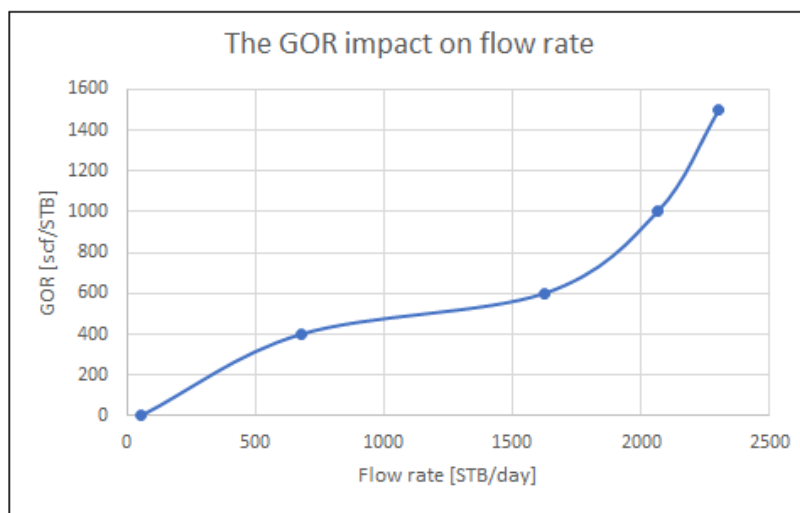


Figure 7.11: Sensitivity analysis of the impact of GOR.

7.3.3 Productivity Index

Because both the empirical inflow models and the simple inflow model are depending on knowledge about the productivity index, a sensitivity analysis was performed to observe how different values of J would affect the oil flow rate of a blowing well. As for the other sensitivity analysis performed in this thesis, one only make adjustments in the productivity index parameter when running the various simulations. Other parameters in the simulation are kept identical to the ones in case study #3 example 1. Several simulations were performed for different values of J , and the results from these simulations are presented in figure 7.12.

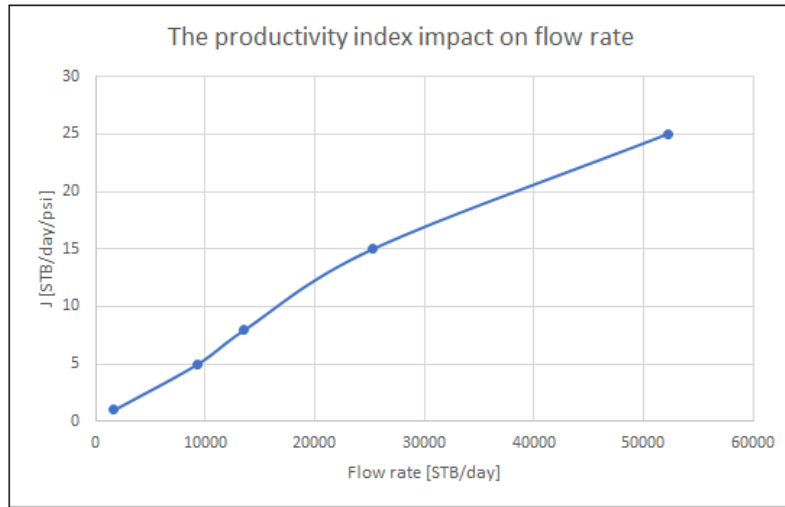


Figure 7.12: *Sensitivity analysis of the impact of productivity index.*

The figure shows that an increase in productivity index causes quite large increase in blowout rate, meaning that the flow rate is highly affected by this parameter. This is expected due to the fact that the productivity index describes the wells ability to produce.

7.3.4 Outlet Pressure - The real pressure at surface

In order for the simulation to work it is essential to state the outlet pressure, namely the boundary condition. This is the pressure we have to ensure that the model reaches at surface. As discussed earlier, there are two ways of defining the boundary condition. The real pressure at surface may be equal to the atmospheric pressure, e.i. 14.7 psi, or it may be set equal to an applied backpressure. The latter being used in the previous case studies conducted in this thesis.

In general, there would be atmospheric pressure at the surface, but in case of a seabed blowout, there would be a backpressure for instance caused by the hydrostatic pressure of seawater. According to Yuan et al. (2017), the application of backpressure on top of the riser has the potential to dampen the unloading of a riser significantly. It should be noted, that the technology established for riser unloading, is more an attempt to prevent the unloading developing into a full blowout, and thus reduce the discharge rate (Yuan et al., 2017).

A test was therefore performed to study the effect of having a backpressure in our simulation examples. If the simulation is run with the assumption that the well is open to the atmosphere, e.i. $P_{surf} = 14.7$ psi, one obtain a flowing rate of $0.1718 \text{ ft}^3/\text{s}$ at 2130.67 psi, corresponding to 2644 STB/day. Furthermore, different values of applied backpressure were tested in the simulation, which can be seen in figure 7.13. Different values of backpressure is caused by variation of water depths.

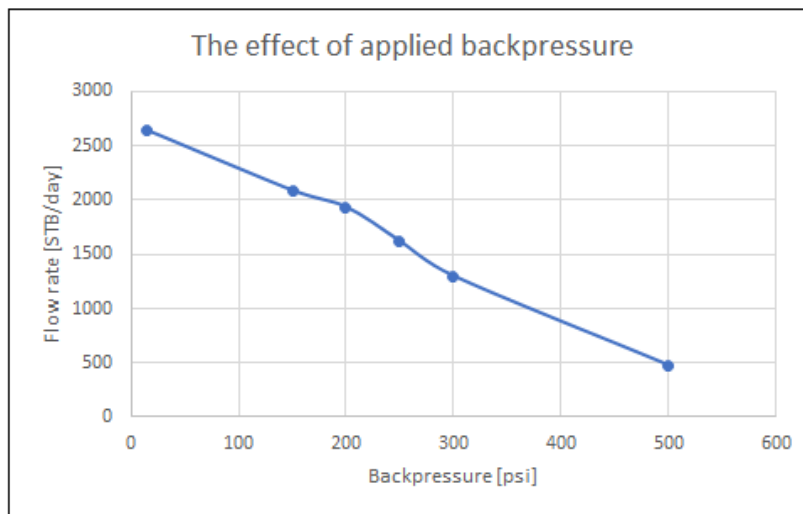


Figure 7.13: Sensitivity analysis of the effect of applying a backpressure at surface.

From the figure above its clear that application of a backpressure has the potential of reducing the blowout flow rate significantly. The result therefore follows the trend in the studies conducted by Yuan et al. (2017) and Liu et al. (2015). Hence, subsea blowouts with an annular flow path will most likely have a lower discharge rate than surface blowouts.

7.4 Discussion of Results

After conducting the different case studies, their corresponding results were compared for validation of the new improved blowout flow rate model. A summary of the results from the various case studies are presented in table 7.7. It should be mentioned that only the result from example 1 in case study #3 is considered here, due to this example being based on the same input parameters as the two

other case studies.

Table 7.7: *Result from the case studies.*

Case study	Rate [STB/day]	BHP [psi]
#1	1600	3390
#2	1627	3390.7
#3	1622	3390.7

The simulation example run with the base code developed in the previous chapter, gave an actual blowout rate of approximately 1600 bbl/day at a BHP of 3390 psi. The approach used in case study #1 is a combination of techniques used in BlowFlow, Gomes (2016) and Gomes et al. (2015). Although the liquid rate at surface conditions is defined in the main program, the model runs the simulation by utilizing a shooting technique from the bottom of the well and up. The solution is then found at the intersection point between the IPR and TPR curves.

The two other case studies were conducted with an alternative approach, where inflow models were incorporated directly in the solution algorithm while still utilizing the shooting technique from bottom to top. These studies provided, based on the same input parameters as case study #1, a solution point flow rate of 1627 STB/day and 1622 STB/day, respectively. The correct rate in both cases was found at a BHP of 3390.7 psi. Hence, the case studies run with the modified code provided results with less than 1% deviation. Therefore, the improved models developed in case studies #2 and #3 are considered compatible for this specific simulation case. This means that the modified model can estimate actual blowout flow rate with a high accuracy, provided the conditions taken into consideration in this specific case. However, it should be mentioned, that in order to increase the robustness of the simulator and gain validation of the model, the results should be compared to other similar models or field data.

When conducting the two first case studies, it was found that the inflow from the reservoir was in fact at multiphase conditions. By analysing the different figures produced by the program, one notice small amounts of free gas present

at downhole conditions. Hence, the well is not deep enough for all the gas to be dissolved in the oil. In these studies the transition between single-phase and multiphase conditions occur at some point between the reservoir and the wellbore, causing the model to present reasonable results regardless of inflow model being used. It should also be mentioned that the bubblepoint pressure of 3565.8 psi in case studies #1 and #2, was higher than the bottomhole pressure found by the model. The author would like to emphasize, that the small difference in results may be caused by the bubble point pressure being so close to the BHP, that the simple inflow model may give accurate enough result. This strengthen our assumption of multiphase inflow from the reservoir. An empirical inflow model should ideally be utilized at such conditions. Therefore, the last case study was conducted with the aim of making the simulator valid for both single-phase and multiphase inflow conditions.

In the attempt of extending the code to cover multiphase inflow in case study #3, the code was initially run with same input as in the other case studies as a test to see if the modified model gave similar result. Example 1 was therefore conducted by using the modified Vogel equation. As discussed earlier the deviation in result was less than 1%. The next step was to see if the improved code worked at other conditions as well. Therefore, simulations were run with single-phase inflow conditions (ex. 3), as well as multiphase inflow conditions where the reservoir pressure is lower than the bubble point pressure (ex.2). The simulation examples in case study #3 gave the results shown in table 7.8.

Table 7.8: *Result from the examples in case study #3.*

Example	Condition	Rate [STB/day]	BHP [psi]
1	Multiphase flow $P_{res} > P_b$	1622	3391
2	Multiphase flow $P_{res} < P_b$	2301	1781
3	Single-phase flow $P_{res} > P_b$	432	4574

It was found that the extended code works for both multiphase and single-phase inflow scenarios. It was determined from the simulation that the program employs correct inflow model depending on the conditions in the well. This was seen by implementing a breakpoint in the simulation inside the inflow model prior to running the simulation. It seems reasonable that there will be a lower well pressure at multiphase conditions because there will be more free gas present in the well, consequently causing more inflow of both oil and gas from the reservoir.

From the study it was found that both solution strategies of computing the blowout rate are accurate. They provide similar results for similar simulation examples. Although the simulations provided reasonable results, it is difficult to determine if they are accurate or not, due to the lack of comparable studies or reservoir data. Because the simulations are based on theoretical data resembling a well by using deterministic inputs, it is difficult to determine if the model illustrate the reality. The approach used in case studies #2 and #3, of including an inflow model inside the code, is undoubtedly the most efficient solution strategy as it saves computational time. This is the case as long as the model is based on a procedure of calculating from bottom to top. In addition, it is believed that the procedure in case studies #2 and #3 is more refined as the model finds the exact point of intersection between the inflow and outflow curves directly by numerical iterations. The strategy in case study #1 leaves room for human error in reading the intersection point between the IPR and TPR curves. This error may be eliminated by extracting this intersection point by performing numerical calculations with cubic spline interpolation, which is the approach used in BlowFlow.

It should also be mentioned that the program experienced problems finding solutions for some of the flow rates tested in case study #1. It is believed that the problem lays in the bisection method, and that some of the rates may cause discontinuities in the model, making the program run in an endless loop. This error may be caused by the wide use of empirical correlations in the simulator. However, because this was only a problem for a few of the rates, the problem was easily solved by adjusting the search interval for these specific rates, which assisted the model in finding a solution. Studies shows that the program, or more

precisely the bisection method, is highly sensitive to choice of search interval.

Because this thesis presents and tests two possible ways of performing blowout modelling, namely by using the BlowFlow engine or by using the developed blowout flow rate model, an attempt was made in comparing the results from the case studies to a similar simulation example in BlowFlow. It is believed that possible similarities in the results can improve the validation of the modified model. In the attempt to produce a similar case in BlowFlow, it was quickly determined that comparisons between the two different programs would be difficult. The author would like to emphasize that this conclusion was drawn based on BlowFlow being more complex and refined, due to a larger set of inputs for the simulation, as well as this engine simulating probabilistic blowouts. There is reason to believe that the blowout flow rate model modified in this thesis has a long way to go, compared to the refined BlowFlow engine with years of testing.

7.5 Additional Improvements

A lot of effort has been put into checking and documenting the original code presented by Gomes (2016). This resulted in various modifications to the original code, most of which have been addressed earlier in this thesis. Additional improvements made to the code will be further described in this section, and may be seen in Appendix A.2. It should be mentioned that the biggest improvement made at this point, is that it is now possible to determine the correct oil flow rate of a blowing well directly from the program by utilizing various inflow models depending on the conditions in a well.

The function `ffric`, is simply removed in the improved code, because there is no need for this function in the simulation as the function is represented in the function `dpdfric`. In addition, the author noticed some confusion in the base code in the function `FVFo`, between saturated and undersaturated oil. For clarity, saturated oil is defined as when $P_{wf} < P_b$, and undersaturated oil is present when $P_{wf} > P_b$. This has been changed in the new improved code.

To summarize the improvements made to the original code by Gomes (2016) to this point, all changes made are listed below.

- All inputs are defined in field units.
- Inflow models implemented directly in the code to simulate both single-phase and multiphase inflow from the reservoir.
- The code is valid for both annular and tubular geometry.
- The temperature model was replaced.
- The parameter *Welldepth* is included as output from *main.m* and *itsolver.m*.
- Considers a transitional zone between laminar and turbulent flow.

7.6 Further Work

Although the developed blowout flow rate model run adequately and present reasonable results, the simulator has room for additional improvements. Due to lack of similar simulator or available field data, it is difficult to obtain validation of the result presented by the model. Hence, there may be lack in the accuracy of the model. There are some points the author would recommend as future work to increase both the accuracy and robustness of the model. A brief description of these recommendations are presented below.

- One of the major challenges when performing simulations is to base the simulation on correct assumption. Factors affecting the blowout rate are uncertain and often unknown. Therefore, to increase the validation of the simulator, the author recommended to invest more time in testing the result with similar cases. This could for example be done by performing comparison with other simulators or preferably field data for production wells. Parameters that match real-life conditions, will provide more realistic results. In addition, more effort should be put into exploring why the developed model did not present similar result as the BlowFlow engine.
- Include a function for the productivity index, as this parameter is affected by various factors. Although, in this thesis, the productivity index is set as a fixed value, it may be defined as a function of effective horizontal

permeability, pay zone thickness, wellbore radius, and skin factor (Guo et al., 2008). This is similar to the approach in BlowFlow, if a OilBasic model is chosen. J is expressed as a function by equation 7.6 (Guo et al., 2008).

$$J = \frac{kh}{141.2B_o\mu_o\left(\ln\frac{r_e}{r_w} - \frac{3}{4} + S\right)} \quad (7.6)$$

- The viscosity of both oil and gas are in the modified code specified as fixed values in the wellpressure script. In real life the viscosity depend on both pressure and temperature, and should therefore ideally be presented as a function in the program, similar to the approach in the BlowFlow engine.
- By utilizing the modified Hagedorn & Brown empirical correlation, the developed simulator does not take into account different flow regimes. The pressure and flow rate are highly affected by the flow regime present in the pipe. Hence, various flow regimes like bubble, slug, churn and annular flow, should ideally be considered in the model to increase the accuracy of the output of the model. The author recommend to include other correlation methods, like Orkiszewski (1967), to calculate the multiphase inflow parameters, or use mechanistic models, like for instance Lage and Time (2000) to perform the calculations. Mechanistic model determine the flow regimes in each box, e.i. the actual type of slip and friction model will be computed based on the flow regime in each box.
- The developed model is only valid for vertical wells. It is important that multiphase models are valid for vertical, inclined and horizontal cases. Therefore an effort should be put into extending the application of the simulator to horizontal/inclined wells, where the reservoir is producing along the horizontal part. An alternative way of making this possible is to include a loop inside the code that calculates the liquid rate in each cell starting from the bottom of the well. For each new cell, the new liquid rate is computed based on using a PI model for that cell, in addition to adding the liquid rate from the previous cell. Inside this loop a PI model for all the cells in the horizontal part of the well must be implemented. Hence, to account for

single-phase flow, the following expression may be added in the code.

$$liquidrate = prodx(P_{res} - P(i))$$

However, for this model to work one need to introduce the inclination as a parameter for the different nodes. This parameter must be used in the hydrostatic pressure loss. One should also introduce a parameter TVD of the well, to account for the depth differences affected by the inclination. An initial test example could be constructed where 1/3 of the nodes are vertical, 1/3 are set to 45 degrees, while 1/3 of the segments are placed horizontally in the reservoir. In the horizontal part, the inflow is expected to be uneven. The well pressure will be higher at the toe of the well (end of well) than at the heel (where the well enters the reservoir). This pressure difference is expected due to more friction acting at the toe compared to the heel. Hence, there will probably be more inflow at the heel, if all other reservoir parameters are kept the same.

- The model experience stability problems regarding finding solutions for some of the rates tested, due to possible discontinuities in the model. These discontinuities are most likely caused by the bisection method and by the wide use of empirical correlations. Applications of mechanistic models in the simulator may eliminate these stability problems, making the model even more robust.
- By applying the shooting technique from the bottom of the well and up, the model gets more sensitive to choosing the right search interval for determining the initial guess of BHP. In addition, the model gets more sensitive to discontinuities in the wellpressure function. This may be solved by using the calculation approach used in BlowFlow. Therefore, an interesting future study would be to study which of the mentioned approaches that are most cost-effective, especially if there is a need to reduce the computational time of the simulator.
- A possible improvement would be to implement and run the simulation with the implicit Colebrook model (5.60), which may increase the accuracy of the solution.

8. Conclusion

A simulation example has been performed using the Oliasoft Blowout Simulator. This engine illustrates a possible approach of simulating blowout rate, volume and duration, which is essential for oil spill preparedness analysis. The BlowFlow model is based on varying the outflow rate at surface conditions, and calculate from top to bottom. This is utilized to numerically calculate the corresponding BHP. The correct solution is found at the intersection point between the IPR and TRP curves. With a Monte Carlo Simulation as framework, and by employing a predictive Bayesian approach, BlowFlow takes into account the uncertainty related to reservoir input parameters, and thus simulate a probabilistic blowout.

In the second part of the thesis, a numerical simulator based on the black oil model, multiphase flow model, simple friction model and inflow model, was developed in Matlab with the purpose of simulating blowout rates. The starting point was a steady state flow model developed by Gomes (2016).

The studies conducted show that in the extended code it is possible to include various inflow models, to numerically calculate the blowout oil flow rate at both multiphase and single-phase inflow conditions. This was possible because the simulator is based on an initial guess of the BHP, where the shooting technique starts at the bottom of the well and works upwards until the outlet is reached. Hence, the method uses iteration to determine the actual BHP. The simulator employs adequate inflow model depending on the conditions in the well. In case of single-phase inflow, one observe undersaturated conditions at the reservoir and at lower parts of the well, in addition to lower inflow rates. It seems reasonable that at multiphase inflow conditions, there would be more free gas present in the well, leading to a lower well pressure, consequently causing more inflow of both

oil and gas from the reservoir. Due to lack of similar simulators or preferably field data, it is difficult to determine if the modified model is accurate or not.

It is possible to determine blowout rate from two different approaches. This is the case for our simulation examples based on theoretical data resembling a well by using deterministic inputs, which makes it difficult to determine if the model illustrates the reality. The first approach is based on assuming various outflow rates at surface condition, and finding the corresponding bottomhole pressure by utilizing a shooting technique from the bottom to top. The correct rate and BHP are found at the intersection point between the IPR and TPR curves. This can be done either manually, as in case study #1, or by finding it by numerical means, like in BlowFlow. The second approach is based on guessing the BHP and calculate upwards, until the calculated outlet pressure at surface satisfy the physical outlet pressure. In this approach, the inflow rate and correct downhole pressure are found directly during the calculation process. The method of integrating an inflow model directly in the program, is without doubt the most efficient solution strategy as it saves computational time. This is the case as long as the modified model is based on a procedure of numerical calculation from bottom to top. The computational time may be even more reduced with the use of the approach in BlowFlow. What approach is most computational efficient may be worth a future study.

Much effort has been put into reviewing and documenting the original code by Gomes (2016), which resulted in various improvements made to the base code. Taking the hydraulic diameter into consideration in the various functions, make the program valid for both annular and tubing configuration. Numerical stability problems were obtained when making the well deeper. As a result the temperature model was substituted with a model that calculates the fixed temperature profile in the well based on specified surface and downhole temperature, such that each box has a fixed temperature. Because the black oil model is included, the various input parameters are now defined in field units, rather than SI units. The welldepth parameter is included as output from both main and itsolver scripts, and the modified model considers a transitional zone between laminar and turbu-

lent flow. All these modification improve the simulator significantly.

The sensitivity analysis performed show that the blowout rate is highly affected by various factors. An increase in the GOR value caused an increase in the blowout flow rate of oil. The reason for this effect is that a higher bubble point pressure will lead to more free gas in the well, reducing the BHP, causing even more inflow from the reservoir. As the productivity index describes the wells deliverability, an increase in this values causes large increase in flow rate. It was found that the potential release point has a great impact on the flow rate and thus the oil-spill. A seabed blowout, will most likely cause a lower discharge rate than surface blowouts. This was also seen in the BlowFlow simulation example. However, cases with very high flow velocity towards the top of the well may lead to a higher rate from a seabed blowout.

Regarding the future work, the author would like to emphasize the advantages of making the model valid for inclined and horizontal wells, where the reservoir is producing along the horizontal part. To increase the validation of the simulator, an effort should be put into testing and comparing the result with similar simulators or field data.

References

- Adams, A., Gibson, C., and Smith, R. (2010). Probabilistic Well-Time Estimation Revisited. SPE Drilling and Completion 25(4). SPE 119287-PA.
- Add Energy (2018). OLGA-WELL-KILL <https://static1.squarespace.com/static/55d2df17e4b0ada576ce3d06/t/5677beb87086d7c6a3dc5436/1450688184041/0lga+Well+Kill.pdf> [Accessed 13.02.19].
- Arild, Ø., Fjelde, K., Merlo, A., Daireaux, B., and Løberg, T. (2008). BlowFlow - a New Tool Within Blowout Risk Management. Paper IADC/SPE 114568 Presented at the IADC/SPE Asia Pacific Drilling Technology Conference and Exhibition. Jakarta, Indonesia, 25-27 August.
- Baker, O. and Swerdloff, W. (1956). *Calculation of Surface Tension 6 - Finding Surface Tension of Hydrocarbons Liquids. Oil Gas J: 125. January 2.*
- Beggs, H. D. (1987). Oil System Correlations. In Petroleum Engineering Handbook, ed. Howard B. Bradly, Chap. 22, Richardson, Texas: Society of Petroleum Engineers. SPE-1987-22-PEH.
- Belayneh, M. A. (2018a). *Advanced Well Engineering, Chapter 5: Well Control Lecture - PET580, UIS.*
- Belayneh, M. A. (2018b). *Advanced Well Engineering, Chapter 8: Drilling Equipment Lecture - PET580, UIS.*
- Blasius, P. (1913). *Das Aehnlichkeitsgesetz bei Reibungscorgangen in Flussigkeiten, p. 1-41. Springer-Verlag. Forschungsheft 131.*
- Brill, J. and Mukherjee, H. (1999). *Multiphase flow in wells. Henry L.Doherty Memorial Fund of AIME, Socceity of Petroleum Engineers, Richardson, Texas.*
- Cacho, B. (2015). A Study on different two-phase flow correlations used in geothermal wellbore modelling. United Nations University. <https://orkustofnun.is/gogn/unu-gtp-report/UNU-GTP-2015-08.pdf>, [Accessed 12.04.19].
- Chen, N. (1979). An Explicit Equation for Friction Factors in Pipes. Industrial and Engineering Chemistry Fundamentals, 18, p.296-297 .
- Coats, K., Thomas, L., and Pierson, R. (1998). Compositional and Black Oil Reservoir Simulation. SPE Reservoir Evaluation & Engineering 1(4): 372-379. SPE-50990-PA.
- Colebrook, C. and White, C. (1937). Experiments with Fluid Friction in Roughenes Pipes. Imperial College, London, p. 367-381. <https://royalsocietypublishing.org/doi/pdf/10.1098/rspa.1937.0150>. [Accessed 21.05.19].
- Danielson, T. J., Brown, L. D., and Bansal, K. M. (2000). Flow Management: Steady-State and Transient Multiphase Pipeline Simulation. Paper OTC 11965 Presented at the Offshore Technology Conference, Houston, Texas, 1-4 May.

- DNV (2010). Environmental Risk Assessment of Exploration Drilling in Nordland VI. Report no. 2010-04-20 prepared for Oljeindustriens Landsforening. <https://www.norskoljeoggass.no/contentassets/bb23a4cb05ed46b4b05dd9312a8b5409/environmental-risk-assessment-of-exploration-drilling-in-nordland-vi.pdf>, Accessed[23.05.19] .
- Dranchuk, P., Purvis, R., and Robinson, D. (1973). Computer Calculation Of Natural Gas Compressibility Factors Using The Standing and Katz Correlation. Presented at the Annual Technical Meeting, May 8-12, Edmonton. Published by the Petroleum Society of Canada, PETSOC-73-112.
- Economides, M., Hill, A., and C.E., E. (1994). *Petroleum Production Systems. 1st Edition. Prentice Hall Petroleum Engineering Series.* .
- EPA (1999). Understanding Oil Spills And Oil Spill Response. United States Environmental Protection Agency. Office of Emergency and Remedial Response. <https://www.epa.gov/sites/production/files/2018-01/documents/ospguide99.pdf>, [Accessed 07.02.19].
- Erichsen, L. L. (2019). User manual: Oliasoft Blowout Simulator. Oliasoft. .
- Fetkovich, M. (1973). The Isochronal Testing of Oil Wells. Paper SPE 4529 Presented at the 48th Annual Fall Meeting of the Society of Petroleum Engineers of AIME, Las Vegas, Nevada, 30 September - 3 October, 1973.
- Fjelde, K. (2016). *Compendium Modelling of Well Flow -PET510, UIS.*
- Fjelde, K. (2017a). *Directional Drilling: lecture 2, Drilling and Operation - PET505, UIS.*
- Fjelde, K. (2017b). *Numerical Solution Techniques for Nonlinear Equations and Applications within Petroleum Engineering - PET510, UIS.*
- Ford, E. (2012). BlowFlow - Technical Report. Report IRIS - 2012/051, Bergen, Norway.
- Gabolde, G. and NGUYEN, J. (2006). *Drilling Data Handbook. Eighth Edition. Editions TECHNIP, IFP PUBLICATIONS, Paris.*
- Gerald, C. and Wheatley, P. (2004). *Applied Numerical Analysis, Pearson, Seventh edition, Boston, United States.*
- Gomes, D. (2016). *Implementation of the black oil model on a base code, PhD course report, UIS.*
- Gomes, D., Naccache, M. F., and Campos, W. (2015). Simplified steady-state numerical solution of multiphase flow in oil production wells. Presented at the 23rd ABCM International Congress of Mechanical Engineering. Rio de Janeiro, Brazil, 6-11 December.
- Guo, B., Sun, K., and Ghalambor, A. (2008). Well Productivity Handbook. Gulf Publishing Company. Houston, Texas. . Technical report, Gulf Publishing Company.
- Hagedorn, A. and Brown, K. (1965). Experimental Study of Pressure Gradients Occurring During Continuous Two-Phase Flow in Small-Diameter Vertical Conduits. Journal of Petroleum Technology 17(4): 475-484. SPE-940-PA .
- Halle, S. (2010). Brønnkontroll. Vett & viten els, 3 utg. Norge. ISBN 9788231500155.
- Herbst, L. (2017). Macondo Blowout, Lessons learned for prevention and mitigation. Presentation by the Bureau of Safety and Environmental Enforcement. http://www.ptil.no/getfile.php/1345593/PDF/Seminar%202017/Lars%20Herbst_%20Macondo.pdf, [Accessed 07.02.19].

- Holand, P. (1996). Offshore Blowouts, causes and trends. Doctoral Dissertation, Norwegian Institute of Technology, Department of Production and Quality Engineering. Trondheim, Norway. <https://www.osti.gov/etdweb/servlets/purl/481374>. [Accessed 11.02.19].
- Holand, P. (2017). Loss of Well Control Occurrence and Size Estimators, Phase 1 and 2. Final Report, ExproSoft, BSEE. <https://www.bsee.gov/sites/bsee.gov/files/tap-technical-assessment-program/765aa.pdf>. [Accessed 12.02.19].
- IPIECA (2015). Oil Spill Preparedness and Response: An introduction. International Petroleum Industry Environmental Conservation Association. IOGP/IPIECA Report 520. http://www.oilspillresponseproject.org/wp-content/uploads/2017/01/Oil_Spill_Preparedness_Response_Introduction_2016.pdf, [Accessed 10.06.2019].
- IRIS (2015). Blowout - A new tool within blowout risk management., <http://www.iris.no/Energy/BlowFlow%20-%20factsheet.pdf>, [Accessed 05.01.19].
- ITOPF (2018). Containment and Recovery of oil spilled (Response Techniques). International Tanker Owners Pollution Federation. <https://www.itopf.org/knowledge-resources/documents-guides/response-techniques/containment-recovery/>, [Accessed 12.02.19].
- Karlsen, H. and Ford, E. P. (2014a). BlowFlow - Next Generation Software for Calculating Blowout Rates. Paper IPTC 17622 Presented at the International Petroleum Technology Conference. Doha, Qatar, 20-22 January.
- Karlsen, H. and Ford, E. P. (2014b). BlowFlow - Next Generation Software for Calculating Blowout Rates. Paper SPE 169226 Presented at the SPE Bergen One Day Seminar. Grieghallen, Bergen, Norway, 2 April.
- Lage, A., Jacinto, C., Martins, F., Vanni, G. S., Santos, O., and Moreiras, J. R. F. (2006). Blowout Contingency and Risk-Reduction Measures for High-Rate Subsea Gas Wells in Mexilao. Paper IADC/SPE 99164 Presented at the IADC/SPE Drilling Conference. Miami, Florida, USA, 21-23 February.
- Lage, A. C. and Time, R. (2000). Mechanistic Model for Upward Two-Phase Flow in Annuli. Paper SPE 63127 Presented at the SPE Annual Technical Conference and Exhibition, Dallas, Texas, 1-4 October .
- Larsen, L. (2001). General Productivity Models for Wells in Homogeneous and Layered Reservoirs. Paper SPE 71613 Presented at the SPE Annual Technical Conference and Exhibition, New Orleans, Louisiana, USA, 30 September- 3 October.
- Liu, Z., Samuel, R., Gonzales, A., and Kang, Y. (2015). Blowout well-flow simulation for deepwater drilling using high-pressure/high-temperature (HP/HT) Black-Oil Viscosity Model. Paper SPE/IADC 173074 Presented at the SPE/IADC Drilling Conference and Exhibition, London, UK, 17-19 March.
- LOVDATA (1981). Pollution Control Act of 13 March 1981 No.6 Concerning Protection Against Pollution and Concerning Waste. https://lovdata.no/dokument/NL/lov/1981-03-13-6#KAPITTEL_6, [Accessed 11.02.19].
- National Commission (2011). *DEEP WATER, The Gulf Oil Disaster and the future of offshore drilling. National Commission on the BP Deepwater Horizon Oil Spill and Offshore Drilling.* <https://www.nrt.org/sites/2/files/GPO-OILCOMMISSION.pdf> [Accessed 29.01.19].
- Newendorp, P. and Schuyler, J. (2000). Decision Analysis for Petroleum Exploration, Planning Press, 2nd Edition.

- Nilsen, T. (2014). Guidance on calculating blowout rates and duration for use in environmental risk analysis. Norwegian Oil and Gas Association. <https://www.norskoljeoggass.no/contentassets/d6c1d516cc4945358fea471a8610becf/guidance-blowoutrates-with-supp-report.pdf>, [Accessed 02.01.2019].
- Norsk Olje og Gass (2013). Veiledning for miljørettede beredskapsanalyser, Rev. 4. <https://www.norskoljeoggass.no/contentassets/e9ab317bb1d44606b95ff4e2e370d03a/veiledning-beredskapsanalyser-2013.pdf>, [Accessed 13.02.19].
- NORSOK D010 (2013). Well integrity in drilling and well operations, NORSOK Standard D-010 Rev.4,2013. Standards Norway. <http://www.npd.no/Global/Norsk/5-Regelverk/Skjema/Bronnregistrering/NORSOK-D-010-2013-Well-integrity-and%20Well-operations-rev%204.pdf>, [Accessed 04.02.19].
- Oldenburg, C. M., Freifeld, B. M., Pruess, K., Pan, L., Finsterle, S., and Moridis, G. (2012). Numerical Simulations of the Macondo Well Blowout Reveal Strong Control of Oil Flow by Reservoir Permeability and Exsolution of Gas. PNAS, Berkley, CA, December 11.
- Oliasoftware (2019). Blowout & Kill Simulations. <https://www.oliasoft.com/products/blowout-kill-simulations/>, [Accessed 15.02.19].
- Orkiszewski, J. (1967). Predicting Two-Phase Pressure Drops in Vertical Pipe. Journal of Petroleum Technology 19(6): 829-838. SPE-1546-PA. .
- Oskarsen, R., Rygg, O., Cargol, M., and Morry, B. (2016). Challenging Offshore Dynamic Kill Operations Made Possible With the Relief Well Injection Spool. Paper SPE 180279 presented at the SPE Deepwater Drilling and Completions Conference, Galveston, Texas, USA, 14-15 September.
- Oudeman, P. (2007). Hydraulic Blowout Control Requirements for Big-Bore and HP/HT Developments: Validation With Field Experience. Paper SPE/IADC 105612 Presented at the SPE/IADC Drilling Conference. Amsterdam, The Netherlands, 20-22 February.
- Oudeman, P. (2010). Validation of Blowout-Rate Calculations for Subsea Wells. Paper SPE 115019 Presented at the IADC/SPE Asia Pacific Drilling Conference and Exhibition, Jakarta, Indonesia, 25-27 August.
- Peaceman, D. (1977). *Fundamentals of Numerical Reservoir Simulation*, Elsevier Science, volume 6, 1st edition, Amsterdam.
- Petrowiki (2015a). Gas Formation Volume Factor and Density. Published by SPE International. https://petrowiki.org/Gas_formation_volume_factor_and_density. [Accessed 20.03.19].
- Petrowiki (2015b). Kicks. <https://petrowiki.org/Kicks>, [Accessed 14.01.19].
- Petrowiki (2015c). Oil Fluid Characteristics. Published by SPE International. https://petrowiki.org/Oil_fluid_characteristics. [Accessed 15.03.19].
- Petrowiki (2015d). Oil Well Performance. Published by SPE International. https://petrowiki.org/Oil_well_performance#Vogel.27s_inflow_performance_relationship. [Accessed 14.03.19].
- Petrowiki (2016). Productivity index (J). Published by SPE International. [https://petrowiki.org/Productivity_index_\(J\)](https://petrowiki.org/Productivity_index_(J)). [Accessed 02.05.19].
- Pettersen, Ø. (1990). *Grunnkurs i Reservoarmekanikk. Matematisk institutt - Universitetet i Bergen*.

- PSA (2019a). Petroleum Safety Authority Norway - Role and area of responsibility. <https://www.ptil.no/en/about-us/role-and-area-of-responsibility/>[Accessed 29.01.19].
- PSA (2019b). Regulations relating to conducting petroleum activities (The Activities Regulations). <https://www.ptil.no/en/regulations/all-acts/?forskrift=613>, [Accessed 07.02.19].
- PSA (2019c). Regulations relating to design and outfitting of facilities, etc. in petroleum activity (The Facilities Regulations). https://www.ptil.no/contentassets/bf47ce8fdec745f4a2c4ed073866f079/2019_eng-26.4.2019/innretningsforskriften_e.pdf, [Accessed 07.02.19].
- Regjeringen (2016). Pollution preparedness and response. <https://www.regjeringen.no/en/topics/energy/oil-and-gas/pollution-preparedness-and-response/id2485367/>. [Accessed 14.05.19].
- Rinde, T., Killie, R., Howard, S., Solli, L., and Lillelokken, N. (2016). Impact of New and Ultra-High Density Kill Fluids on Challenging Well-Kill Operations. Paper SPE 180047 Presented at the SPE Bergen One Day Seminar, Grieghallen, Bergen, Norway, 20 April.
- Rygg, O., Smestad, P., and Wright, J. (1992). Dynamic Two-Phase Flow Simulator: A Powerful Tool for Blowout and Relief Well Kill Analysis. Paper SPE 24578 Presented at the 67th Annual Technical Conference and Exhibiton of the Society of Petroleum Engineers, Washington, DC, 4-7 October.
- Santos, O. (2001). A Study on Blowouts in Ultra Deep Waters. Paper SPE 69530 Presented at the SPE Latin American and Caribbean Petroleum Engineering Conference. Buenos Aires, Argentina, 25-28 March.
- Schlumberger (2019). Drillbench Blowout Control <https://www.software.slb.com/products/drillbench/drillbench-blowout-control>, [Accessed 13.02.19].
- Schubert, J. (1995). Well Control. Texas A&M University, Department of Petroleum Engineering. http://www1.uis.no/Fag/Learningspace_kurs/PetBachelor/webpage/tech%5Cdrilling%5CwellControl.pdf, [Accessed 06.02.19].
- Schubert, J., Valko, P., Jourine, S., Oskarsen, R. T., Noynaert, S., Meyer, H., Walls, S., and Weddle, C. (2004). Development of a Blowout Intervention Method and Dynamic Kill Simulator for Blowouts Occurring in Ultra-Deepwater. Final Project Report - Phase One, prepared for the Mineral Management Service - BSEE. <https://www.bsee.gov/sites/bsee.gov/files/tap-technical-assessment-program/408aa.pdf>, [Accessed 03.05.19].
- Singh, T. and Hosein, R. (2012). PVT Correlations for Trinidad Oil the Offshore Southwest Coast. Paper SPE 158805 Presented at the SPETT 2012 Energy Conference and Exhibiton, Port-of-Spain, Trinidad, 11-13 June.
- SINTEF (2010). Oil Spill Response - recommendation for further development. <https://www.sintef.no/globalassets/project/oilandgas/pdf/oil-spill-response.pdf>, [Accessed 30.01.19].
- SINTEF (2014). OSCAR - Oil Spill Contingency And Response. <https://www.sintef.no/programvare/oscar-oil-spill-contingency-and-response/>, [Accessed 13.02.19].
- SINTEF (2017). SINTEF Offshore Blowout Database. <https://www.sintef.no/en/projects/sintef-offshore-blowout-database/>, [Accessed 30.01.19].

- Standing, M. (1947). A pressure-Volume-Temperature Correlation For Mixtures of California Oils And Gases. *Drilling and Production Practice*, 1 Januray, New York. Paper API-47-275.
- Standing, M. (1968). Concerning the Calculation of Inflow Performance of Wells Producing from Solution Gas Drive Reservoirs. *Journal of Petroleum Technology* 23(9): 1141-1142. SPE-3332-PA.
- Statoil (2010). Individual Development Well, Activity Program Drilling Well NO 6608/10-K-2 H and AH, NORNE field.
- Sutton, R. and Farshad, F. (1990). Evaluation of Emperically Derived PVT Properties for Gulf of Mexico Crude Oils. *SPE Reservoir Eningeering* 5(1). SPE-13172-PA.
- UNEP (1997). Environmental management in oil and gas exploration and production. Joint UNEP IE and EP Forum publication, <https://wedocs.unep.org/bitstream/handle/20.500.11822/8275/-Environmental%20Management%20in%20oil%20%26%20Gas%20Exploration%20%26%20Production-19972123.pdf?sequence=2&isAllowed=y>, [Accessed 10.06.2019].
- Vandenbussche, V., Bergsli, A., Brandt, H., Nissen-Lie, T., and Brude, O. (2012). Well-specific Blowout Risk Assessment. Paper SPE 157319 Presented at the SPE/APPEA International Conference on Health, Safety and Environment in oil and gas exploration and production, Perth, Australia, 11-13 September.
- Vasques, M. and Beggs, H. (1980). Correlations for Fluid Physical Property Prediction. *Journal of Petroleum Technology* 32(6): 968-971. SPE 6719-PA.
- Vogel, J. (1968). Inflow Performance Relationships for Solution-Gas Drive Wells. *Journal of Petroleum Technology* 20(1): 83-92. SPE-1476-PA.
- Watson, D., Brittenham, T., and Moore, P. (2003). *Advanced Well Control*. SPE Textbook Series, Vol. 10. Richardson, Texas, Society of Petroleum Engineers. ISBN 1-55563-101-0.
- Wild Well (2019). Well Control Modeling. <https://wildwell.com/engineering/modeling/>, [Accessed 13.02.19].
- Willson, S. M. (2012). A Wellbore Stability Approach For Self-Killing Blowout Assessment. Paper SPE 156330 Presented at the SPE Deepwater Drilling and Completions Conference. Galveston, Texas, USA, 20-21 June.
- Yahaya, A. U. and Gahtani, A. (2010). A Comparative Study Between Empirical Correlations and Mechanistic Models of Vertical Multiphase Flow. Paper SPE 136931 Presented at the SPE/DGS Annual Technical Symposium and Exhibition, Al-Khobar, Saudi Arabia, 4-7 April. .
- Yuan, Z., Hashemian, Y., and Morell, D. (2014). Ultra-Deepwater Blowout Well Control Analysis under Worst Case Blowout Scenario. Paper SPE 170256 Presented at the SPE Deppwater Drilling and Completion Conference. Galveston, Texas, USA, 10-11 September.
- Yuan, Z., Morrell, D., Sonnemann, P., and Leach, C. (2017). Mitigating Gas-in-Riser Rapid Unloading for Deepwater-Well Control. *SPE Drilling & Completion* 32(2). SPE 185179-PA.

A. Appendix

A.1 Simple Inflow Model Calculations

Simple inflow model calculations performed in case study #1 in order to plot a graph of both the IPR and the TPR. These calculations are performed in Excel.

Liquid rate [STB/day]	Liquid rate [ft ³ /s]	BHP [psi]	Inflow rates [STB/day]
1,539	0,0001	4482,3	517,7
100	0,00650	4414,1	585,9
250	0,01625	4299,7	700,3
300	0,01950	4255,5	744,5
400	0,02599	4171	829
500	0,03249	4078,6	921,4
700	0,04549	3899,9	1100,1
800	0,05199	3818,7	1181,3
900	0,05849	3744	1256
1000	0,06499	3674,5	1325,5
1100	0,07148	3613,8	1386,2
1200	0,07798	3555,5	1444,5
1300	0,08448	3508,1	1491,9
1400	0,09098	3466,8	1533,2
1500	0,09748	3429,5	1570,5
1600	0,10398	3390,7	1609,3
1700	0,11048	3364,3	1635,7
1800	0,11697	3334,2	1665,8
1900	0,12347	3310,2	1689,8
2000	0,12997	3286,6	1713,4
3000	0,19496	3151,6	1848,4
5000	0,32493	3072,3	1927,7

<i>Productivity index</i>	1 [STB/day/psi]
<i>Reservoir Pressure</i>	5000 [psi]
<i>Bubble point pressure</i>	3565,8 [psi]
<i>Pres>Pb</i>	

A.2 Modified Code with Implemented Inflow Model

A.2.1 Main.m

```

%% A BLOWOUT WELL FLOW MODEL

% A program developed for calculating well pressures in a
% well where we have both oil and gas flow. The model assumes that we
% have steady state conditions (constant flowrates at surface) and no time
% variations. The model is based on calculating the correct bottomhole
% pressure for certain gas and oil flow rates and takes into account
% both the hydrostatic pressure and frictional pressures.

% As the black oil model is implemented into the program, all
% calculations are done using field units, thus [psi] for pressure,
% [ft3/s] for rates.

clear;

% Here we specify the vertical depth of the well and
% and the number of boxes we want in our calculations.
% Based on this, the boxlength is found and used in the calculations.

welldepth = 4000; %m
nobox = 200;
nopoints = nobox+1;
boxlength = welldepth/nobox; %m
% nopoints is an j array keeping track of the end point of the boxes.

% Now we will call a function that calculates the pressure along the well
% for a given liquid flowrate. We call this function
% itsolver because it is the zero point solver, meaning that the function
% iterates until it finds the correct pressure. This solver routine again
% calls upon a function "f(Pbottom)" called wellpressure. The routine
% solver actually finds the correct bottomhole pressure that makes the
% function wellpressure become zero "f(Pbottom) = 0".
% Then we have found the correct pressure profile.

% Rates are given in ft3/s. We assume only liquid flow first.

liquidrate = 0.12347; %liquid rate at surface [ft3/s]

[pbot,error,rate] = itsolver(nopoints,boxlength,welldepth,liquidrate);
%[pbot,error]=itsolver(nopoints,boxlength,welldepth,liquidrate);

```

A.2.2 Itsolver.m

```

%% FUNCTION ITSOLVER
function [pbot,error,rate] = itsolver(nopoints,boxlength,welldepth,liquidrate)
%function [pbot,error] = itsolver(nopoints,boxlength,welldepth,liquidrate)

% The numerical solver implemented here for solving the equation f(x)= 0
% "wellpressure(pbot)= 0" is called the
% Method of Halving the Interval (Bisection Method)

% You will not find exact match for f(x)= 0. By using
% ftol we say that if f(x)<ftol, we are satisfied.

ftol = 1; %Specified tolerance [psi]

% Set number of iterations to zero. This number will tell how many
% iterations are required to find a solution with the specified accuracy.

```

```

noit = 0;

% Here one need to specify the search interval. xguess is the pressure you
% guess for the bottomhole. We here use hydrostic pressure of liquid in the
% well as our initial guess. This is of course not nes. correct since we have
% gas and friction effects in addition. But it might be a good starting point for
% the iteration.

xguess = 500*9.81*welldepth*0.000145038;%initial guess for BHP, [psi]
% The search interval can be adjusted to help find a solution.
xint = 725.19; %Selected search interval, [psi]
x1 = xguess-xint/2.0;
x2 = xguess+xint/2.0;

[f1,rate] = wellpressure(x1,liquidrate,nopoints,boxlength,welldepth);
[f2,rate] = wellpressure(x2,liquidrate,nopoints,boxlength,welldepth);
% f1 = wellpressure(x1,liquidrate,nopoints,boxlength,welldepth);
% f2 = wellpressure(x2,liquidrate,nopoints,boxlength,welldepth);

% First include a check on whether f1xf2<0. If not you must adjust your
% initial search intervall. If error is 1 and zero pbot, then you must
% adjust the intervall here.

while (f1*f2)>=0
    xint= xint+100;
    x1 = xguess-xint/2.0;
    x2 = xguess+xint/2.0;

    [f1,rate] = wellpressure(x1,liquidrate,nopoints,boxlength,welldepth);
    [f2,rate] = wellpressure(x2,liquidrate,nopoints,boxlength,welldepth);
    %f1 = wellpressure(x1,liquidrate,nopoints,boxlength,welldepth);
    %f2 = wellpressure(x2,liquidrate,nopoints,boxlength,welldepth);
    error = 1;
    %pbot = 0;
end

% start iterating, we are now on the track.
x3 = (x1+x2)/2.0;
[f3,rate] = wellpressure(x3,liquidrate,nopoints,boxlength,welldepth);
%f3 = wellpressure(x3,liquidrate,nopoints,boxlength,welldepth);

while (f3>ftol | f3 < -ftol)
    noit = noit +1

    if (f3*f1) < 0
        x2 = x3;
    else
        x1 = x3;
    end

    x3 = (x1+x2)/2.0;
    [f3,rate] = wellpressure(x3,liquidrate,nopoints,boxlength,welldepth);
    [f1,rate] = wellpressure(x1,liquidrate,nopoints,boxlength,welldepth);
    %f3 = wellpressure(x3,liquidrate,nopoints,boxlength,welldepth);
    %f1 = wellpressure(x1,liquidrate,nopoints,boxlength,welldepth);
end
error = 0;
pbot = x3
noit
end

```

A.2.3 Wellpressure.m

```

%% FUNCTION WELLPRESSURE
function[f,rate]=wellpressure(pbotguess,liquidrate,nopoints,boxlength,welldepth)
% function [f] = wellpressure(pbotguess,liquidrate,nopoints,boxlength,welldepth)

% At first we need to state the outlet pressure, namely also the physical
% boundary condition, that we have to ensure that our model reaches.
% One may assume the outlet pressure to be equal to the atmospheric
% pressure, 14.7 psi. However, if a choke is present, the surface pressure
% will be different. This means that the outlet pressure should be set
% equal to desired choke pressure. It means that if the choke pressure is
% 250 psi, then the variable, prealsurface, should be set to this.

prealsurface = 250; %If there is a back-pressure present [psi]
%prealsurface=14.7; %If the outlet pressure is the atmospheric pressure

% We now start by the deepest box with the pressure we assume: pbotguess
% and for each box, we calculate the pressure and flowrates. In the end, we
% end up with some surface rates and a surface outlet pressure. The
% calculated outlet surface pressure should equal the physical outlet
% condition. The function will be zero if the correct bottomhole pressure
% is found.

% One assume a annular geometry, and therefore need to set outer/inner
% diameter of annulus. Assume a 8.5" casing, and a 5.0" drillpipe.

%% Defining initial parameters:
do = 8.5; % Outer diameter, [in]
di = 5.0; % Inner diameter, [in]
e = 0.000288; %inner rugosity in [ in]
RGL = 600; % = gas-liquid ratio, [scf/STB]
% RGL = GOR, because we assume only oil and gas flow.
%fw=zeros(nopoints, 1);
fw = 0; % water fraction, zero because we assume only gas and oil flow
gamaoil=0.87;% oil relative density
gamagas=0.75;% gas relative density
rowater= 62.4; %water density [lbm/ft3]
Mair = 29; % air molar mass [g/mol]
roair = 0.0765; % air density [lbm/ft3]

%% CASE STUDY #2
% This PI model is used in case study #2 for single-phase flow.

%% The PI model (Simple reservoir inflow model )
% prodinx = 1; %Productivity index, [STB/day/psi]
% Pres = 5000; % Average reservoir pressure [psi]
%
% if (pbotguess < Pres)
% liquidrate = prodinx*(Pres - pbotguess); %[STB/day]
% else
% liquidrate = 0;
% end
%
% % need to convert the liquidrate from STB/day to ft3/s, hence
% liquidrate = liquidrate * 0.000065; %[ft3/s]

%% Preliminary calculations:
Rsb = RGL / (1 - fw); %solubility ratio at bubble point [scf/STB],
% hence Rsb = RGL = GOR.

%If the simple PI model is used, Qost, Qgst and Qwst needs to be
%activated before running the simulation.
% Qost=(1-fw)*liquidrate; %oil flowrate [ft3/s] at surface
% Qgst=RGL*liquidrate/5.61; % gas flowrate [ft3/s] at surface
% Qwst=fw*liquidrate; % Water rate in [ft3/s] at surface
K=e/(do-di); % relative rugosity
rodeadoil=gamaoil*rowater; %density of dead oil, [Lbm/ft3]

```

```

rogassc=gamagas*roair; %density of gas at standard conditions, [lbm/ft3]
API= 141.5/gamaoil-131.5; %API grade
flowarea = 3.14/4*(do*do-di*di); % The flow area [in2]

%% Specify viscosities [cP]

viscw = 1; %water viscosity cP
visco= 12; %Oil viscosity, cP
viscg = 0.01;%Gas viscosity, cP

%%
% Now we loop from the bottom to surface and calculate accross all the
% segments until we reach the outlet.

%vls = zeros(nopoints,1);
%vgs = zeros(nopoints,1);
p = zeros(nopoints,1);
T = zeros(nopoints,1);
depth = zeros(nopoints,1);
%PB = zeros(nopoints,1);
Rs = zeros(nopoints,1);
Bo = zeros(nopoints,1);
%Z = zeros(nopoints,1);
%sigma = zeros(nopoints,1);
Bg = zeros(nopoints,1);
%Ql = zeros(nopoints,1);
%vls = zeros(nopoints,1);
%Qg = zeros(nopoints,1);
%vgs = zeros(nopoints,1);
%vmix = zeros(nopoints,1);
roliq = zeros(nopoints,1);
rooil = zeros(nopoints,1);
rogas = zeros(nopoints,1);
%Nvl = zeros(nopoints,1);
%Nvg = zeros(nopoints,1);
%Nd = zeros(nopoints,1);
%Nl = zeros(nopoints,1);
H.l = zeros(nopoints,1);
%Hg = zeros(nopoints,1);
%romix = zeros(nopoints,1);
%viscmix = zeros(nopoints,1);
%Re = zeros(nopoints,1);
%dpdlfric = zeros(nopoints-1,1);
%dpdlhid = zeros(nopoints-1,1);

% Before we loop, we define all variables at the inlet of the first
% segment(at bottom). As starting point we use the fact that we know the
% mass rate of the different phases (same as on top of the well)
% Calculations that must be updated in each cell
% (parametres that verie with P and T) :

% Set pressure equal to guessed pressure
p(1) = pbotguess; %Inital guess for pressure in node 1, [psi]
T(1)= 302;% Bottomhole temperature, [F]
depth(1)=welldepth* 3.28084;%welldepth converted from [m] to [ft]

%% Temperature Model
%Include a simple temperature model, in order to determine the
%temperatures in the different nodes.
T(1)=302;
T(nopoints)=100;
tempgrad=(T(nopoints)-T(1))/(nopoints-1); %Temperature gradient [F]
for i=1:nopoints-1
    T(i+1)=T(i)+tempgrad;
end

```

```

%% CASE STUDY #3
%% PI Model (Inflow model for both undersaturated and saturated reservoirs)
PB=Pbubble (gamagas, T(1), API, Rsb);% Bubble point pressure, [psi]
prodinx = 1; %Productivity index [STB/day/psi]
Pres =5000; %Average reservoir pressure [psi]
qmax = (prodinx*Pres)/1.8; %Maximum inflow rate [STB/day]

if pbotguess < Pres
    if (Pres > PB) & (pbotguess ≥ PB)
        liquidrate = prodinx*(Pres - pbotguess); % [STB/day]
    elseif (pbotguess ≤ PB) & (Pres < PB)
        %Standard Vogel inflow model [STB/day]
        liquidrate = qmax* ( 1 - 0.2*(pbotguess/Pres)- 0.8*(pbotguess/Pres)^2);
    else
        %Modified Vogel inflow model [STB/day], a combination of both the
        %simple inflow model and the standard Vogel equation.
        liquidrate = prodinx*(Pres-PB)+ (prodinx*PB/1.8)*(1 - 0.2*(pbotguess/PB)
        - 0.8*(pbotguess/PB)^2);
    end
else
    liquidrate = 0;
end

%need to convert the liquidrate from STB/day to ft3/s, hence
liquidrate = liquidrate * 0.000065; %[ft3/s]

%% Additional preliminary calculations
Qost=(1-fw)*liquidrate; %oil flowrate at surface [ft3/s]
Qgst=RGL*liquidrate/5.61; % gas flowrate at surface [ft3/s]
Qwst=fw*liquidrate; %water flow rate at surface [ft3/s]
%%
% Now we loop across the segments.
for i =1:nopoints-1

% use the inlet values for each segment to calculate hydrostatic
% and friction pressure across each segment.

%if (i==8)
%disp('here')
%end

% If the simple inflow model is used, the bubble point pressure equation
% needs to be activated.
PB=Pbubble (gamagas, T(i), API, Rsb);% Bubble point pressure, [psi]
Rs=Rsolu (gamagas,API,PB, p(i),T(i));% solubility ratio
Bo(i)= FVFo (Rs,API,gamagas,T(i),p(i),PB);% Oil fomration volume factor
CompFactor= zgas (gamagas,p(i),T(i)); %Gas compressibility factor
sigma=tension (p(i),T(i),API); % [dyna/cm]
Bg(i)=FVFg (T(i),CompFactor,p(i));%Gas formation volume factor [ft3/scf]
Ql=Qwst+Qost*Bo(i); %in situ liquid rate, [ft3/s]
vls = Ql/flowarea*144; %liquid superficial velocity, [ft/s]
Qg = (Qgst-Qost*Rs/5.61)*Bg(i);%gas rate in situ, [ft3/s] [1 bbl = 5.61 ft3]
    if Qg<0
        Qg=0;
    end
vgs=Qg/flowarea*144;%gas superficial velocity, [ft/s]
vmix=vls+vgs; %misxture velocity in ft/s

%in situ density of liquid in Lbm/ft3
roliq(i)=(rodeadoil*Qost+ Rs*Qost*rogassc/5.61+rowater*Qwst)/(Bo(i)*Qost+Qwst);
rooil(i)=(rodeadoil+Rs*rogassc/5.61)/Bo(i);%in situ density of oil in Lbm/ft3
%in situ density of gas in Lbm/ft3
rogas(i)=p(i)*gamagas*144*Mair*CompFactor/1545.349/(T(i)+460);

%% Liquid holdup
% now, we apply modified Haggdorn & brown method to find liquid fraction
N_vl = Nvl(vls, roliq(i), sigma);%liquid velocity number
N_vg = Nvg(vgs, roliq(i), sigma);%gas velocity number

```

```

N_d = Nd(do,di, roliq(i), sigma ); %pipe diameter number
N_l = Nl(visco, roliq(i), sigma);%liquid viscosity number
H_l(i) = Hl(N_vl, N_vg, N_d, N_l, vgs, vmix, p(i), do, di); %liquid holdup

%A test to see if there are any errors in the Hagedorn and Brown correlation;
% No slip formula for fraction:
%H_l(i)= vls/(vls+vgs);

%With known liquid holdup, the gas holdup can be determined from
Hg=(1-H_l(i)); %gas holdup

%the holdups obtained from the Hagedorn & Brown correlation may be used
%to determine the mixture properties of a multiphase flow.

romix= roliq(i)*H_l(i)+rogas(i)*Hg;%mixture density , [Lbm/ft3]
viscmix = (viscw*fw+visco*(1-fw))^H_l(i)*viscg^Hg; %Viscosity mixture, [cP]
Re=124.01 * ((do-di) * vmix * romix) / viscmix; %Reynolds number

%% Pressure drop
dpdlfric = dpfric(Re, K, di, do, vmix, romix); %Pressure loss due friction[psi/ft]
dpdlhid = romix / 144; % hydrostatic pressure loss [psi/ft]

p(i+1)=p(i)-dpdlhid*boxlength*3.28084-dpdlfric*boxlength*3.28084;

% A test to see if there are any problems in the friction model
%p(i+1)=p(i)-dpdlhid*boxlength*3.28084;
depth (i+1)= depth(i)-boxlength*3.28084;
    end

%% Results
pout = p(nopoints);
f = pout-prealsurface;
rate = liquidrate;
    if f ≤ 1 %psi. This value is the value copied of ftol in itsolver

%% Plotting figures
%Simply remove % to show some of the parameters profile

%Plot of the pressure drop in the well
% plot(depth(1:nopoints-1),p(1:nopoints-1))
% grid on
% title('Pressure drop profile')
% xlabel('Depth(ft)')
% ylabel('Pressure (psi)')

%Plot of the Oil Formation Volume Factor
% plot(depth(1:nopoints-1),Bo(1:nopoints-1))
% grid on
% title('Oil Formation Volume Factor profile')
% xlabel('Depth (ft)')
% ylabel('Bo')

%Plot of the Gas Formation Volume Factor
% plot(depth(1:nopoints-1),Bg(1:nopoints-1))
% grid on
% title('Gas Formation Volume Factor profile')
% xlabel('Depth (ft)')
% ylabel('Bg')

%Plot of the gas density profile
% plot(depth(1:nopoints-1),rogas(1:nopoints-1))
% grid on
% title('Gas Density profile')
% xlabel('Depth(ft)')
% ylabel('Density (Lbm/ft3)')

%Plot of the oil density profile

```

```

% plot(depth(1:nopoints-1),rhoil(1:nopoints-1))
% grid on
% title('Oil Density profile')
% xlabel('Depth(ft)')
% ylabel('Density (Lbm/ft3)')

%Plot of the liquid holdup
plot(depth(1:nopoints-1),H_l(1:nopoints-1))
grid on
title('Liquid Holdup profile')
xlabel('Depth(ft)')
ylabel('Liquid Holdup')

    end
end

```

A.2.4 Function for solubility ratio

```

%% SOLUBILITY RATIO
function Rs= Rsolu(gamag, API, PB, P, T)
% Standing correlation is employed to calculate Rs.
%Rsolu = solubility ratio, [scf/STB]
%gamag= gas specific gravity
%API= API (dead oil)
%PB = Bubble point pressure, [psia]
%p: pressure [psia]
%T: temperature [F]
if (P<14.7)
    P=14.7;
end

    Yg = 0.00091 * T - 0.0125 * API;
    if (P < PB)
        Rs = gamag * ((P - 14.7) / 18 / 10 ^ Yg) ^ (1 / 0.83);
    else
        Rs = gamag * ((PB - 14.7) / 18 / 10 ^ Yg) ^ (1 / 0.83);
    end
end

```

A.2.5 Function for bubble point pressure

```

%% BUBBLE POINT PRESSURE
function PB = Pbubble (gamag, T, API, Rsb)
% The Standing correlation is employed to calculate the bubble point
% pressure, Pb [psia]
%T = temperature [F]
%gamagas = gas specific gravity
%API = API (of dead oil)
%Rsb = Solubility Ratio at bubble point [scf/STB]
    Yg = 0.00091 * T - 0.0125 * API;
    PB = 18 * (Rsb / gamag) ^ 0.83 * 10 ^ Yg + 14.7; % The factor of 14.7psi
    %is added to the formula in order to get the absolute pressure.

end

```

A.2.6 Function for frictional pressure loss

```

%% FRICTIONAL PRESSURE LOSS
function friclossgrad = dpfric(Re, K, di,do, v, ro)

%friclossgrad = frictional pressure loss [psi/ft]

```

```

%f = Fanning friction factor
%Re = Reynolds number
%K = relative rugosity
%v = mixture velcocity [ft/s]
%d = diameter [in]
%ro: mixture density [lbm/ft3]

%One need to distinguish between laminar and turbulent flow regime, as
%different flow patterns yields different calculations of the friction
%factor.

if (Re ≤ 2000)
    f = 24 / Re;

elseif ((Re≥2000) & (Re≤3000))
    xint = (Re-2000)/1000;
    f1 = 24 / Re;
    A = (-4) * log((K / 3.7065) - (5.0452 / Re) * log(((K ^ 1.1098) /
    2.8257) + ((7.149 / Re) ^ 0.8981)));

    f2 = (1 / A) ^ 2; %Chens friction factor
    %f2 = 0.052*(Re)^(-0.19); %Blasius friction factor
    f = xint*f2+(1-xint)*f1;

else
    A = (-4) * log((K / 3.7065) - (5.0452 / Re) * log(((K ^ 1.1098) /
    2.8257) + ((7.149 / Re) ^ 0.8981)));

    f = (1 / A) ^ 2; %Chens friction factor
    %f = 0.052*(Re)^(-0.19); %Blasius friction factor

end
friclossgrad = (2 * f * ro * v ^ 2) / (32.17*( do-di)/12 * 144);

end

```

A.2.7 Function for oil formation volume factor

```

%% OIL FORMATION VOLUME FACTOR

function Bo=FVFo(Rs, API, gg, T, p, pb)
%Standing correlation is used to determine this parameter.
%FVFo= oil formation volume factor [bbl/STB]
%Rs= solubility of the gas in the oil [scf/STB]
%gg= gas specific gravity
%API: API (dead oil)
%pb = bubble point pressure [psia]
%p = pressure [psia]
%T = temperature [F]
%co = compressibility factor of oil [1/psi]
%go = oil specific gravity
%Bob = Oil Formation Volume Factor above bubble point [bbl/STB]

if (p < pb) %saturated oil
    go = 141.5 / (131.5 + API); % Density relative to water
    f = Rs * (gg / go) ^ 0.5 + 1.25 * T;
    Bo = 0.972 + 0.000147 * f ^ 1.175;
else %undersaturated oil
    Yg = 0.00091 * T - 0.0125 * API;
    Rsb = gg * ((pb- 14.7) / 18 / 10 ^ Yg) ^ (1 / 0.83);
    %The value 14.7 psia is added into the equation to get the absolute
    %pressure.
    go = 141.5 / (131.5 + API);
    f = Rsb * (gg / go) ^ 0.5 + 1.25 * T;
    Bob = 0.972 + 0.000147 * f ^ 1.175;
    %because, the standing correlation is only valid for p < pb, one
    %need to include the Vasques-Beggs correlation for cases above the

```

```

    %pb, hence one need to include the following
    co = (5 * Rsb + 17.2 * T - 1180 * gg + 12.61 * API - 1433) / (p * 10 ^ 5);
    Bo = Bob * exp(co * (pb - p));
end
end

```

A.2.8 Function for gas formation volume factor

```

%% GAS FORMATION VOLUME FACTOR

function Bg = FVFg(T,Z,P)
%Bg = Gas formation volume factor [scf/scf]
% P = pressure[psia]
% T = Temperature [F]
% Z = Compressibility factor of gas
Bg = (14.7 / 520) * Z * (T + 460) / P;
end

```

A.2.9 Function for liquid holdup

```

%% LIQUID HOLDUP

function liquidholdup = Hl(Nvl, Nvg, Nd, Nl, vsupg, vmist, P, do,di)
% The modified Hagedorn & Brown method to find liquid holdup
Lb1 = 1.071 - 0.2218 * (vmist ^ 2) / (do-di);
%Lb1 = 1.071 - 0.2218 * (vmist ^ 2) / 2.8;
if (Lb1 < 0.13)
Lb = 0.13;
else
Lb = Lb1;
end

alphag = vsupg / vmist; %alpha g (no slip gas holdup)
%-----
if (alphag < Lb)
% then there is a bubble flow, and the Griffth correlation is used to
% obtain the liquid holdup
vs = 0.8; % [ft/s]
liquidholdup = 1 - (1 / 2) * (1 + vmist / vs - ((1 + vmist / vs) ^ 2 - 4
* vsupg / vs) ^ (1 / 2));
else
% If the flow regime in the pipe is not bubble flow, the original
% Hagedorn & Brown correlation is used to obtain HL
CNL = -4.2757 * Nl ^ 5 + 5.0934 * Nl ^ 4 - 1.9063 * Nl ^ 3 + 0.1478 * Nl ^ 2
+ 0.0505 * Nl + 0.0018;
A = Nvl * P ^ 0.1 * CNL / (Nvg ^ 0.575 * 14.7 ^ 0.1 * Nd);
%-----
if (A <= 0.0009)
B = 14.195 * A ^ 0.4094;
else
B = 7 * 10 ^ 6 * A ^ 3 - 80723 * A ^ 2 + 316.19 * A + 0.5649;
end
%-----
%B = Hl / PSI
c = Nvg * Nl ^ 0.38 / (Nd ^ 2.14);
if (c <= 0.012)
PSI = 1;
else
PSI = 124923 * c ^ 4 - 24628 * c ^ 3 + 1446.7 * c ^ 2 - 12.246 * c
+ 0.9953;
end
liquidholdup = B * PSI;

end
end

```

A.2.10 Function for liquid velocity number

```

%% THE LIQUID VELOCITY NUMBER

function liqvelnumber=Nvl(vsl, ro_l, sigma)
%vsl = Superficial velocity [ft/s]
%ro_l = Liquid density [lbm/ft3]
%sigma = Interracial tension [dyna/cm]
gc = 32.2; % [lbm*ft/lbf/s2]
g = 32.174; % gravity constant [ft/s2]
signal = sigma * 6.85 * 10 ^ (-5); % conv from dyna/cm to lbf/ft
liqvelnumber= vsl * (ro_l / gc / g / signal) ^ (1 / 4);
end

```

A.2.11 Function for gas velocity number

```

%% THE GAS VELOCITY NUMBER

function Gasvelnum=Nvg(vsg, ro_l, sigma)
%vsg = Superficial velocity [ft/s]
%ro_l = Liquid density [lbm/ft3]
%sigma = Interracial tension [dyna/cm]
gc = 32.2; % [lbm*ft/lbf/s2]
g = 32.174; % gravity constant [ft/s2]
signal = sigma * 6.85 * 10 ^ (-5); % [lbf/ft]
Gasvelnum = vsg * (ro_l / gc / g / signal) ^ (1 / 4);
end

```

A.2.12 Function for viscosity liquid number

```

%% THE VISCOSITY LIQUID NUMBER

function liqvisnum=Nl(viscL, ro_l, sigma)
%viscL = Liquid viscosity [cP]
%ro_l = Liquid density [lbm/ft3]
%sigma = Interracial tension [dyna/cm]
g = 981; %gravitational constant [cm/s2]
ro_l1 = ro_l * 0.016; % [g/cm3]
viscL = viscL / 100; % cP =dyn*s/cm2
liqvisnum = viscL * (g / ro_l1 / (sigma ^ 3)) ^ (1 / 4);
end

```

A.2.13 Function for diameter number

```

%% THE DIAMETER NUMBER

function dvelnum=Nd(do,di, ro_l, sigma)

%Diameter = d [in]
%Liquid density = ro_l [lbm/ft3]
%Interracial tension = sigma [dyna/cm]
gc = 32.2; % [lbm*ft/lbf/s2]
g = 32.174; % gravity constant [ft/s2]
signal = sigma * 6.85 * 10 ^ (-5); % [lbf/ft]
dvelnum = (do-di)/12 * (ro_l / gc * g / signal) ^ (1 / 2);
end

```

A.2.14 Function for tension

```

%% GAS-OIL INTERFACIAL TENSION
function sig = tension(p,T,API)

```

```

%p = pressure [psia]
%T = Temperature [F]
C = 1 - 0.024 * p ^ 0.045;
ts68 = 39 - 0.2571 * API;
ts100 = 37.5 - 0.2571 * API;
tsT = ts68 - (T - 68) * (ts68 - ts100) / 32;

if (T ≤ 68)
    sig = ts68 * C;
elseif (T ≥ 100)
    sig = ts100 * C;
else
    sig = tsT * C; % [dyna/cm]
end

end

```

A.2.15 Function for compressibility factor of gas

```

% COMPRESSIBILITY FACTOR OF GAS

function Z=zgas(gg,p,T)
%Real gas equation: Z=(pV)/(nRT)
%gg = gas specific gravity, air=1
%p = pressure [psia]
%T = temperature [F]

if(p<14.7)
    p=14.7;
end

A1 = 0.31506237;
A2 = -1.0467099;
A3 = -0.57832729;
A4 = 0.53530771;
A5 = -0.61232032;
A6 = -0.10488813;
A7 = 0.68157001;
A8 = 0.68446549;
ppc = 702.5 - 50 * gg; %pseudo-critical pressure [psia]
Tpc = 167 + 316.67 * gg; % pseudo-critical temperature [R]
ppr = p / ppc; %pseudo-reduced pressure [psia]
Tpr = (T + 460) / Tpc; %pseudo-reduced temperature
% 460 is included to covert the temperature from Rankine to Farenheit
Z = 1;
error = 999;
while (error > 0.001);
    ropr = 0.27 * ppr / Z / Tpr;
    Z1 = 1 + (A1 + A2 / Tpr + A3 / Tpr / Tpr / Tpr) * ropr;
    Z1 = Z1 + (A4 + A5 / Tpr) * ropr * ropr;
    Z1 = Z1 + (A5 * A6 * ropr * ropr * ropr * ropr * ropr) / Tpr;
    Z1 = Z1 + (A7 * ropr * ropr / Tpr / Tpr / Tpr) * (1 + A8 * ropr * ropr)
    * exp(-A8 * ropr * ropr);

    error = 2 * abs((Z - Z1) / (Z + Z1));
    Z = (Z1 + Z) / 2;
end

end

```